USE OF NIMROD IN FLOOD FORECASTING

S. J. Cole, V. A. Bell, A. J. Robson and R. J. Moore

This report is an official document prepared under contract between the Natural Environment Research Council, the Environment Agency and the Met Office.

CEH Wallingford
Crowmarsh Gifford
Wallingford
Oxfordshire
OX10 8BB
UK

Project C02328
August 2004

CONTENTS

List of Figures **iv**

List of Tables **vii**

Executive Summary **viii**

1 Introduction **1**

1.1 Motivation 1
1.2 Research Design 1
1.3 Other requirements 2
1.4 Report overview 3

2 Catchment characteristics and instrumentation **4**

2.1 The Upper Calder 4
2.2 River network and forecast points 5
2.3 Drainage areas and reservoirs 5
2.4 Raingauges 7
2.5 Weather Radar 7
2.6 River Gauging Stations 10

3 Data availability and quality **11**

3.1 Digital terrain model 11
3.2 Raingauge data 11
3.3 Radar data 13
3.3.1 Pre-2001 Met Office retrieved radar data 14
3.3.2 Post-2001 CEH retrieved radar data 16
3.3.3 Further analysis of radar data 19
3.4 River level data 26
3.5 Rating curves 30
3.6 Event Selection 31

4 Model calibration **33**

4.1 The Probability Distributed Model 33
4.2 Strategy for model calibration 35
4.2.1 Peak analysis 36
4.3 Raingauge-based model calibration 36
4.3.1 Calculating catchment average rainfall using raingauge weightings 36
4.3.2 Model calibration using raingauges 44
4.4 Radar-based model calibration 56
4.5 Summary 60

5 Model assessment and sensitivity analysis **62**

5.1 Model Assessment 62

5.2 Sensitivity Analysis 73
5.2.1 Radar-based sensitivity analyses 73
5.2.2 Raingauge-based sensitivity analysis 78
5.3 Summary 80

6 Summary, conclusions and recommendations 82

7 References 89

Appendix A Synoptic conditions for the peak rainfall periods 91

Appendix B Radar rainfall accumulation maps 110

Appendix C Cumulative rainfall time-series 124

LIST OF FIGURES

Figure 2.1 The Upper Calder, showing raingauges and gauging stations. Heavy lines show the catchment boundaries. Overlaid is the grid used for the 5km Nimrod radar data. 4

Figure 2.2 Reservoir drainage areas (1-6) and naturally draining areas (others). Overlaid is the grid used for the 2km radar data. 6

Figure 2.3 A schematic representation of the problem areas associated with the measurement of precipitation by radar (after Collier, 1989) 8

Figure 3.1 Cumulative rainfall of the available raingauges over the period January to March 2000 exposing a raingauge anomaly 12

Figure 3.2 Rainfall accumulation using Nimrod 5km analysis for Event 4; 69 days to 6 June 2000 20

Figure 3.3 Cumulative rainfall plots for Event 4: 29 March to 5 June 2000. Comparison of a given raingauge (RG) with the 5km radar grid-square containing it (RD) 21

Figure 3.4 Rainfall accumulation using Nimrod 5km analysis for Event 5; 66 days to 28 October 2000 22

Figure 3.5 Cumulative rainfall plots for Event 5: 24 August to 29 October 2000. Comparison of a given raingauge (RG) with the 5km radar grid-square containing it (RD) 23

Figure 3.6 Rainfall accumulation using Nimrod 5km and 2km analysis products for Event 7; 24 hours to 00:00 11 June 2002. 24

Figure 3.7 2 km raw and Nimrod 2 km data at 12:15 27 October 2002. 25

Figure 3.8 A level hydrograph for the Mytholmroyd station; 1 September to 31 October 2002. 27

Figure 3.9 A level hydrograph for the Walsden station; 1 January to 25 February 2002. Unnatural jumps in the level have been circled. 27

Figure 3.10 A level hydrograph for the Nutclough station; 1 May to 13 June 2002. 28

Figure 3.11 A level hydrograph for the Nutclough station covering Event 6: 1 to 12 November 2002. 28

Figure 3.12 Level hydrographs for the period 12 September to 12 October 2000. 29

Figure 4.1 The PDM rainfall-runoff model. 34

Figure 4.2 Raingauge area allocations based on the Thiessen method for the Mytholmroyd catchment. 38

Figure 4.3 Maps of SAAR (1km grid) and relief for the Upper Calder catchment. 40

Figure 4.4 Raingauge area allocations for the Mytholmroyd catchment, based on different weighting measures. 41

Figure 4.5 Daily potential evaporation estimated by the standard sine curve profile used in the PDM (solid line) and MORECS mean monthly estimates (+). 45

Figure 4.6 Hydrographs for Event 2: 09:00 20 September to 09:00 26 October 1998 (plus 1 day warm-up). The figure below the axis is the maximum rainfall (from either raingauge or 5km radar) for that catchment. 49

Figure 4.7 Hydrographs for Event 3: 09:00 13 December 1998 to 09:00 18 January 1999 (plus 1 day warm-up). The figure below the axis is the maximum rainfall (from either raingauge or 5km radar) for that catchment. 50

Figure 4.8 Hydrographs for the last ten days of Event 4: 09:00 2 April to 09:00 5 June 2000. The figure below the axis is the maximum rainfall (from either raingauge or 5km radar) for that catchment. 51
Figure 4.9 Hydrographs for Event 5a: 09:00 25 August to 22:00 28 October 2000 (plus 1 day warm-up). The figure below the axis is the maximum rainfall (from either raingauge or 5km radar) for that catchment. 52
Figure 4.10 Hydrographs for Event 6: 09:00 2 November to 09:00 12 November 2002 (plus 1 day warm-up). The figure below the axis is the maximum rainfall (from either raingauge or 5km radar) for that catchment. 53
Figure 5.1 Hydrographs for Event 7: 00:00 10 June to 12:00 11 June 2002 (plus 2 day warm-up). The figure below the axis is the maximum rainfall (from either raingauge or 5km radar) for that catchment. 68
Figure 5.2 Hydrographs for Event 8: 00:00 9 August to 00:00 11 August 2002 (plus 1 day warm-up). The figure below the axis is the maximum rainfall (from either raingauge or 5km radar) for that catchment. 69
Figure 5.3 Hydrographs for Event 9: 12:00 9 September to 00:00 11 September 2002 (plus 1 day warm-up). The figure below the axis is the maximum rainfall (from either raingauge or 5km radar) for that catchment. 70
Figure 5.4 Hydrographs for Event 10: 12:00 20 October to 00:00 29 October 2002 (plus 1 day warm-up). The figure below the axis is the maximum rainfall (from either raingauge or 5km radar) for that catchment. 71
Figure 5.5 Hydrographs for Event 11: 00:00 16 January to 00:00 17 February 2002 (plus 1 day warm up). The figure below the axis is the maximum rainfall (from either raingauge or 5km radar) for that catchment. 72
Figure 5.6 Hydrographs for Event 8: 00:00 9 August to 00:00 11 August 2002 and Event 9: 12:00 9 September to 00:00 11 September 2002 (plus 1 day warm up). The figure below the axis is the maximum rainfall (from any rainfall source) for that event. 76
Figure 5.7 Hydrographs for Event 10: 12:00 20 Oct - 00:00 29 Oct 2002 and Event 11: 00:00 16 Jan - 00:00 17 Feb 2002 (plus 1 day warm up). The figure below the axis is the maximum rainfall (from any rainfall source) for that event. 77
Figure 5.8 Hydrographs for a selection of assessment events at Walsden. Two different raingauge weights are used: one excluding the Blackstone Edge raingauge (left-hand column) and one including it (right-hand column). 79
Figure A.1 Surface pressure chart at 12:00 24 October 1998 92
Figure A.2 Nimrod 5km rain-rate analysis (12:30) and Nimrod 5km analysis (19:45) on 15 January 1999 93
Figure A.3 Nimrod 5km analysis at 10:00 and 19:30 15 January 1999 93
Figure A.4 Surface pressure chart at 12:00 15 January 1999 94
Figure A.5 Surface pressure chart at 00:00 4 June 2000 95
Figure A.6 Nimrod 5km analysis at 23:15 3 June 2000 96
Figure A.7 Nimrod 5km analysis at 10:45 and 14:15 9 October 2000 96
Figure A.8 Surface pressure chart at 12:00 9October 2000 97
Figure A.9 Surface pressure chart at 12:00 2 November 2002 99
Figure A.10 Surface pressure chart at 12:00 8 November 2002 100
Figure A.11 Nimrod 5km analysis for two times in November 2002 101
Figure A.12 Nimrod 5km and 2km analysis at 11:15 10 June 2002 101
Figure A.13 Surface pressure chart at 12:00 10 June 2002 102
Figure A.14 Surface pressure chart at 12:00 9 August 2002 103

Figure A.15 Nimrod 2km analysis at 12:00 and 23:20 9 August 2002 104
Figure A.16 Nimrod 5km and 2km analysis at 14:15 9 September 2002 104
Event 9: 9 September 2002 105
Figure A.17 Surface pressure chart at 12:00 9 September 2002 105
Figure A.18 Surface pressure charts at 12:00 25 October 2002 and 00:00 27 October 2002 106
Figure A.19 Nimrod 2km analysis at 18:50 25 October 2002 107
Figure A.21 Surface pressure chart at 00:00 11 February 2002 108
Figure A.22 Nimrod 2km analysis for two times in February 2002 109
Figure B.1 Rainfall accumulation, using Nimrod 5km analysis, for Event 2; 38 days to 27 October 1998 111
Figure B.2 Rainfall accumulation, using Nimrod 5km analysis, for Event 3; 38 days to 18 January 1999 112
Figure B.3 Rainfall accumulation, using Nimrod 5km analysis, for Event 4; 69 days to 6 June 2000 113
Figure B.4 Rainfall accumulation, using Nimrod 5km analysis, for Event 5; 66 days to 28 October 2000 114
Figure B.5 Rainfall accumulation, using Nimrod 5km and 2km analysis, for Event 6; 11 days to 12 November 2002 116
Figure B.6 Rainfall accumulation, using Nimrod 5km and 2km analysis, for Event 7; 24 hours to 00:00 11 June 2002. 117
Figure B.7 Rainfall accumulation, using Nimrod 5km and 2km analysis, for Event 8; 36 hours to 12:00 10 August 2002. 119
Figure B.8 Rainfall accumulation, using Nimrod 5km and 2km analysis, for Event 9; 12 hours to 00:00 10 September 2002. 120
Figure B.9 Rainfall accumulation, using Nimrod 5km and 2km analysis, for Event 10; 9 days to 29 October 2002. 122
Figure B.10 Rainfall accumulation, using Nimrod 5km and 2km analysis, for Event 11; 33 days to 17 February 2002. 123
Figure C.1 Cumulative rainfall time-series for Event 1: 10 January to15 February 1997 125
Figure C.2 Cumulative rainfall time-series for Event 2: 19 September to 27 October 1998 126
Figure C.3 Cumulative rainfall time-series for Event 3: 11 December 1998 to 18 January 1999 127
Figure C.4 Cumulative rainfall time-series for Event 4: 29 March to 5 June 2000 128
Figure C.5 Cumulative rainfall time-series for Event 5: 24 August to 29 October 2000 129
Figure C.6 Cumulative rainfall time-series for Event 6: 1 to 12 November 2002 130
Figure C.7 Cumulative rainfall time-series for Event 7: 10 to 11 June 2002 131
Figure C.8 Cumulative rainfall time-series for Event 8: 00:00 9 August to 12:00 10 August 2002 132
Figure C.9 Cumulative rainfall time-series for Event 9: 12:00 9 September to 00:00 10 September 2002 133
Figure C.10 Cumulative rainfall time-series for Event 10: 20 to 29 October 2002 134
Figure C.11 Cumulative rainfall time-series for Event 11: 15 January to 17 February 2002 135

LIST OF TABLES

Table 2.1 Catchment, reservoir and natural drainage areas 5
Table 2.2 Telemetry raingauges 6
Table 2.3 Details of Nimrod products used in this study 9
Table 2.4 River gauging stations 9
Table 3.1 Availability and quality of recent raingauge data 13
Table 3.2 Availability of the infilled 5km Nimrod analysis (pre-2001) provided by the Met Office 15
Table 3.3 Details of the infilled radar data (post-2001) retrieved from the CEH archive 17
Table 3.4 Availability and quality of river level data 26
Table 3.5 Rating curve coefficients provided by the Environment Agency 30
Table 3.6 Calibration events 31
Table 3.7 Assessment events 32
Table 4.1 Parameters of the PDM model 34
Table 4.2 Raingauges allocated to each catchment 38
Table 4.3 Raingauge weightings for Mytholmroyd catchment 42
Table 4.4 Raingauge weightings for Walsden catchment 43
Table 4.5 Raingauge weightings for Todmorden catchment 43
Table 4.6 Raingauge weights for Nutclough catchment 44
Table 4.7 Comparison of raingauge-calibrated PDM parameters across catchments. The radar-calibrated PDM parameters are identical except for the rainfall factor and time delay which are also listed. 48
Table 4.8 Calibration performance (R^2 statistic) for each catchment using raingauge and Nimrod 5km analysis rainfall 54
Table 4.9 Peak analysis for calibration events. Unbracketed terms relate to raingauge calibrations and bracketed terms to radar calibrations. 55
Table 5.1 Evaluation performance (R^2 statistic) for each catchment using raingauge, Nimrod 5km analysis, Nimrod 2km analysis and Nimrod 1-hour lead-time forecast rainfalls. 66
Table 5.2 Peak analysis for assessment events. Unbracketed terms relate to raingauge calibrations and bracketed terms to radar calibrations. 67

EXECUTIVE SUMMARY

It is common practice within the Environment Agency to calibrate rainfall-runoff models using raingauge data. Operationally these models are used in flood forecasting systems with raingauge data as input up to the time that the forecast is made. Radar rainfall forecasts are used beyond this for lead-times up to 6 hours to provide the potential for earlier flood warnings. There is an acknowledged reluctance to employ weather radar data for rainfall-runoff model calibration at the present time. This stems from concern regarding the consistency of the radar product in time and space, offset by the knowledge that raingauge networks of low density may provide poor spatial estimates of rain especially for spatially-varying convective storms. What is needed is some sound evidence that points to the value of using weather radar data in rainfall-runoff models for both model calibration and forecasting.

The "Use of Nimrod in Flood Forecasting" project aimed to establish a body of evidence that will serve to clarify the relative merits of using radar or raingauge data for rainfall-runoff model calibration and forecasting. The study is timely since there have been substantial efforts in recent years by the Met Office to improve the quality of the weather radar product under the Nimrod programme. For the first time, these improved Nimrod products are evaluated systematically in this study for use in flood model calibration and forecasting.

A set of four catchments in the Upper Calder part of the Yorkshire Ouse drainage basin were used as the focus of the study. The gauging locations for these catchments feature as operational flood forecast points within the River Flow Forecasting System used for flood forecast construction. The catchments are well served by the weather radar at Hameldon Hill, being at a distance of between 6 and 21 km. Three of the catchments are nested within the fourth, the Calder at Mytholmroyd (near Caldene Bridge) with a natural drainage area of 121 km^2, and the smallest being 10 km^2. Only one tipping-bucket raingauge is located within the larger catchment although three are located on its outer periphery. The prospect for radar being useful is therefore good.

The main Nimrod radar product used was the Nimrod 5 km analysis, available as a rain-rate every 15 minutes over the period of the study. This was chosen as being available over the period of the selected events from September 1998 to November 2002. Detailed quality control of the study dataset led to a set of 11 events being identified, of which 6 were used for model calibration and 5 for independent assessment. Three of the assessment events were chosen specifically to encompass spatially-varying convective rainfall. Radar might be expected to outperform raingauges in such situations, when used in rainfall-runoff models to estimate catchment runoff.

The form of rainfall-runoff model used was the PDM (Probability Distributed Model), selected as representative of models used in practice and employed operationally for flood forecasting in the Upper Calder by the Environment Agency. It was found that the raingauge-calibrated models provided a basis to set the parameters of the radar-based models, with revisions only needing to be considered for the rainfall factor and time delay parameters affecting flow volumes and timing respectively. This has beneficial implications to operational models that use raingauge data up to the time of the forecast and Nimrod rainfall forecasts beyond this.

A major finding of the study was that raingauge-based models provided more consistent flow simulations than those employing radar. This stemmed from the lack of consistency in the Nimrod radar product, with a tendency on occasions to over- and under-estimate rainfall. This was aggravated at times by changes affecting the product, notably the Cyclops radar processing upgrade on 1 September 2000. In contrast, the raingauge network provided a consistent rainfall measurement product, apart from the addition of one gauge over the study period. The radar-based model for the smallest 10 km^2 catchment did occasionally perform best, with the nearest raingauge being 2 km away. This leads to the conjecture that for a given gauge density (or proximity) there is some threshold catchment size below which radar may, on occasions, provide superior estimates of catchment average rainfall for input to a rainfall-runoff model. There was also some evidence for flood peak timings to be better predicted, on occasions, using radar-based models although peak magnitudes were usually inferior. Temporal synchronisation of hydrometric networks and possibly quantisation of raingauge estimates are issues to bear in mind here.

A sensitivity analysis was performed using the higher resolution Nimrod 2 km analysis available at a 5 minute frequency. Although this provided a minor improvement over the use of the Nimrod 5 km analysis, the overall finding relating to the superiority of the raingauge-based models was unaffected. Model sensitivity to using a Nimrod 5 km rainfall forecast, for a lead-time of one hour, in place of the Nimrod 5 km analysis was also investigated. This demonstrated the consistency of the radar-based models when used with Nimrod analysis or forecast products, and an expected overall fall in performance using the forecast product. The beneficial implications referred to above are reinforced by this finding. A third sensitivity test focussed on the impact of including an additional raingauge on raingauge-based model performance. The successful simulations obtained, without changing the model parameters, served to support the raingauge-weighting strategy for catchment average rainfall estimation developed in the study.

The report's summary, conclusions and recommendations provide further details of the knowledge acquired by the study and the implications for Environment Agency and Met Office operational practices.

1 INTRODUCTION

1.1 Motivation

There is an acknowledged reluctance at the present time within the Environment Agency to employ radar data routinely as input to rainfall-runoff models for flood forecasting. This is due to reasons concerning the lack of consistent quality in time and space of the weather radar estimates of rainfall. Up to the time the forecast is made, more reliance is often placed on information from a raingauge network, although this may be of poor quality at times due to low gauge density and high spatial variability of rain. For future times, however, radar rainfall forecasts are seen as the best available source of information for extending the lead-time of flow forecasts from rainfall-runoff models.

The above position is now being challenged as a result of significant efforts in recent years by the Met Office to produce improved quality-controlled (QC) radar products within the Nimrod environment. Some of these developments are reported by Harrison *et al*. (2000), whilst others are scheduled for implementation in 2004 as part of the RadarnetIV release. Past assessments involving radar data and rainfall-runoff models by the Centre for Ecology & Hydrology (CEH), and its predecessor Institute of Hydrology, have been limited to the use of raw radar products with Hyrad methods of correction and raingauge merging (Moore *et al*., 1993, 2000; Bell *et al*., 2001). This strategy reflected the wish to employ the highest resolution data (at the time, 2 km, 5 minute rain-rate) with efficient raingauge-merging procedures. There was also a reluctance to use a quality-controlled product still under development and subject to change and only available at a coarser space and time-resolution (5 km, 15 minute rain-rate).

The purpose of the present study is to carry out, for the first time, a detailed examination of the performance of rainfall-runoff models when used with Nimrod Quality-Controlled estimates of rainfall as input. This aims to provide the Environment Agency with the confidence to use, or not to use, Nimrod rainfall estimates routinely in rainfall-runoff models for flood forecasting in preference to raingauges. The lessons learnt will aim to steer future research on improvements to weather radar estimation of rainfall and the use of such estimates in rainfall-runoff models for flood forecasting.

1.2 Research Design

The research design was set down by the Environment Agency and the Met Office, and agreed with CEH. The focus of the study would be the Calder catchment in Yorkshire, previously studied by the Institute of Hydrology back in 1997. The report "Austin, R.M., Bell, V.A., Jones, D.A., Moore, R.J. (1997) River Calder Flood Warning Improvements RFFS Model Network. Contract Report to the Environment Agency, November 1997, Institute of Hydrology, 39pp." will be referred to as the Calder 1997 Report.

Three catchments were selected with existing raingauge-based rainfall-runoff model calibrations: Walsden Water at Walsden, the Calder at Todmorden, and Hebden Water at Nutclough. These catchments feature as forecast points within the River Flow Forecasting System (RFFS) operated by the Agency within its Northeast Region. A fourth catchment – the Calder at Mytholmroyd (immediately upstream of Caldene Bridge) - encompassing these three, was included to provide a larger catchment (147 compared to circa 14, 20 and 56 km^2) in the research design. The type of rainfall-runoff model used is the PDM (Probability Distributed Model), a popular and easy-to-use lumped conceptual catchment model based on continuous water accounting principles and simple translation functions (Moore, 1999; CEH Wallingford, 2001). The PDM is used operationally within the RFFS Model Network for the River Calder.

The Calder catchment is well served by the Hameldon Hill radar, being at a range of between 6 and 21 km depending on location. This C-band radar is one of the 15 radars providing network coverage over the British Isles. The density of the telemetry raingauge network is typical for areas of this kind with only one gauge within the larger catchment and three surrounding it. Thus the potential benefit of spatially-distributed radar rainfall estimates should be tested within this research design.

Choosing storms of both widespread stratiform/frontal rain and localised convective nature within the calibration and assessment framework would also ensure that the potential benefit of weather radar would be exposed. In practice, a set of 6 typically 2 month long periods over the period 1997 to 2002 were prescribed for model calibration and chosen to be characterised by predominant widespread rainfall. A set of 4 typically 2 day events in 2002 characterised by localised convective rainfall was prescribed for independent model assessment. This initial research design was relaxed to better reflect the recommended operational procedure for model calibration and assessment, which is to encompass both types of rainfall in both calibration and assessment as both types of event need to be forecast in practice. This was done by allowing further convective periods to be identified and added to the calibration set, and similarly including widespread rainfall events in the assessment set.

A dual model calibration strategy was set down in which separate models would be calibrated using radar and raingauge data as input, so that neither approach to forecasting would be unduly prejudiced. An important perceived advantage of calibration using radar data was that the use of rainfall forecasts based on radar data would be more consistent, and likely to be better, than had a raingauge-calibrated model been used. The scope of the project was constrained to focus on radar estimates of rain, as opposed to forecasts. However, a sensitivity analysis using Nimrod rainfall forecasts (Golding, 1998) for a given lead-time in place of radar estimates was included in the research design for application to the assessment events only.

1.3 Other requirements

An important outcome of this research project was seen to be the documentation of a step-by-step procedure for preparing a rainfall-runoff model for operational use which made use of radar rainfall data as input. This procedure needs to consider the radar archive, retrieval of data from it, quality control procedures applied subsequently to the radar and raingauge data in forming the modelling database, the use of Hyrad for deriving catchment average rainfall time-series, and quality control and management of the river level/flow data used in model calibration and assessment.

1.4 Report overview

The report begins by outlining the characteristics of the study catchments in the Upper Calder and reviewing the hydrometric network and available Nimrod rainfall radar products. Section 3 then considers the availability of data and particularly procedures for data quality control and infilling. This leads to the selection of two sets of events for independent model calibration and assessment. Appendices A, B and C provide supporting detailed information relating to each event including synoptic summaries, and maps and time-series of rainfall accumulations used in quality control.

Section 4 begins with a brief overview of the PDM rainfall-runoff model and then sets down a strategy for model calibration. For the raingauge-based model calibration, a procedure is first developed for combining raingauges to estimate catchment average rainfall. The results of the raingauge-based model calibration are then presented for each catchment in turn. This is followed by the radar-based calibrations and a summary which highlights the relative merits of raingauge- and radar-based models.

Section 5 gives comparable results obtained for the assessment events. In contrast, these are interpreted on an event by event basis to highlight event specific error characteristics and their effect across the study catchments. This section also explores the sensitivity of the results to using the Nimrod 5 km rainfall forecast and the 2 km analysis products in place of the Nimrod 5 km analysis as model input. The sensitivity to incorporating an additional raingauge in the raingauge-based models is also examined.

Finally, Section 6 provides a summary of the report, encompassing conclusions and recommendations, arranged in a thematic manner.

2 CATCHMENT CHARACTERISTICS AND INSTRUMENTATION

This chapter details the characteristics of the Upper Calder catchment. The location and properties of the instrumentation (raingauges, radar and flow gauging stations) are discussed along with possible sources of error in their readings.

2.1 The Upper Calder

The Upper Calder river basin (Figure 2.1) is located in the Southeast Pennines, in West Yorkshire. For the purposes of this study the Upper Calder is taken to comprise the catchment upstream of Caldene Bridge (SE 012 260), encompassing an area of 147 km^2 with altitude ranging from 88m to over 400m. Note that immediately upstream of Caldene Bridge is the Mytholmroyd river gauging station.

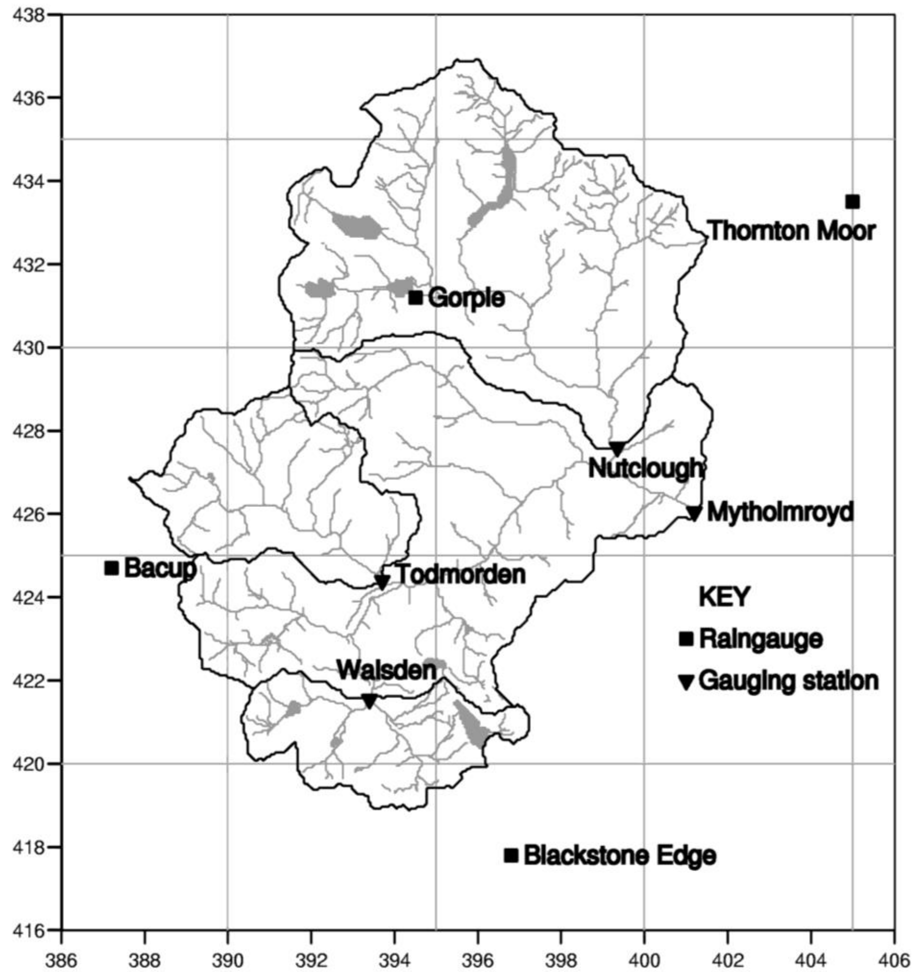

Figure 2.1 The Upper Calder, showing raingauges and gauging stations. Heavy lines show the catchment boundaries. Overlaid is the grid used for the 5km Nimrod radar data.

The catchment lies entirely on Carboniferous rocks of Millstone Grit and Coal Measures, with the former predominating in the high moorland areas. The river and its tributaries flow through steep and relatively narrow valleys. About 18% (26 km^2) of the area drains to reservoirs. Typically these are reservoirs for direct water supply, releasing only compensation flows unless spilling at times of flood. The natural flow regime has also been modified by various channel improvements and flood defences, including those at Todmorden and Mytholmroyd.

2.2 River network and forecast points

This project is concerned with river level forecasts at four locations within the Upper Calder, each corresponding to an established or recently-installed river gauging station (see Section 2.6). These locations are shown in Figure 2.1 in relation to the river network, the boundaries of their drainage areas, and the telemetry raingauges in the vicinity.

2.3 Drainage areas and reservoirs

To support detailed hydrological modelling and analysis of relative runoff contributions, the Upper Calder was divided into 10 non-overlapping contributing areas, of which the 6 labelled in Figure 2.2 show the reservoir drainage areas and the remainder show the naturally draining areas.

Table 2.1 gives the overall and natural drainage areas for each of the forecast locations, also identifying which reservoirs are contained in each subcatchment. Note that the CEH Digital Terrain Model has been updated since the original drainage areas were calculated at the time of the Calder 1997 Study. This accounts for the increased drainage area to the Gorple reservoir.

Table 2.1 Catchment, reservoir and natural drainage areas

Catchment (total area)	Reservoir (reservoir catchment area, km^2)						Natural drainage area
	Widdop (3.50)	Gorple (7.23)	Gorpley (2.86)	Walshaw Dean (9.59)	Ramsden Clough (1.93)	Warland (1.25)	
Walsden Water at Walsden (13.61)					✓	✓	10.43
Calder at Todmorden (19.59)							19.59
Hebden Water at Nutclough (56.24)	✓	✓		✓			35.92
Calder at Mytholmroyd (147.03)	✓	✓	✓	✓	✓	✓	120.67

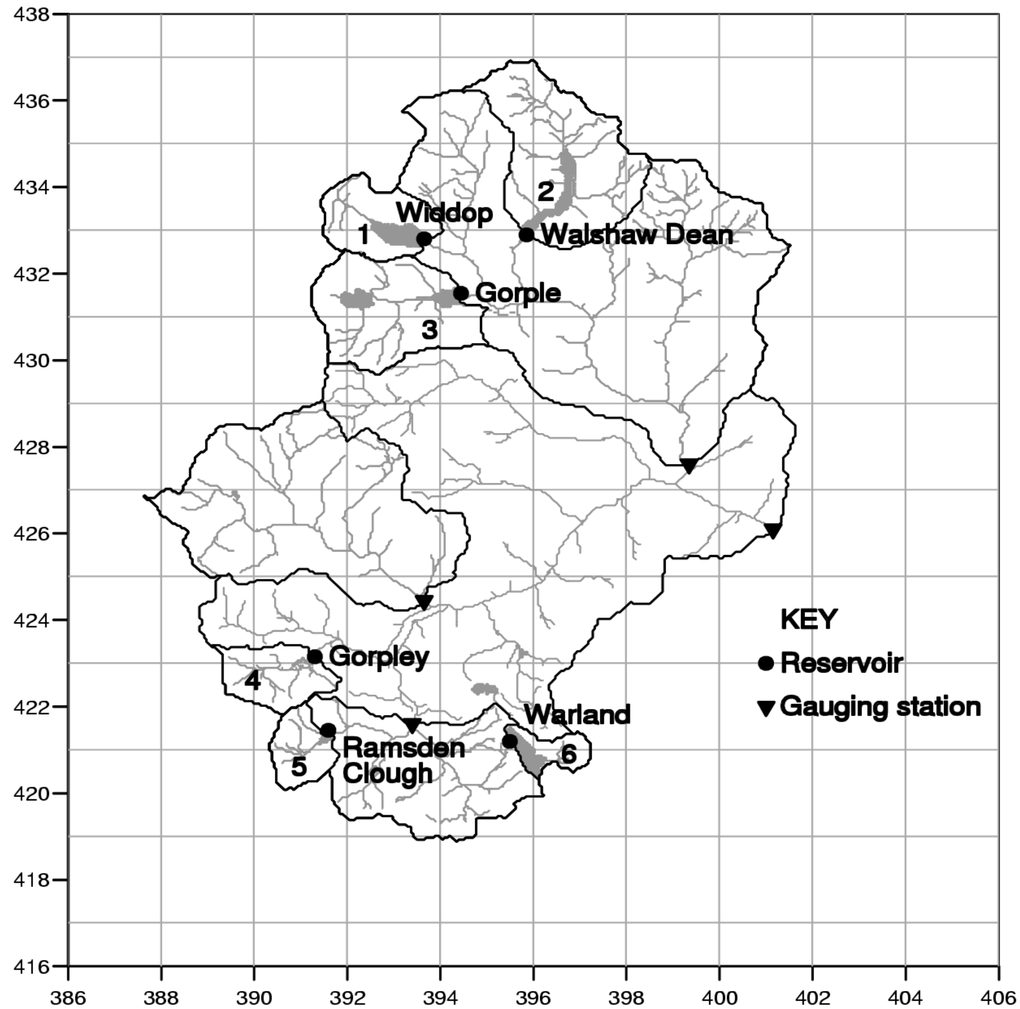

Figure 2.2 Reservoir drainage areas (1-6) and naturally draining areas (others). Overlaid is the grid used for the 2km radar data.

Table 2.2 Telemetry raingauges

Raingauge	Grid Ref.	Altitude (m)	SAAR
Bacup	SD 872 247	307	1398
Gorple	SD 945 312	306	1400
Thornton Moor	SE 050 335	371	1204
Blackstone Edge	SD 968 179	372	1300

2.4 Raingauges

Figure 2.1 shows the locations of the four telemetry tipping-bucket raingauges in and around the Upper Calder. The raingauges at Bacup and Blackstone Edge are operated by the Agency's Northwest Region, but telemetry links to Northeast Region are provided. These raingauges are used to provide 15 minute rainfall accumulations for forecasting purposes. Potential problems with raingauge measurements are well known and can be affected by any of the factors set down below.

- Instrument design
- Prevailing weather conditions, e.g. local wind, freezing temperatures, precipitation other than rain
- The situation of the gauge including the height above ground
- Heavy rainfall causing splashing (in or out) and losses whilst tipping
- Time sampling of the measurements.

Table 2.2 gives details of the telemetry raingauge sites.

2.5 Weather Radar

The Upper Calder is primarily served by the network weather radar at Hameldon Hill (SD 811 487), and lies between radii of 6km and 21km. The radar emits pulses of electromagnetic waves at various beam elevations. As these waves propagate through the atmosphere they interact with raindrops, snowflakes and hail. The power of the back scattered energy from this interaction and the time taken for the return signal to reach the radar can be used to infer rain rates and distances of objects respectively. The estimation of the rain rate can be subject to considerable uncertainty. The main factors which can affect the accuracy of these inferred rain rates are represented schematically in Figure 2.3 and set down with reference to the figure labels below.

- Overshooting of precipitation by the beam at long ranges (1)
- Low level evaporation occurring below the beam (2)
- Low level orographic based effects (3)
- Enhanced reflectivity or 'bright band' caused by the beam intersecting the melting layer (4)
- Underestimation of drizzle intensity due to the lack of large droplets (5)
- Strong temperature and moisture gradients at low levels can cause the beam to bend towards the ground causing an anomalous return of precipitation called 'anaprop' (6)
- Other anomalous echoes of ground clutter
- Occultation of the beam(s) due to topography

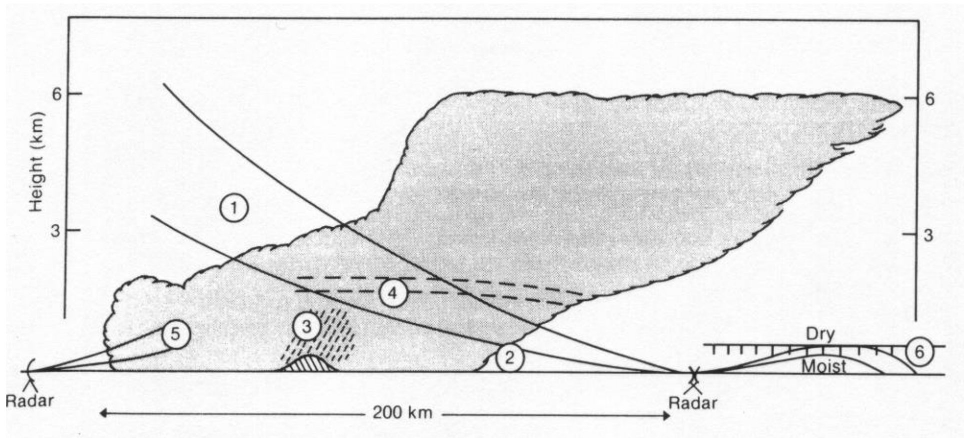

Figure 2.3 A schematic representation of the problem areas associated with the measurement of precipitation by radar (after Collier, 1989)

Point (1) is of little importance in this study due to the proximity of the radar to the catchment. However the other problems highlighted are all relevant.

The radar data are corrected and processed by Nimrod to produce analyses (of the current weather state) and short-range forecasts (nowcasts) of key surface weather variables, including rain rates. The correction procedure includes adjustment of the radar data using raingauge measurements and suppression of "bright band" effects. The mean field bias correction of radar data using raingauge data historically occurred on a weekly basis. However since 2002, the method employed is based on the NEXRAD system developed in the USA which performs the correction when suitable raingauge data are available (typically this is more frequent than weekly).

The Nimrod products used in this study are summarised in Table 2.3. The grids used for the 2km and 5km spatial resolution are shown in Figures 2.1 and 2.2 respectively. Note that whilst the product details are correct for the period studied (1997-2002), some have been updated since. For example, the Nimrod 5km analysis product is now available every 5 minutes rather than 15.

The Centre for Ecology & Hydrology's Hyrad software is used in this project to calculate catchment average rainfall totals over a given time interval (here 15 minutes from the Nimrod rain-rates). It is the 15 minute catchment average rainfall totals that are needed for rainfall-runoff modelling purposes.

Table 2.3 Details of Nimrod products used in this study

Product description	Resolution	Reference name	Delivery Frequency	Forecast time step
Single site radar, Nimrod quality controlled	5km	Nimrod 5km analysis	15	-
Single site radar, Nimrod quality controlled	2km	Nimrod 2km analysis	5	-
Radar composite, Nimrod Quality controlled	5km	Nimrod 5km radar composite analysis	15	-
Nimrod rain-rate analysis (single site radar with infill from NWP, satellite and synoptic gauge reports)	5km	Nimrod 5km rain-rate analysis	15	-
Nimrod rain-rate forecast	5km	Nimrod 5km forecast	30	Intervals of 15 mins up to 6hrs

Table 2.4 River gauging stations

Station	Grid Ref.	Total Catchment		Naturally Draining	
		Area (km^2)	SAAR (mm)	Area (km^2)	SAAR (mm)
Walsden Water at Walsden	SD 934 216	13.61	1387	10.43	1366
Calder at Todmorden	SD 937 244	19.59	1390	19.59	1390
Hebden Water at Nutclough	SD 993 276	56.24	1376	35.92	1365
Calder at Mytholmroyd	SE 012 260	147.03	1365	120.67	1354

2.6 River Gauging Stations

Each of the four forecast locations has a river gauging station providing measurements of river level. The gauging stations at Mytholmroyd and Todmorden on the River Calder also provide measurements of river flow via multi-path ultrasonic gauges. Only river level data have been used in this study since there are problems with the flow estimates at Mytholmroyd and the flow gauge at Todmorden was only recently installed during December 2000. Rating equations have been provided by the Environment Agency for all stations, including the newest station at Nutclough (on the Hebden Water tributary to the Calder) which was installed during the summer of 2000. The details of the forecast points are given in Table 2.4.

3 DATA AVAILABILITY AND QUALITY

The availability and quality of data used to support the project are considered in this section. First, the Digital Terrain Model (DTM) used to derive the characteristics of the study catchments, presented in Section 2, is outlined. Then the availability of each type of data and the quality control procedures used to assess them are discussed. This information is used as background in selecting events for the model calibration and assessment.

3.1 Digital terrain model

The Centre for Ecology & Hydrology's Integrated Hydrological Digital Terrain Model (IHDTM) and the digitised Standard Average Annual Rainfall (SAAR) dataset were used to derive many of the catchment characteristics described in Section 2. The IHDTM is updated occasionally when improved elevation or river network data or improved DTM procedures become available. As stated earlier, use of a version of the IHDTM updated since the Calder 1997 Study accounts for the change in the reservoir drainage area for the Gorple reservoir.

The IHDTM comprises a grid, with a spacing of 50 m, covering most of the UK. For each grid cell, the following data are available:

- Altitude (held to a precision of 0.1m)
- Cumulative catchment area to cell
- Inflow directions
- Outflow direction
- Surface classification (land, sea, river, lake)

SAAR data for the standard period 1941-1970 are held on a grid with a 1 km spacing.

3.2 Raingauge data

The Environment Agency provided the rainfall data from their telemetry tipping-bucket raingauge network. These data were inspected to identify any missing periods: these are listed in Table 3.1. To assess the quality of the available data, time-series of cumulative rainfall were plotted over blocks of three months for each raingauge. This allowed anomalously large rainfall values to be easily detected and removed. By comparing the cumulative plots for different raingauges, it is possible to identify suspect periods where a single gauge may be under- or over-estimating the rainfall or simply not recording rainfall at all (i.e. the data are zero rather than missing). These comparisons can also identify if any single gauge is *consistently* over- or under-estimating the rainfall. However, there is no evidence of this occurring in the available data. The cumulative rainfall plots for each selected event are presented in Appendix C, Figures C.1-10 (c), whilst an example exposing an anomaly is presented on Figure 3.1.

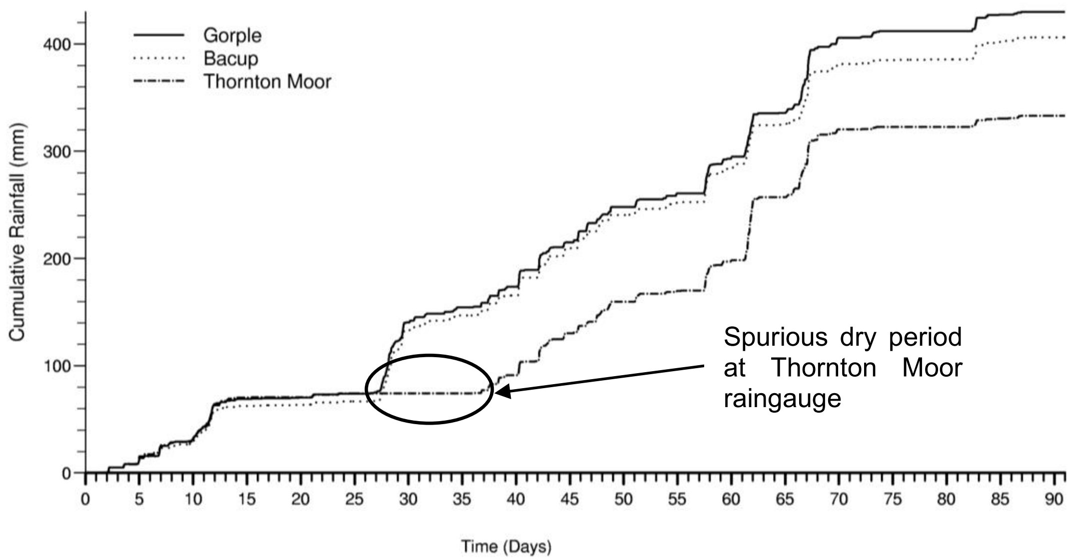

Figure 3.1 Cumulative rainfall of the available raingauges over the period January to March 2000 exposing a raingauge anomaly

Table 3.1 summarises the availability and quality of the rainfall data from the telemetry raingauges. Note that the Blackstone Edge raingauge is relatively new with data only available since 1 February 2001. Since the date of installation falls within the period of study, this has certain implications for the method of model calibration; this is explained later.

Gorple raingauge data

There is a Met Office daily raingauge at Gorple, sited adjacent to the telemetry raingauge, which was found to be reliable in the Calder 1997 Study. Investigations revealed that from 1994 to 1995 the daily totals from the Gorple telemetry raingauge were around 50% of the readings from the daily gauge. This was accommodated in the RFFS operational model network configuration by introducing a weighting factor of 1.5 for the Gorple raingauge data. However, for several flood events between 1998 and 2000 comparisons between the daily and telemetry raingauges, performed by the Environment Agency, show no evidence of the telemetry raingauge under-recording. This suggests that the telemetry raingauge is now recording reliably and a weighting factor is no longer required. Examination of the cumulative rainfall plots for all raingauges also supports this view (see Figure 3.1 and Figures C.1-10 (c)).

Table 3.1 Availability and quality of recent raingauge data

Raingauge	Period	Comments
Bacup	26 Apr 1994 – 1 Jan 2003	Small periods of missing data (about one day's worth) in May 1995, Oct and Nov 2001. Three large values (180mm +) in the period Aug to Nov 1995 removed.
Gorple	1 Sep 1996 – 1 Jan 2003	No evidence of underestimation. No data for the period 2 Aug to 1 Sep 1999.
Thornton Moor	7 Jul 1997 – 1 Jan 2003	Week long periods of missing data in Jul and Aug 1997. Small periods of missing data (about one day's worth) in Oct and Dec 1997 and Feb 1998. Spurious dry period 28 Jan to 6 Feb 2000. No data for the period 30 Apr to 17 May 2001. 3 days of missing data in May 2002.
Blackstone Edge	1 Feb 2001 – 1 Jan 2003	Raingauge only operational from 1 Feb 2001. No data for the period 3 Aug to 30 Aug 2001. Missing day in Dec 2001.

3.3 Radar data

As mentioned in Section 2.5, the Nimrod system processes radar data to produce analyses (of the current weather state) or very short-term (up to 6 hour) forecasts of the surface rain-rate on a 2km or 5km grid. The Hyrad software can then be used to produce catchment-average rainfall accumulations over 15 minute periods from these rain-rates. Currently the Environment Agency only have access to catchment boundaries that *include* the reservoir drainage areas. As highlighted in Section 2.3, the naturally draining area is appropriate for reservoir-dominated catchments. The naturally draining catchment boundaries that *exclude* the reservoir drainage areas have been derived using the IHDTM and are available to the Agency as an output of this study.

Suitable events for model calibration and assessment were selected at project inception, along with which Nimrod products to use, in order to avoid retrieving and storing large periods of radar data from the Met Office archive. Calibration events (event numbers 1-6) were selected from the period 1997-2002 whilst assessment events (event numbers 7-11) were selected from the year 2002. It is important that the calibration and assessment events do not overlap (in time) to ensure an objective evaluation of the performance of the calibrated models.

The Nimrod 5km analysis for the Hameldon Hill radar was used as the basic radar product type for use in model calibration and assessment. In addition, the Nimrod 2km analysis and the Nimrod 5km 1-hour lead-time forecast products were used over the assessment periods to evaluate the sensitivity of the PDM models to different radar products. A lead-time of 1 hour was selected as not too long to still be of relevance to forecasting short-lived convective events whilst a shorter lead-time would not differ significantly enough from the 5km Nimrod analysis.

When considering the radar data one must appreciate that radar technology is constantly evolving. The most significant recent development is the new Met Office radar control and data processing software package called "Cyclops". This has been installed across the radar network and has been in use at Hameldon Hill since September 2000. This brought the following improvements:

- Increase of the 5km radar data range from 210km to 250km
- Increase of the 2km radar data range from 75km to 100km
- Introduction of 1km radar data with a range of 50km
- Faster data processing
- Transfer of polar data direct to Bracknell allowing centralised processing

Radar hardware is also upgraded or replaced on occasions. Notably, the magnetron at Hameldon Hill was upgraded to the co-axial type in August 2001. Both the software and hardware upgrades have taken place during the period of study and must be taken into account when comparing radar data from different points in time. Another important factor to consider is the infill maps used. For the Hameldon Hill radar, a higher beam (Beam 1, 1.5 degree) is used out to a range of 25 km to infill the surface beam (Beam 0, 0.5 degree). Discontinuities in the resulting Nimrod analysis should not usually be noticeable but can be if brightband is present and not perfectly corrected for (an example is presented in Figure 3.7). Crucially, the study catchments lie within a 25 km range of the radar and so the higher beam is used for rainfall estimation.

Originally the Nimrod 5km analysis was to be provided by the Met Office for *all* events and the Nimrod 2km analysis and 5km 1-hour lead-time forecast were to be retrieved from the CEH archive. However, during the relocation to Exeter, some Met Office radar data (for 2002) were irretrievably lost. Therefore pre-2001 radar data were provided by the Met Office and post-2001 radar data were retrieved from the CEH archive. The retrieval, availability and quality of the two sources of data used in this study are considered separately in the following sections.

3.3.1 Pre-2001 Met Office retrieved radar data

The 5km Nimrod analysis data pre-2001 (events 1-5) were retrieved by the Met Office and a quality control procedure applied. Instances of missing data were identified and data outside of realistic meteorological bounds removed. These periods of absent data

Table 3.2 Availability of the infilled 5km Nimrod analysis (pre-2001) provided by the Met Office

Event	Period	Missing Data	Comments
1	00:00 8 Jan 1997 - 00:00 15 Feb 1997	8 Jan 00:00 – 9 Jan 10:00 9 Jan 10:45 - 13:30 20 Jan 14:00 22 Jan 19:00	Very large rain rates over catchment for the period 04:15-05:15 22 Jan 1997 see Figure C.1 (a)
2	00:00 19 Sep 1998 - 00:00 27 Oct 1998	24 Sep 04:15 -10:00 9 Oct 13:45	Visual check of radar shows rain disappearing between images during 15, 24 and 26 Oct
3	00:00 11 Dec 1998.- 00:00 18 Jan 1999	25 Dec 23:45	
4	00:00 29 Mar 2000.- 00:00 5 Jun 2000	None	
5	00:00 15 Aug 2000.- 00:00 3 Nov 2000	23 Aug 22:15 - 24 Aug 10:00 1 Oct 23:15 2 Oct 07:15 16 Oct 14:45, 15:15 28 Oct 22:15 –30 Oct 22:00	The Cyclops upgrade to the radar processing software took place during the event in Sep 2000. After the upgrade, spurious circular bands occasionally appear in the data but do not affect the Upper Calder catchment area. Significant periods of data missing near the start and end of the event period.

were then infilled by two other Nimrod products, depending on availability, in the following order of preference:

1. Nimrod 5km rain-rate analysis
2. Nimrod 5km composite radar analysis

Table 3.2 lists the periods when no alternative data were available. This has restricted some of the proposed calibration event periods. A list of actual event periods used for calibration is presented in Table 3.6. The Met Office also visually checked the radar data for potentially unrealistic precipitation: the resulting comments are presented in Table 3.2.

3.3.2 Post-2001 CEH retrieved radar data

The Nimrod 5km analysis data for the single calibration event and four assessment events in 2002 (events 6-10) were retrieved from the CEH archive. Nimrod 2km analysis and Nimrod 5km 1-hour lead-time forecast products were also retrieved from the archive for the assessment events. Instances of missing data were identified and are listed in Table 3.3. This reveals that there were not many instances of missing data (although there were more Nimrod 2km analysis data missing due to this products more frequent delivery time) and most consisted of only one or two radar images. These periods of absent data for each radar product type were then infilled in the following order of preference:

Nimrod 5km analysis:

(1) If a single image is missing use an average of the neighbouring images
(2) 2km Nimrod analysis
(3) 5km raw data

Nimrod 2km analysis:

(1) If a single image is missing use an average of the neighbouring images
(2) Use the completed 5km dataset

Nimrod 5km 1-hour lead-time forecast:

(1) Use the completed 5km dataset

All three radar product types were entirely infilled by the above method apart from one day during Event 11. The details are presented in Table 3.3, including a comment on the rain over the catchment under the indicative categories none, slight or rain. Although the infill method for the Nimrod 5km analysis product differs between the Met Office retrieved data and the CEH retrieved data, it is a minor point since very few images are actually absent in the CEH archive.

Table 3.3 Details of the infilled radar data (post-2001) retrieved from the CEH archive
(a) Nimrod 5km analysis

Event	Period	Missing Images	Rain?	Infill Method
6	00:00 1 Nov 2002 – 00:00 12 Nov 2002	5 Nov 17:15 5 Nov 22:15,23:15	None Slight	(1) (1)
7	00:00 10 Jun 2002 – 12:00 11 Jun 2002	10 Jun 10:15-10:45	Rain	(3)
8	00:00 9 Aug 2002 – 00:00 11 Aug 2002	None		
9	12:00 9 Sep 2002 – 00:00 11 Sep 2002	10 Sep 15:15-15:45	None	None
10	12:00 20 Oct 2002 – 00:00 29 Oct 2002	27 Oct 20:45,21:15 27 Oct 21:45	Slight Slight	(1) (1)
11	00:00 16 Jan 2002 – 00:00 17 Feb 2002	18 Jan 02:00-02:30 20 Jan 19:15-20:00 25 Jan 00:00-23:45 28 Jan 13:00-16:30 28 Jan 17:15 2 Feb 17:00 2 Feb 18:00-19:00 2 Feb 20:00, 21:00 2 Feb 22:00, 23:00 3 Feb 00:00, 01:00 3 Feb 02:00	None None Rain Slight Rain None None None None None None	None None None* (2) (2) (1) None (1) (1) (1) (1)

** No infill data available*

(b) Nimrod 2km analysis

Event	Period	Missing Images	Rain?	Infill Method
7	00:00 10 Jun 2002 – 12:00 11 Jun 2002	10 Jun 10:05-10:45 11 Jun 09:50-10:30 11 Jun 11:00	Rain Rain Slight	(2) (2) (1)
8	00:00 9 Aug 2002 – 00:00 11 Aug 2002	None		
9	12:00 9 Sep 2002 – 00:00 11 Sep 2002	8 Sep 17:30,21:20 9 Sep 10:20,14:35 10 Sep 00:35	None Rain Rain	(1) (1) (1)
10	12:00 20 Oct 2002 – 00:00 29 Oct 2002	21 Oct 01:15 25 Oct 08:25-10:20 25 Oct 11:10 27 Oct 20:50,21:40 27 Oct 21:50-22:00 27 Oct 23:55 28 Oct 03:20,09:40	Rain Rain None Slight Slight Slight None	(1) (2) (1) (1) (2) (1) (1)
11†	00:00 16 Jan 2002 – 00:00 17 Feb 2002	25 Jan 00:00-23:45 2 Feb 22:45-23:05	Rain Rain	None* (2)

** No infill data available*
† Other images were missing (too many to list) and were infilled by method (1)

(c) Nimrod 5km 1-hour lead-time forecast

Event	Period	Missing Images	Rain?	Infill Method
7	00:00 10 Jun 2002 – 12:00 11 Jun 2002	10 Jun 11:30-11:45 10 Jun 12:30-12:45	Rain Rain	(1) (1)
8	00:00 9 Aug 2002 – 00:00 11 Aug 2002	None		
9	12:00 9 Sep 2002 – 00:00 11 Sep 2002	None		
10	12:00 20 Oct 2002 – 00:00 29 Oct 2002	25 Oct 09:30-11:15 25 Oct 12:00-12:15 27 Oct 22:00-22:45 27 Oct 23:15 28 Oct 01:30-01:45	Rain Slight Slight Slight Rain	(1) (1) (1) (1) (1)
11	00:00 16 Jan 2002 – 00:00 17 Feb 2002	25 Jan 00:00-23:45 26 Jan 00:00 28 Jan 14:00-15:15 28 Jan 18:00-18:15 1 Feb 06:30-06:45 5 Feb 06:45	Rain None None Rain None None	None* None None (1) None None

** No infill data available*

3.3.3 Further analysis of radar data

Beyond simply noting missing radar images and infilling the absent periods, several other forms of analysis were also performed. The main focus was on the Nimrod 5km analysis, as this is the dataset used for model calibration, although the Nimrod 2km analysis dataset was also used. The Nimrod forecast dataset has not been quality-controlled in detail, other than identifying and infilling missing images, since it is only used in the sensitivity analysis.

Hyrad was used to calculate and map cumulative rainfall accumulations for the 5km grid squares (and the 2km grid squares for the assessment events) covering the Upper Calder catchment. Such maps allow the spatial variability of rainfall over the study catchments to be examined as well as the identification of any suspect behaviour related to the radar. These have been calculated for all events and are presented in Appendix B. To further highlight the spatial variability from catchment to catchment, Hyrad was used to produce cumulative time-series of catchment-average rainfall accumulations for each study catchment: these are presented in Figures C.1-10 (a).

Comparison of the Nimrod 5km (and 2km for 2002) products with the raingauge data was achieved by using Hyrad to produce time-series plots of radar rainfall accumulations for the radar grid-square coincident with a given raingauge. Examples are shown in Appendix C for the Gorple and Bacup raingauges. Of course, it is not expected that the radar accumulations and the raingauge accumulations will be exactly the same, especially during convective events which operate on small length scales. However, these comparisons can still be informative. Some examples of the findings resulting from this further analysis are given below. These relate to events 4, 5, 7 and 10 which are discussed in turn.

Event 4

Figure 3.2 shows the rainfall accumulation for Event 4 over 69 days during spring/summer 2000. The orographic signature of the mid and southern Pennines is evident but the rainfall over this period is generally more evenly distributed. The rainfall near the radar site is clearly being over-estimated (see the light blue squares surrounding the radar site) with the grid-square covering Hameldon Hill accumulating 104cm of rainfall which is obviously wrong. The variability over the Upper Calder catchment is highlighted in the magnified image with the southern part accumulating more rain. However, for this event, the area of over-estimation near the radar appears to affect the grid-square coincident with the Bacup raingauge (the magenta grid square to the southwest of the Upper Calder catchment) which encompasses a small part of the catchment. Indeed, the comparison of the Nimrod 5km accumulations with those for the Gorple and Bacup raingauges (see Figure 3.3) confirms that the grid-square coincident with the Bacup raingauge over-estimates badly during days 13-16 of Event 4, whereas the grid-square coincident with the Gorple raingauge only slightly over-estimates. This suggests that over the majority of the Upper Calder, other than the grid-square coincident with the Bacup raingauge, the radar is performing satisfactorily.

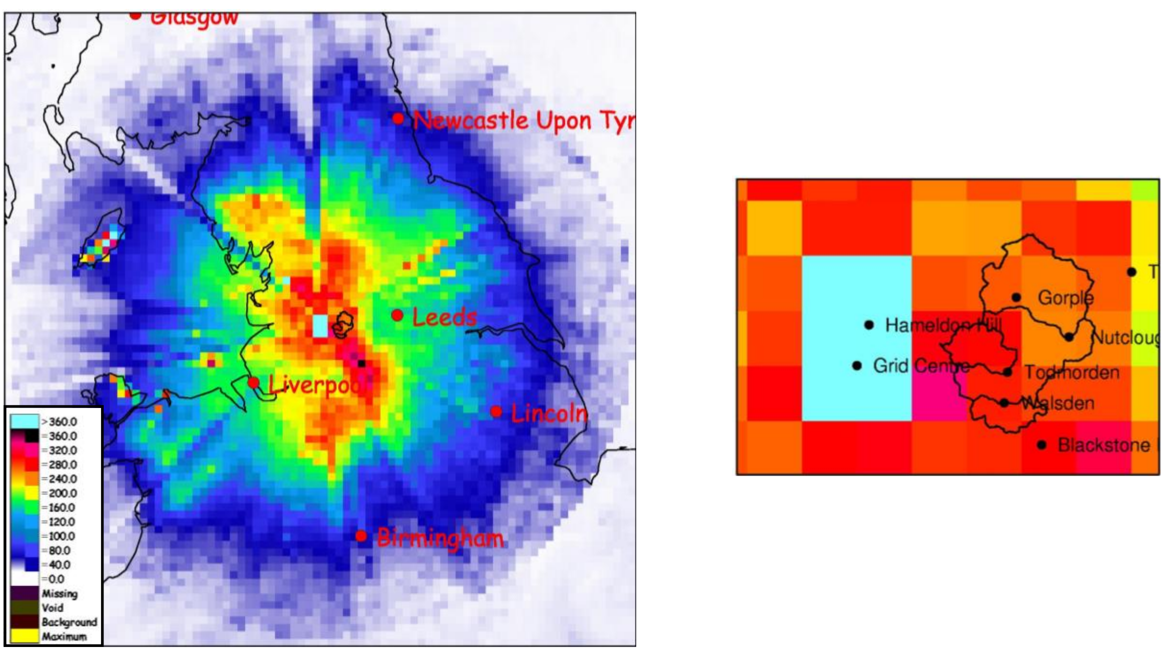

Figure 3.2 Rainfall accumulation using Nimrod 5km analysis for Event 4; 69 days to 6 June 2000

The tendency for the radar to overestimate rain in its immediate vicinity is evident in all events prior to the Cyclops upgrade (see the accumulation maps for events 2-4 in Appendix B). After the upgrade, there appears to be no significant over-estimation near the radar (see the accumulation maps for events 5-10 in Appendix B). These anomalous estimations prior to the upgrade are not fully explained but the most probable causes are nearby ground clutter, the relatively small pulse volume and the effect of the Fresnel region. The Fresnel region is the region where the electromagnetic waves are not planar (and so the approximations based on the wave being planar are not valid, e.g. Sauvageot (1992)). For a wavelength (λ) of 5cm and an antenna with a circular aperture (d) of 3.7m in diameter, the Fresnel region extends up to $2d^2/\lambda \approx 550$m.

(a) Gorple

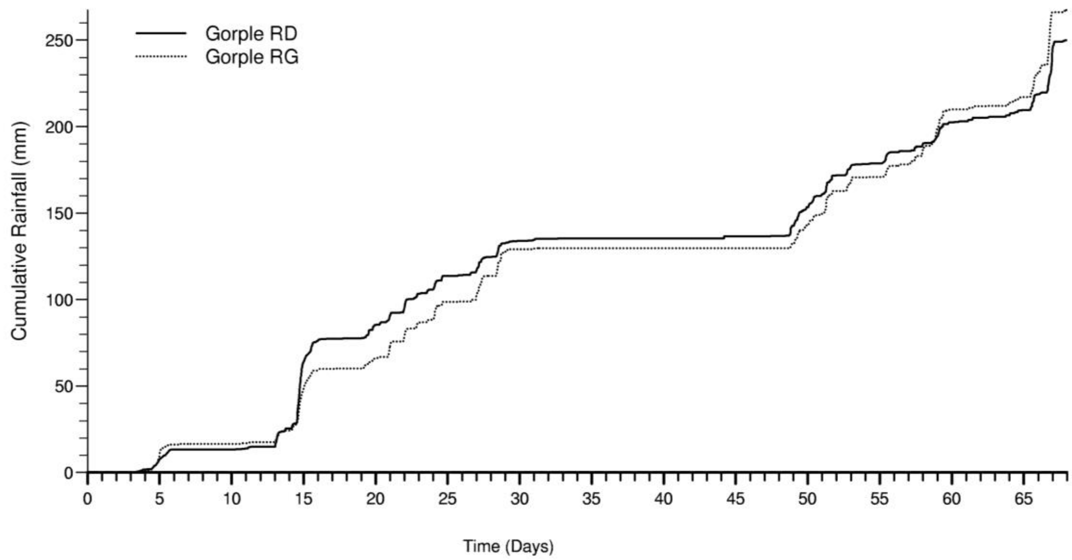

(b) Bacup

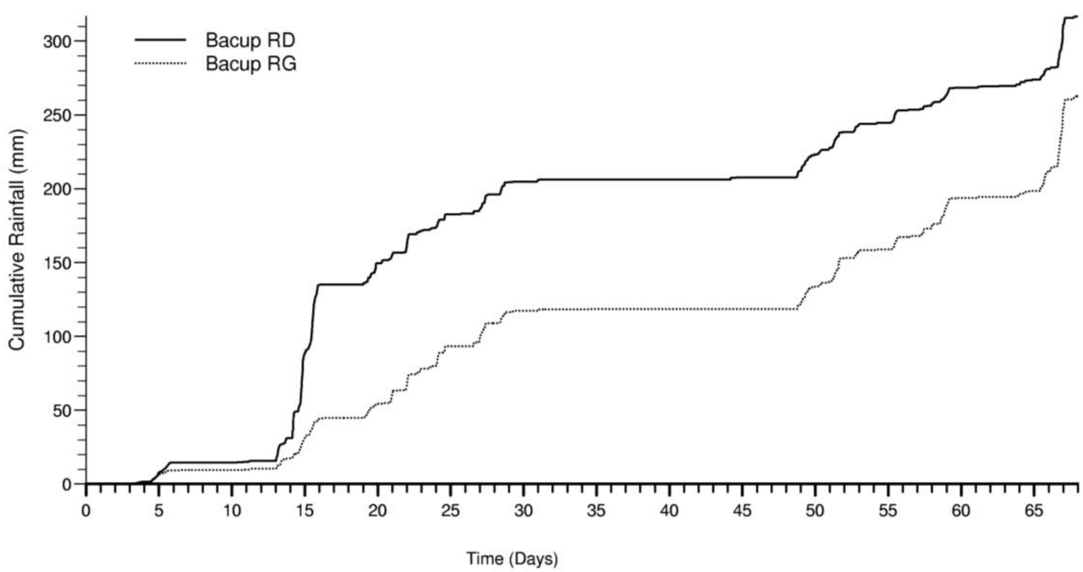

Figure 3.3 Cumulative rainfall plots for Event 4: 29 March to 5 June 2000. Comparison of a given raingauge (RG) with the 5km radar grid-square containing it (RD)

Event 5

Figure 3.4 shows the rainfall accumulation for Event 5 over 66 days during summer/autumn 2000 with orographically-enhanced rainfall over Snowdonia and the Pennines. The Cyclops upgrade to the processing software occurred on 1 September 2000 which is during the period of Event 5. There is no evidence of severe over-estimation near the radar with the rainfall accumulation in the grid-square over Hameldon Hill being a far more realistic 68cm. There is significant spatial variation of the rainfall over the Upper Calder: the west experienced most rain with 60cm in the grid-square west of centre whilst the least rain fell on the far eastern side of the catchment with only 45cm.

Examination of the cumulative map alone (Figure 3.4) suggests that the radar is performing satisfactorily before and after the upgrade. However, comparing the Nimrod 5km analysis with the Gorple and Bacup raingauges (see Figure 3.5) strongly suggests that the radar is significantly overestimating the rainfall immediately after the upgrade. Note that this general overestimation after the upgrade is not apparent in subsequent events (see events 6-10 in Appendix C).

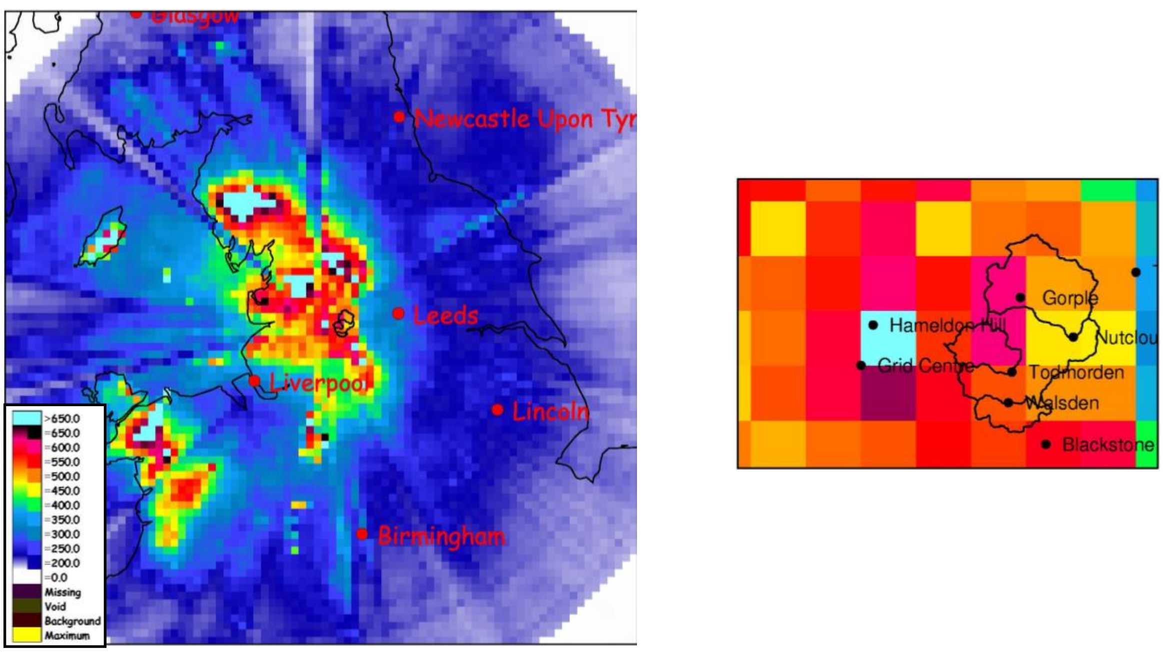

Figure 3.4 Rainfall accumulation using Nimrod 5km analysis for Event 5; 66 days to 28 October 2000

(a) Gorple

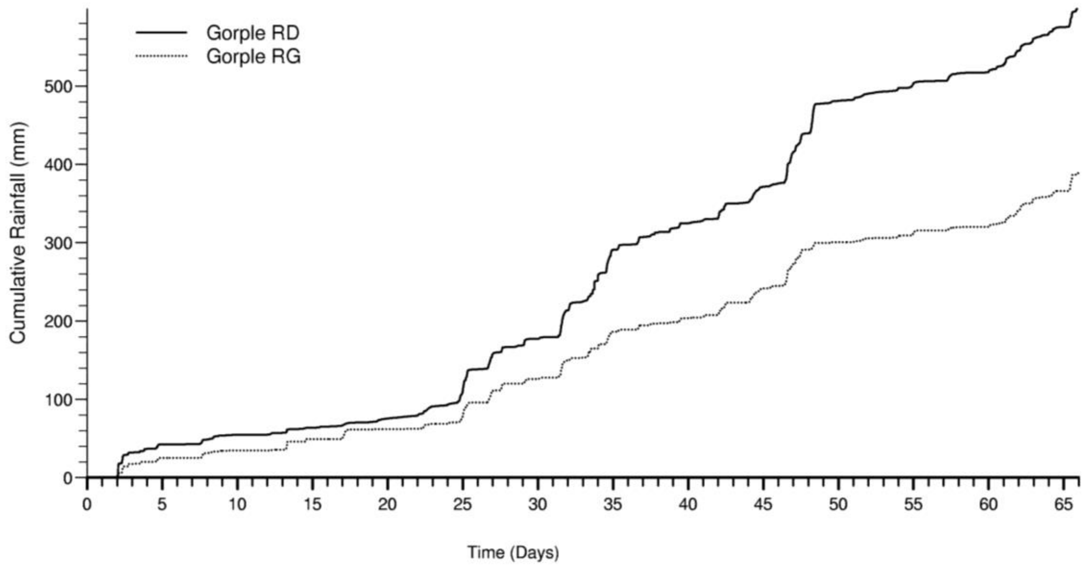

(b) Bacup

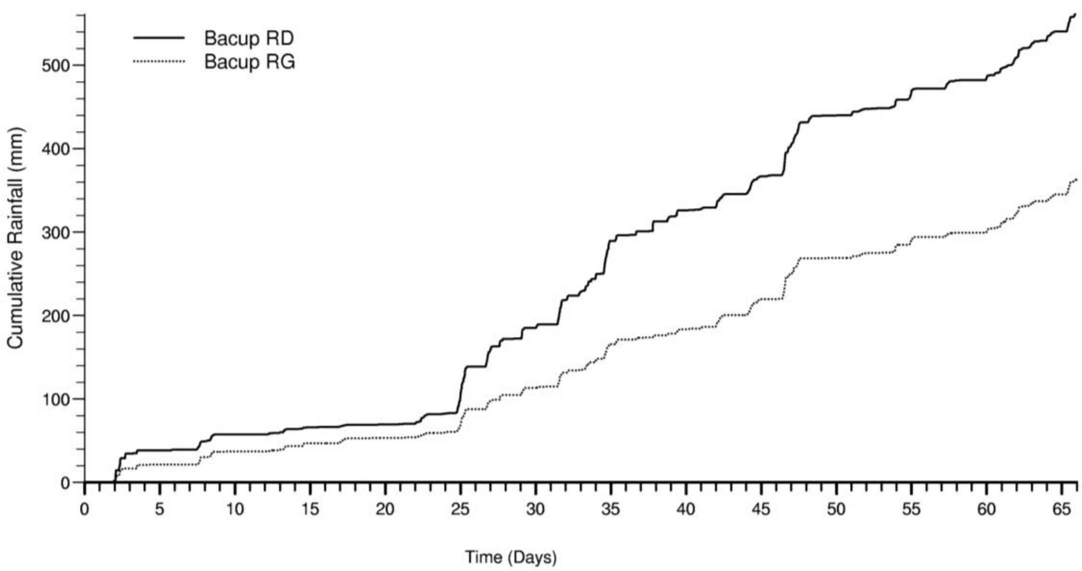

Figure 3.5 Cumulative rainfall plots for Event 5: 24 August to 29 October 2000. Comparison of a given raingauge (RG) with the 5km radar grid-square containing it (RD)

Event 7

Figure 3.6 shows the rainfall accumulations for Event 7 over 24 hours using both Nimrod 2km and 5km analysis products. This event is characterised by localised showers and, because the event is only a day in length, the traces of the heaviest showers are evident in Figure 3.6. Clearly there are some differences between the 2km and 5km accumulations. This is partly due to the fact that the Nimrod 2km analysis is available every five minutes (as opposed to every 15 minutes for the 5km analysis) and this is particularly significant for localised convection-driven rain. However, the 2km accumulations also show a discontinuity at a range of approximately 25km which is attributed to the infill map used (see earlier discussion). This also affects the 5km accumulations but the sharp discontinuity is not apparent because of the coarser resolution. This discontinuity was unnoticeable when viewing each individual radar image.

(a) Nimrod 5km analysis

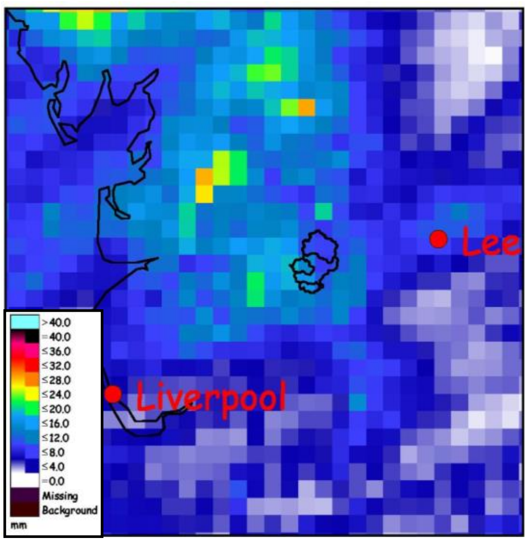

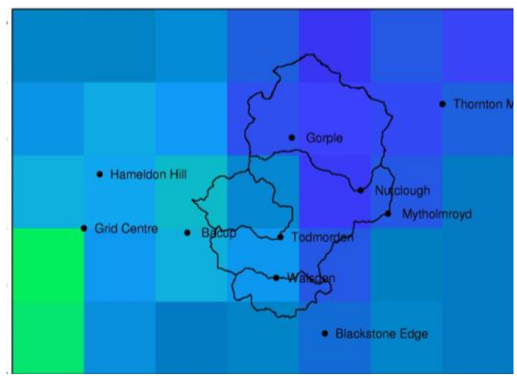

(b) Nimrod 2km analysis

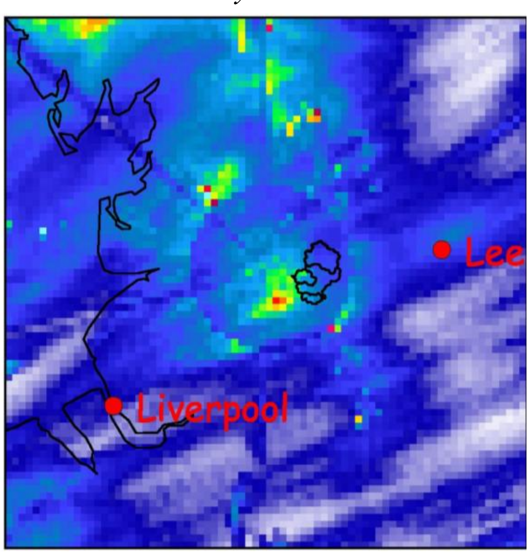

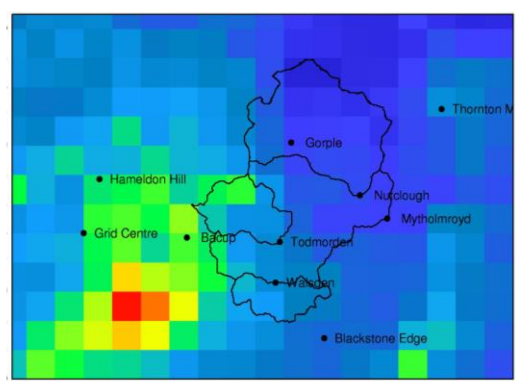

Figure 3.6 Rainfall accumulation using Nimrod 5km and 2km analysis products for Event 7; 24 hours to 00:00 11 June 2002.

Event 10

As discussed previously, the infill region should not normally be noticeable. This is found to be the case for the majority of the events considered. However, Event 7 and Event 10 are examples where the infill regions *are* noticeable and are most likely to have been caused by brightband effects not being perfectly corrected. An example of an individual radar image displaying this discontinuity is given in Figure 3.7. Nimrod 2km analysis and 2km raw data are both shown to emphasise that the discontinuity is not due to the Nimrod processing.

(a) 2 km raw (b) Nimrod 2 km

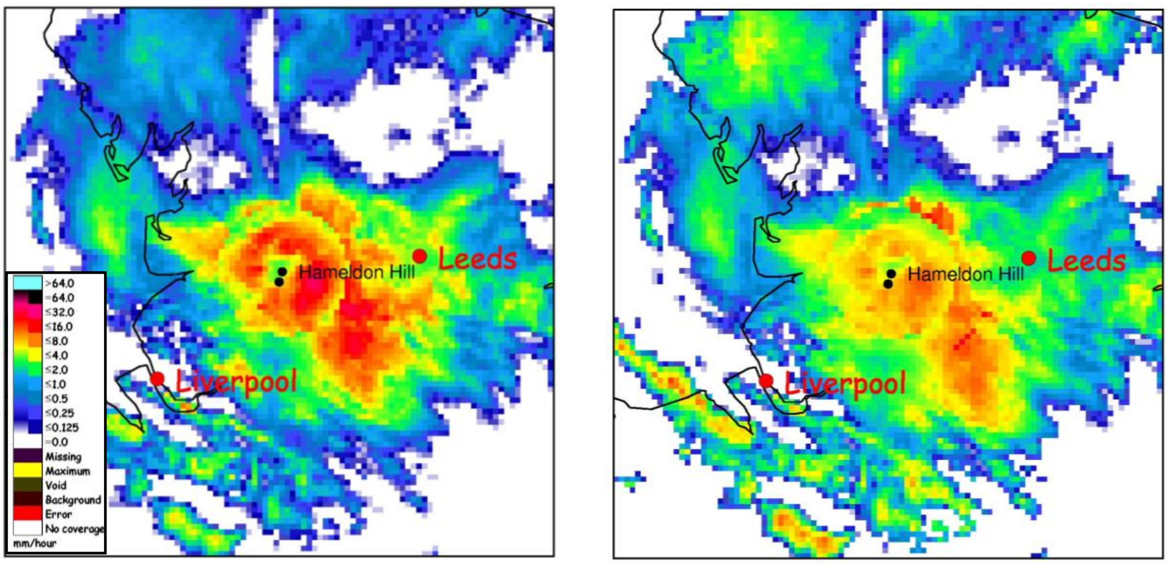

Figure 3.7 2 km raw and Nimrod 2 km data at 12:15 27 October 2002.

3.4 River level data

River level data for the four study catchments in the Upper Calder have been provided by the Environment Agency. A summary of the availability and quality of these data is given in Table 3.4. Examining the flow hydrographs allowed anomalous readings to be identified, examples of which are given below.

Table 3.4 Availability and quality of river level data

Station	Period	Comments
Calder at Mytholmroyd	19 Jul 1989 – 1 Jan 2003	Significant periods of missing data during May – Jul and Oct - Dec 2001 and Apr 2002. Small periods of missing data (< 1day) during Jun, Aug and Dec 2002 but not affecting event periods. Several anomalous stage values of either 1.999 or 2.499 removed during 2002 and affects Event 6. Anomalous oscillatory behaviour evident in Sep 2002 (affects Event 9).
Hebden Water at Nutclough	14 Aug 2000 – 1 Jan 2003	Only installed in Aug 2000. Significant missing data during Nov 2000 and Jun 2001. Anomalous oscillatory behaviour during Jan – Jun 2002, affects Event 7. Two anomalous peaks during 6 Nov 2002 affecting Event 6.
Calder at Todmorden	19 Aug 1996 – 1 Jan 2003	Data unreliable prior to 15 Feb 1997. Missing data Aug 2000, Sep 2000 (affecting Event 5), Aug 2002 and Sep 2002 (affects all of Event 9). Spurious large values removed in Sep 1999 and Jun 2001 and low values removed in Mar 2001 and Aug 2002.
Walsden Water at Walsden	17 Aug 1996 – 1 Jan 2003	Data unreliable prior to 4 Feb 1997. Only significant period of missing data is 4 days in Oct 2002. At lower stages there are frequent anomalous jumps in values.

Calder at Mytholmroyd

Figure 3.8 is a level hydrograph for the months of September and October 2002. The early part shows the oscillatory readings which affect Event 9 (the first peak in Figure 3.8). There is a jump in the stage which occurs near the start of October after which the oscillations fade away. Figure 3.8 presents an example of how the anomalously large river level values were easily identified from the level hydrographs.

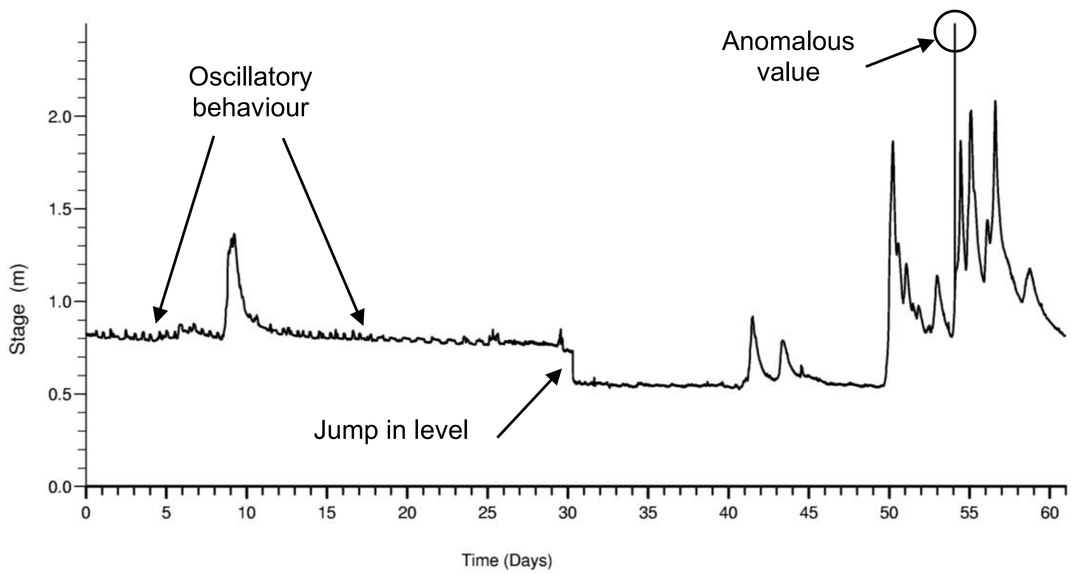

Figure 3.8 A level hydrograph for the Mytholmroyd station; 1 September to 31 October 2002.

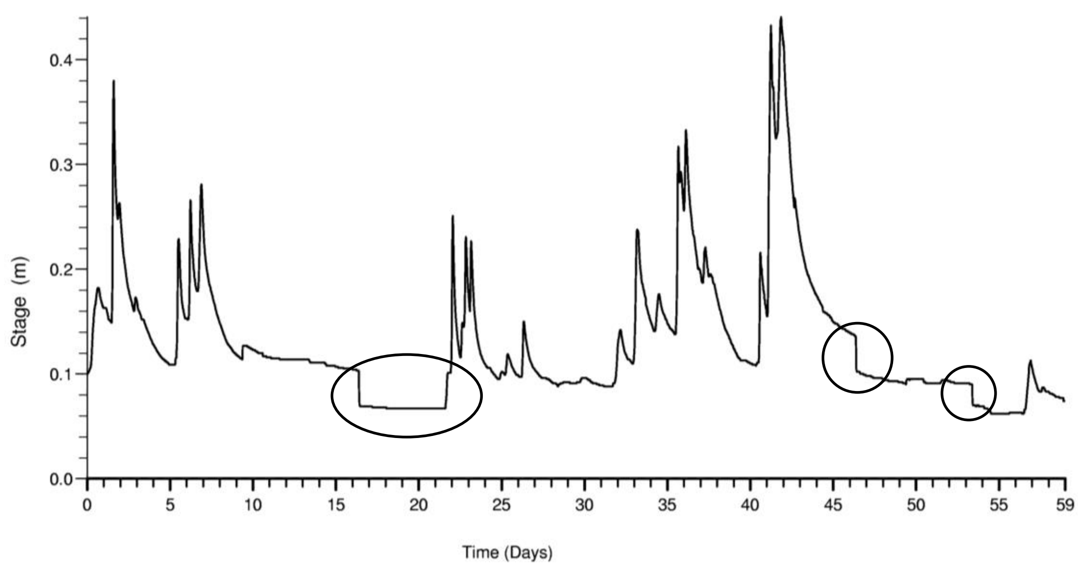

Figure 3.9 A level hydrograph for the Walsden station; 1 January to 25 February 2002. Unnatural jumps in the level have been circled.

Walsden Water at Walsden

As mentioned in Table 3.4, the Walsden stage reading appears to jump frequently at low levels. An example is given in Figure 3.9 depicting a level hydrograph for early 2002. This does not cover a particular event but highlights the problematic behaviour that can occur. As this only affects low levels the importance to model calibration is less.

Hebden Water at Nutclough

Figure 3.10 presents a level hydrograph for the period 1 May to 13 June 2002. This clearly shows the oscillatory behaviour, occuring with an almost daily frequency, and that this affects Event 7 (highlighted). The oscillatory behaviour disappears after this event. Figure 3.11 shows the two anomalous peaks which affect Event 6.

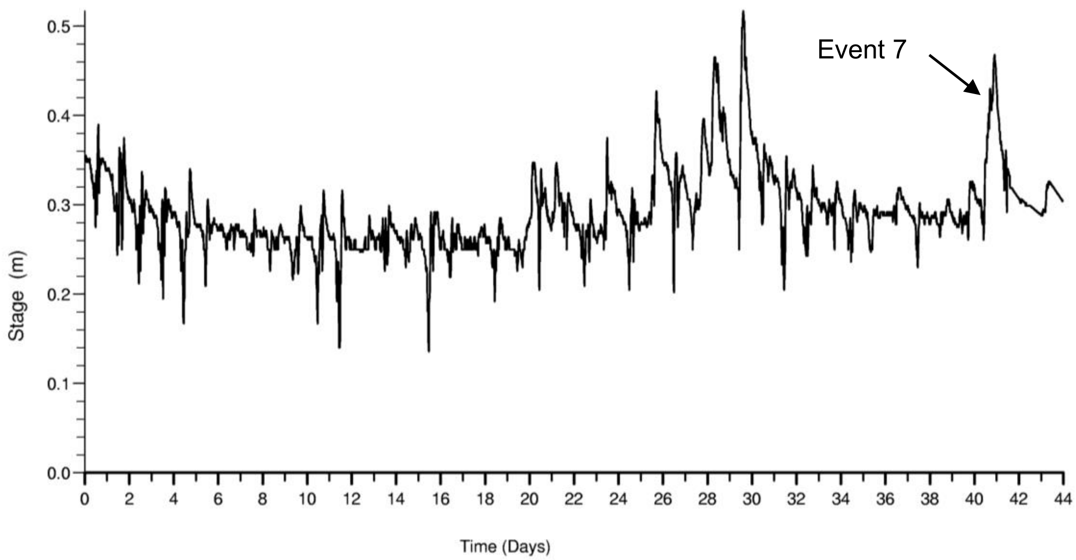

Figure 3.10 A level hydrograph for the Nutclough station; 1 May to 13 June 2002.

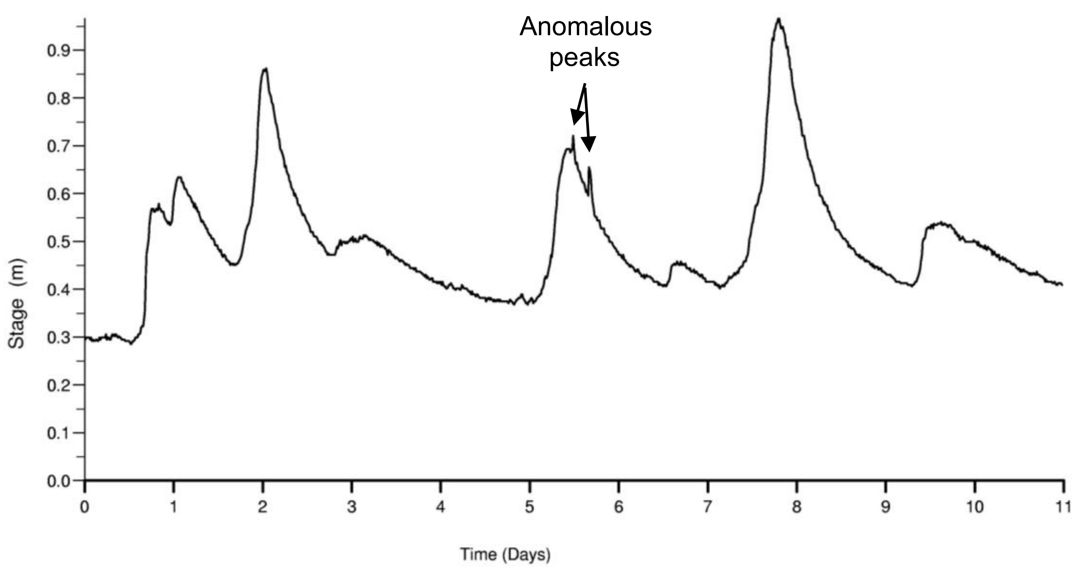

Figure 3.11 A level hydrograph for the Nutclough station covering Event 6: 1 to 12 November 2002.

Calder at Todmorden

Examining the level hydrograph for the Todmorden station over the period 12 September to 12 October 2002 (see Figure 3.12 (a)) identified a period of missing data around 25 September and a very large peak on 20 September. By comparing the level hydrograph for Todmorden to that for Mytholmroyd downstream (see Figure 3.12 (b)), it can be inferred that the large peak in the Todmorden record is an anomaly and should be discarded. This occurs during Event 5 and therefore a shorter event period, avoiding the anomaly, is used for the Todmorden catchment (see Table 3.6).

(a) Todmorden

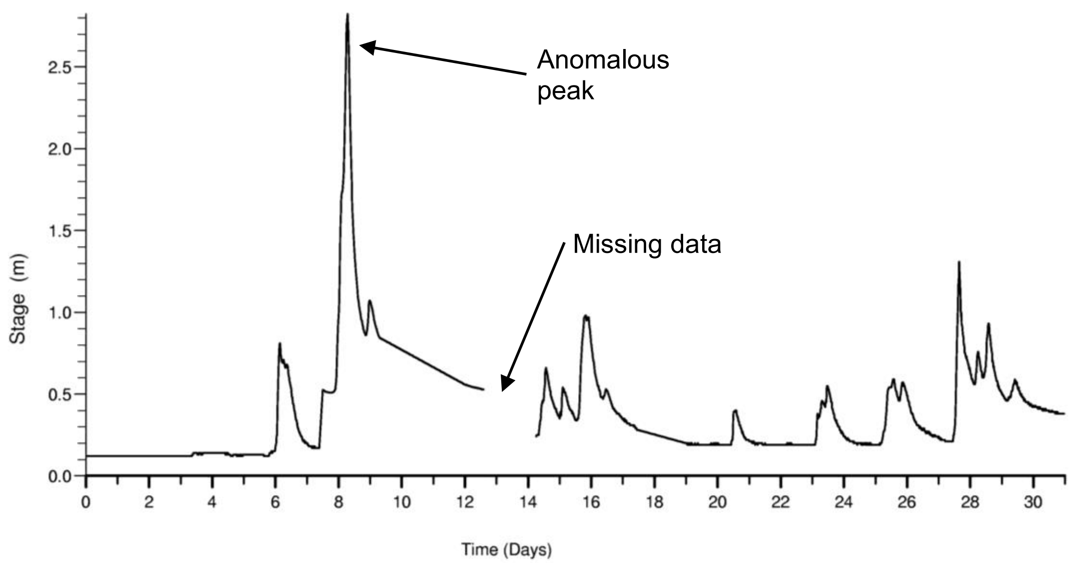

(b) Mytholmroyd

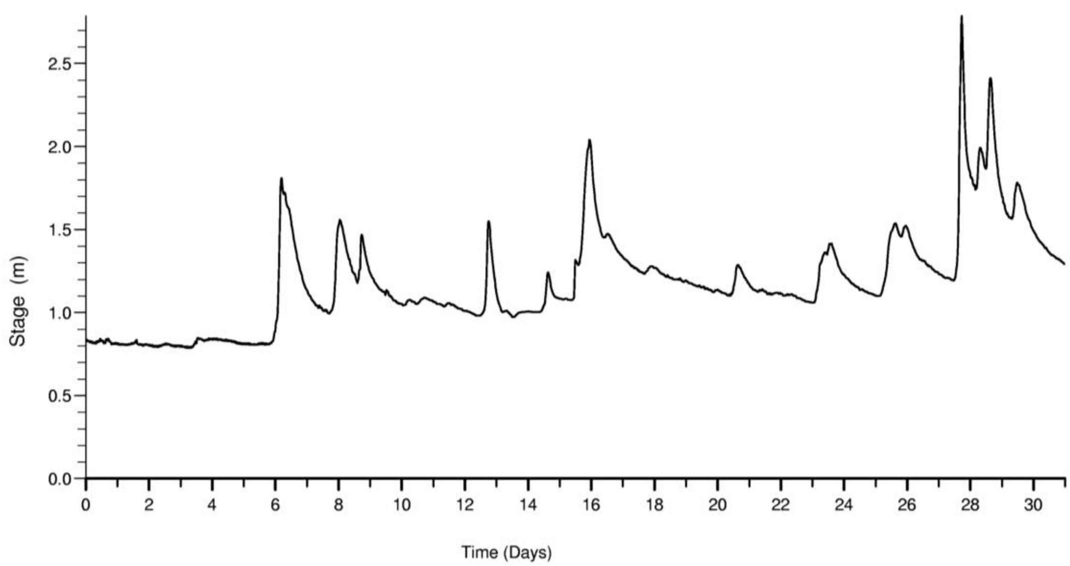

Figure 3.12 Level hydrographs for the period 12 September to 12 October 2000.

3.5 Rating curves

Details of the rating curves currently used by the Environment Agency are given in Table 3.5. The form of the rating equation is $Q = \alpha(h + d)^{\beta}$ for $h < h_T$, where Q is flow in.m^3s^{-1}, h is stage in m with h_T the threshold stage for validity, and α, d and β are parameters of the relation. Note that Mytholmroyd has a two-part relation. The rating curves for Mytholmroyd, Todmorden and Walsden are all well established. Although ultrasonic multi-path instruments are available at Mytholmroyd and Todmorden, only river level measurements and rating curves are used to derive flows for this study. The rating for Walsden has been derived via the joint calibration of the PDM model and rating curve over several events using the PDM model calibration software.

For the recently installed station at Nutclough, a rating curve has been derived by the Environment Agency. They found that initial attempts to derive the rating curve coefficients via the PDM calibration were unsuccessful. Unrealistic flow values were produced that were out of proportion with those for other stations in the Upper Calder. The rating curve coefficients were actually derived by comparing the level readings at Nutclough with the flow (from the ultrasonic gauge) readings at Mytholmroyd since the Calder to Mytholmroyd catchment encompasses the Hebden Water to Nutclough catchment. Deriving rating equations by this comparison method is not ideal, especially when the catchment areas differ considerably (in this case by almost a factor of 4). Therefore, it was decided to review the rating equation for Nutclough during model calibration.

Details on the maximum stage for which the Agency's rating curves are valid were not provided.

Table 3.5 Rating curve coefficients provided by the Environment Agency

Station	h_T	α	d	β
Mytholmroyd	2.109	8.459	-0.342	2.2388
		15.0828	-0.483	1.4321
Nutclough*		23.27421	-0.22362	1.405546
Todmorden		5.267	0.120	2.174
Walsden		9.3762	-0.00667143	1.3682

** The Nutclough rating curve is reviewed during model calibration.*

3.6 Event Selection

Having assessed the availability and quality of data required to support the project, informed decisions could be made about the actual events to use for calibration and assessment. For the calibration events, suitably low flow levels without recent rain were selected as starting points for the model simulations to strengthen model initialisation. To maintain consistency, the radar and raingauge model calibrations are derived from the same set of events.

The set of calibration and assessment events selected for this study are presented in Tables 3.6 and 3.7 respectively. These tables also indicate the approximate peak flow for each event. Event 1 has been discarded from the calibration set since data are only available for one of the four gauging stations, namely Mytholmroyd. As discussed in Section 3.4, river level data for Todmorden are only available for the latter part of Event 5 whereas they are available for the other catchments for the entire event. Therefore Event 5b is used for the Todmorden catchment whilst Event 5a is used for the other catchments. The end of Event 5 is constrained by the availability of the radar data. Also Event 5 should be used with caution for the calibration of radar-based models as the Cyclops upgrade to the radar processing software occurred (see Section 3.3) within the event.

Table 3.6 Calibration events

Event	Period	Peak flow of event (approx), $m^3 s^{-1}$			
		Mytholmroyd	**Nutclough**	**Todmorden**	**Walsden**
2	09:00 20 Sep 1998- 09:00 26 Oct 1998	87	N/A	26	5.6
3	09:00 13 Dec 1998- 09:00 18 Jan 1999	59	N/A	12	3.6
4	09:00 2 Apr 2000- 09:00 5 Jun 2000	113	N/A	45	7.1
5a	00:00 25 Aug 2000- 22:00 28 Oct 2000	50	19	N/A	2.7
5b	09:00 2 Oct 2000- 22:00 28 Oct 2000	N/A	N/A	11	N/A
6	09:00 2 Nov 2002 09:00 12 Nov 2002	40	12	6.9	2.6

Initially only events 7 to 10 were selected for assessment by the Environment Agency and Met Office. The main emphasis of their selection was to capture more spatially-varied convective-driven rain events. This selection yielded the three short duration events 7 to 9 characterised by comparatively low peak flows. The Agency and Met Office also selected Event 10 which has a longer duration of nine days but still has a relatively low peak flow. To broaden the set of assessment events to embrace higher flows, a longer period with a substantial flow peak was selected from early 2002 (Event 11).

Table 3.7 Assessment events

Event	Period	Peak flow of event (approx), $m^3 s^{-1}$			
		Mytholmroyd	Nutclough	Todmorden	Walsden
7	00:00 10 Jun 2002- 12:00 11 Jun 2002	14	2.7	2.7	1.7
8	00:00 9 Aug 2002- 00:00 11 Aug 2002	25	8.8	3.7	1.3
9	12:00 9 Sep 2002- 00:00 11 Sep 2002	8.9	2.5	N/A	1.0
10	12:00 20 Oct 2002- 00:00 29 Oct 2002	29	6.5	4.2	2.6
11	00:00 16 Jan 2002- 00:00 17 Feb 2002	81	30	12	4.8

4 MODEL CALIBRATION

The rainfall-runoff model used in this study is the Probability Distributed Model (PDM). This lumped conceptual rainfall-runoff model is briefly outlined in Section 4.1 below. The PDM was chosen since it has been successfully calibrated for some of the study catchments as part of the 1997 Calder Report. It is also used operationally within the River Flow Forecasting System, or RFFS, for Northeast Region which encompasses forecasting for the River Calder. The PDM can be used to compute flows in either *simulation* mode, based solely on rainfall and potential evaporation inputs, or in *updating* mode, when additional use is made of observed flow data up to the time the forecast is made. Since the main concern here is the comparison of raingauge- and radar-estimated rainfall as input to a rainfall-runoff model, the PDM is only used in simulation-mode for this study. This avoids the added complications of interpretation arising from using the PDM in updating mode clouding any conclusions. An outline of the strategy for model calibration is given in Section 4.2.

Raingauge-based calibrations are performed first and are discussed in Section 4.3. When more than one raingauge is located in the vicinity of a catchment their readings need to be pooled to derive catchment average rainfall. Various methods have been considered for calculating areal rainfall from multiple raingauges and these are detailed in Section 4.3.1. Once the raingauge-based model calibrations are complete they are used as a starting point for the radar-based calibrations. Calibration of the PDM models using the Nimrod 5km analysis rainfalls are discussed in Section 4.4.

4.1 The Probability Distributed Model

The PDM is a fairly general conceptual rainfall-runoff model which transforms rainfall and potential evaporation to flow at the catchment outlet. Figure 4.1 illustrates the general form of the model. The PDM has been designed more as a toolkit of model components than a fixed model construct. A number of options are available in the overall model formulation which allows a broad range of hydrological behaviours to be represented.

Runoff production at a point in the catchment is controlled by the absorption capacity of the soil to take up water: this can be conceptualised as a simple store with a given storage capacity. By considering that different points in a catchment have differing storage capacities and that the spatial variation of capacity can be described by a probability distribution, it is possible to formulate a simple runoff production model which integrates the point runoffs to yield the catchment surface runoff. This runoff is translated via a surface storage, representing channels and other “fast” pathways, to the catchment outlet. The form of PDM used here employs a Pareto distribution of store capacities, with the shape parameter b controlling the form of variation between minimum and maximum capacity values c_{min} and c_{max} respectively. Drainage from the probability-distributed store passes into subsurface storage as recharge. The rate of drainage is in proportion to the water in store in excess of a tension water storage threshold. The subsurface storage, representing translation along slow pathways to the basin outlet, is chosen here to be of cubic form, with outflow proportional to the cube of the water in store.

Table 4.1 Parameters of the PDM model

Parameter name	Unit	Description
f_c	None	rainfall factor
τ_d	h	time delay
Soil moisture		
c_{min}	mm	minimum store capacity
c_{max}	mm	maximum store capacity
b	none	exponent of Pareto distribution controlling spatial variability of store capacity
Evaporation function		
b_e	none	exponent in actual evaporation function
Recharge function		
k_g	h mm^{b_g-1}	groundwater recharge time constant
b_g	none	exponent of recharge function
S_t	mm	soil tension storage capacity
Surface routing		
k_1	h	time constant of first linear reservoir
k_2	h	time constant of second linear reservoir
Baseflow storage (cubic)		
k_b	h mm^{m-1}	baseflow time constant

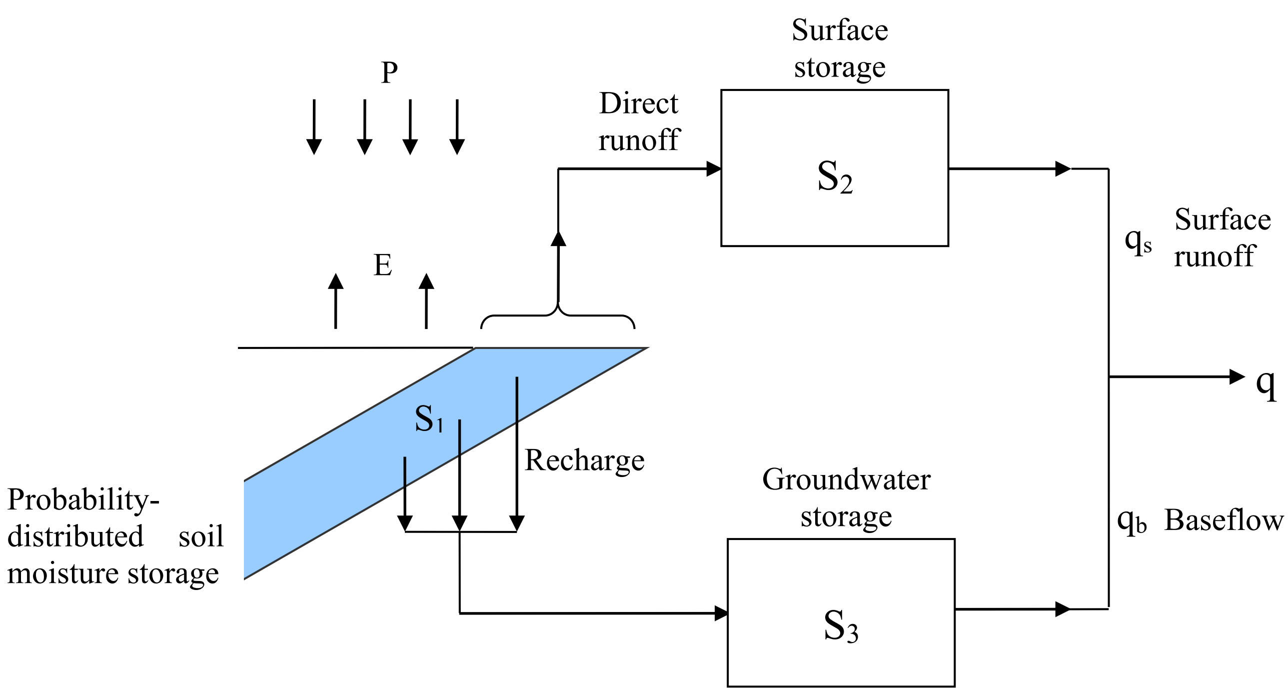

Figure 4.1 The PDM rainfall-runoff model.

Runoff generated from the saturated probability-distributed store contributes to the surface storage, representing the fast pathways to the basin outlet. This is modelled here by a cascade of two linear reservoirs cast as an equivalent transfer function model (O'Connor, 1982). The outflow from surface and subsurface storages, together with any fixed flow representing, say, compensation releases from reservoirs or constant abstractions, forms the model output. The parameters involved in this standard form of PDM model are summarised in Table 4.1.

4.2 Strategy for model calibration

As stated earlier, the PDM is used to compute flows in simulation-mode only for the purposes of this study. Model calibration is first carried out to estimate the PDM parameters listed in Table 4.1. This is achieved by comparing observed and modelled flows over the set of calibration events detailed in Table 3.6. Initially the parameters governing the long-term baseflow response of the model are calibrated manually by simply visually inspecting the hydrograph. These "slow" parameters can then be refined along with the calibration of the fast response parameters using a mixture of manual adjustment and automatic optimisation over all the calibration events.

The goal of automatic optimisation is to minimise an *objective function*. In this study the objective function used is the root mean square error (*rmse*) of the differences between observed and modelled flows at each time-step t, denoted by Q_t and q_t respectively. Over n observations the *rmse* is given by

$$rmse = \left(n^{-1} \sum_{t=1}^{n} e_t^2 \right)^{1/2}$$

where $e_t = Q_t - q_t$ is the error at time t. The *rmse* is measured in the same units as the flow (usually $m^3 s^{-1}$). The automatic optimisation employs a robust and straightforward simplex minimisation procedure (Nelder and Mead, 1965) modified to incorporate the ideas suggested by Gill, Murray and Wright (1981).

Another commonly used performance measure is the R^2 statistic:

$$R^2 = 1 - \frac{\sum_{t=1}^{n} e_t^2}{\sum_{t=1}^{n} (Q_t - \overline{Q})^2}$$

where $\overline{Q}$ is the mean of the observed flows over the n observations. The R^2 statistic is a dimensionless measure which gives the proportion of variability in observed flows accounted for by the model forecast and allows comparison across different events and catchments. A value of 1 indicates a perfect model. Note that the R^2 statistic is period/event specific due to the calculation of $\overline{Q}$ and can be negative if the modelled flow is worse than that provided by the (unknown) mean flow.

4.2.1 Peak analysis

The *peak analysis* is another useful indicator of a model's performance and is particularly relevant in the context of issuing flood warnings. Peak analysis is an analysis of the model accuracy in forecasting the flow peaks in terms of the percentage error in the peak and the timing error of the peak. Formally these errors are defined as follows:

$$\%\,peak\,error = \frac{(Q_{peak} - q_{peak})}{Q_{peak}} \times 100$$

$$Peak\ timing\ error = T_{peak} - t_{peak}$$

where Q_{peak} and q_{peak} denote the observed and predicted peak values, and T_{peak} and t_{peak} their corresponding times.

4.3 Raingauge-based model calibration

4.3.1 Calculating catchment average rainfall using raingauge weightings

In order to carry out the raingauge-based calibrations, catchment average rainfall needs to be derived from the network of raingauges. The methods considered involve a linear weighted average of the raingauge values for each of the four catchments, and the choice of appropriate raingauge weights. Figure 2.1 shows the location of the four raingauges in the Upper Calder catchment and Table 3.1 summarises the availability and quality of the data. The Blackstone Edge raingauge is the most recent addition to the network and is available from 1 February 2001. As the Blackstone Edge raingauge is only available for a single calibration event (Event 6), weightings with and without this raingauge have been derived. Calibration will be performed using the weightings that exclude the Blackstone Edge raingauge; however, the weightings derived including it will be used as part of the sensitivity analysis in Section 5.2.

The raingauge weights for the various methods investigated were calculated using the CEH Digital Terrain Model or CEHDTM. The algorithm applied is outlined below.

1. Use the CEHDTM to obtain the set of M gridpoints (on a 50m resolution grid) contained within the catchment.

2. Using a prescribed *distance measure* or *metric,* d_{ij}, between the i^{th} raingauge, which is located at (x_i, y_i), and the j^{th} gridpoint in the catchment, (x_j, y_j), the 'nearest' raingauge to the gridpoint can be determined (i.e. the raingauge that gives the smallest value of d_{ij}). The j^{th} grid point is then allocated to the 'nearest' raingauge.

3. Repeat Step 2 for *all* gridpoints in the catchment. The i^{th} raingauge weighting, w_i, is then calculated as

$$w_i = \frac{M_i}{M}$$

where M_i is the number of grid-points allocated to the i^{th} raingauge and M is the total number of grid-points in the catchment.

This algorithm provides the standard weightings for a given distance measure. The catchment average rainfall, $\bar{p}$, is calculated as the linear weighted sum of n raingauge measurements, such that

$$\bar{p} = \sum_{i=1}^{n} w_i p_i$$

where p_i is the rainfall measured at the i^{th} raingauge.

A correction can be applied to the standard weightings in an attempt to account for the possible unrepresentivity of the raingauges in relation to their allocated area. The correction factor, c_i, consists of the average SAAR of the area allocated to gauge i ($\text{SAAR}_{i,\text{ area}}$), divided by the SAAR at the gauge location ($\text{SAAR}_i = \text{SAAR}(x_i, y_i)$). That is

$$c_i = \frac{\text{SAAR}_{i,area}}{\text{SAAR}_i}.$$

Calculating $\text{SAAR}_{i,\text{ area}}$ can easily be incorporated in Step 2 of the algorithm by recording the SAAR of the allocated gridpoints.

Five methods of raingauge weighting are considered below based on different choices of distance measure.

(i) Thiessen method

The Thiessen weighting (Thiessen, 1911) uses the Euclidean distance measure:

$$d_{ij} = \sqrt{(x_i - x_j)^2 + (y_i - y_j)^2}\ .$$

This works on an intuitive ‘nearest neighbour’ principle with each raingauge weighted according to the proportion of the catchment for which it is the closest gauge. Figure 4.2 shows a map of the Mytholmroyd catchment indicating the area allocations derived using the Thiessen method, including and excluding the Blackstone Edge raingauge. Note that the subcatchments are also shown and that the reservoir drainage areas have been excluded.

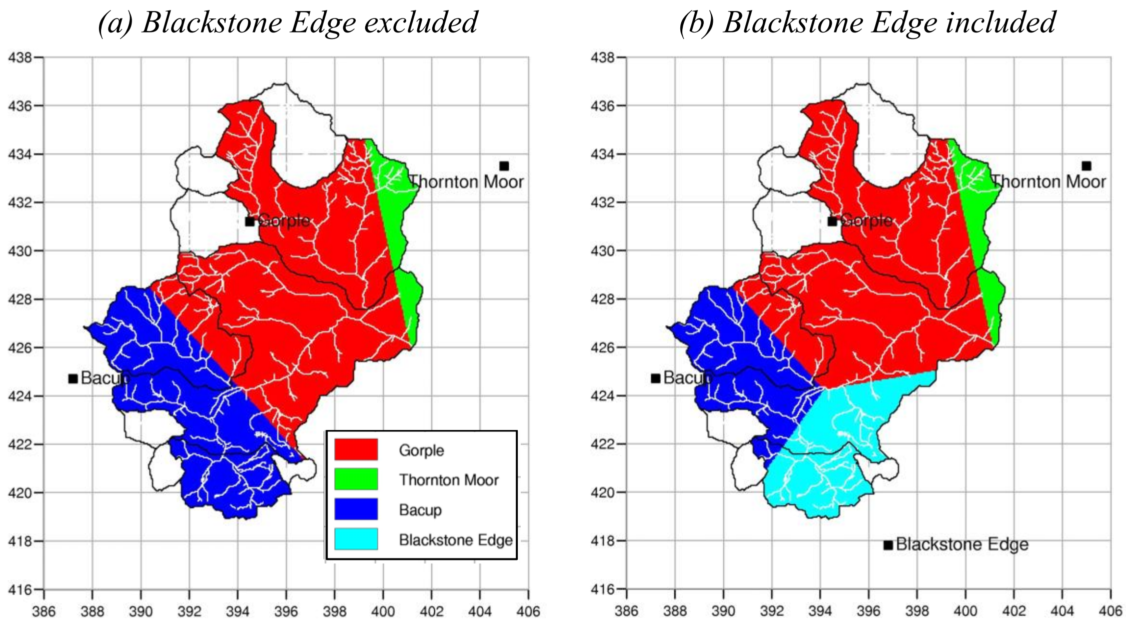

Figure 4.2 Raingauge area allocations based on the Thiessen method for the Mytholmroyd catchment.

Table 4.2 Raingauges allocated to each catchment

Catchment	**Raingauge**			
	Gorple	**Thornton Moor**	**Bacup**	**Blackstone Edge**
Mytholmroyd	✓	✓	✓	✓
Todmorden	✓		✓	
Nutclough	✓	✓		
Walsden			✓	✓

The Thiessen method is used to infer a suitable subset of nearest raingauges to use for each of the catchments. That is, gauges that would not be included in the Thiessen scheme are similarly excluded from the other weighting methods considered here. Details of the relevant raingauges selected for each catchment are contained in Table 4.2.

(ii) Elevation method

Across the Upper Calder catchment the elevation ranges considerably from 88m to 493m (see the relief map Figure 4.3 (b)) and this topographic variation can influence precipitation amounts. Using the appropriate subset of raingauges, as given in Table 4.2, the elevation method calculates the weights according to the proportion of the catchment that is closest in *elevation* to each gauge. The distance measure used is given by

$$d_{ij} = \sqrt{(z_i - z_j)^2}$$

where z_i is the elevation of the i^{th} raingauge and z_j is the elevation of the j^{th} grid-point. The weightings derived for the Mytholmroyd catchment, including the Blackstone Edge raingauge, are illustrated in Figure 4.4 (a). It is evident that only small proportions of the catchment are allocated to the Bacup and Thornton Moor raingauges. This is a consequence of the elevation of the Bacup and Thornton Moor gauges being very close to Gorple and Blackstone Edge gauges respectively; see Table 2.2.

(iii) SAAR method

Standard Average Annual Rainfall, or SAAR, data are available as a gridded dataset at a 1km resolution. SAAR, like elevation, varies significantly across the Upper Calder from 1100 to 1535mm as illustrated in Figure 4.3 (a). The SAAR weighting method is very similar to the elevation method but uses SAAR instead of elevation. The raingauge weights are calculated according to the proportion of the catchment that is closest in *SAAR* to each gauge. The distance measure used is given by

$$d_{ij} = \sqrt{\mathrm{SAAR}(x_i, y_i)^2 + \mathrm{SAAR}(x_j, y_j)^2}$$

where $\mathrm{SAAR}(x_i, y_i)$ is the SAAR at the i^{th} raingauge and $\mathrm{SAAR}(x_j, y_j)$ is the SAAR at the j^{th} grid-point. The area allocations based on this method for the Mytholmroyd catchment, including the Blackstone Edge raingauge, are presented in Figure 4.4 (c).

(iv) 3D method

The elevation method has no knowledge of the horizontal distances between the grid-point (in the catchment) under consideration and the raingauge locations. This can result in the unsatisfactory allocation of some grid-points where it would be preferable to use a nearer (in terms of horizontal distance) raingauge; see Figure 4.4 (a). This has been addressed by the construction of the 3D method which is defined by the distance measure:

$$d_{ij} = \sqrt{(x_i - x_j)^2 + (y_i - y_j)^2 + 100(z_i - z_j)^2}$$

which includes a measure of the horizontal distance. The elevation component has been multiplied by a factor of 100 to increase its influence and to alter the 3D method sufficiently from the standard Thiessen method. The area allocation derived using this method for the Mytholmroyd catchment, including the Blackstone Edge raingauge, is presented in Figure 4.4 (b) and is seen to sit somewhere between the standard Thiessen allocations (Figure 4.2 (b)) and the elevation allocations (Figure 4.4 (a)).

(a) SAAR

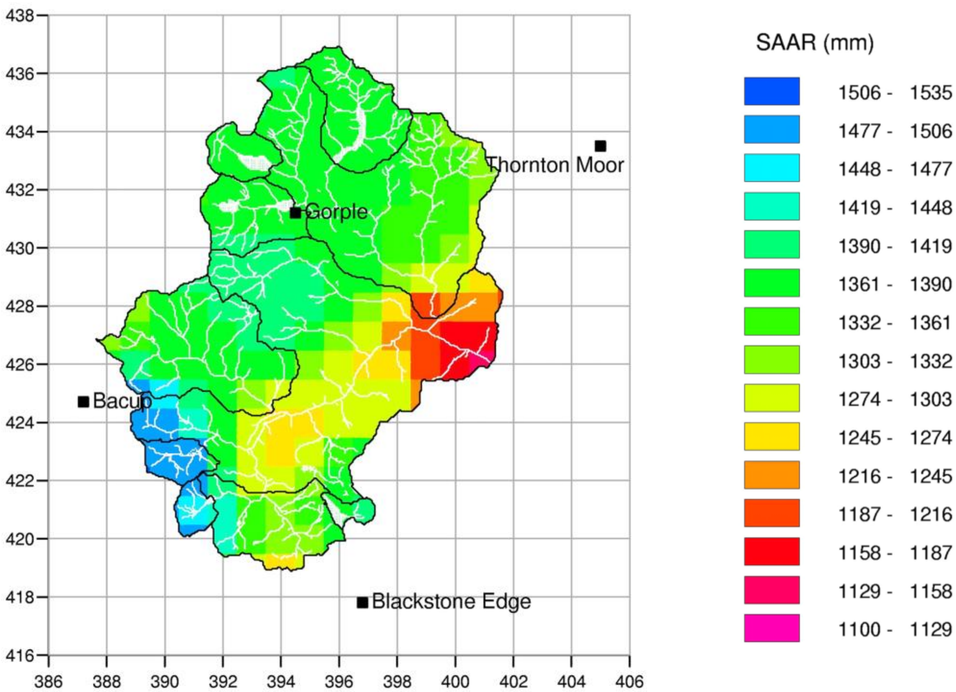

(b) Relief

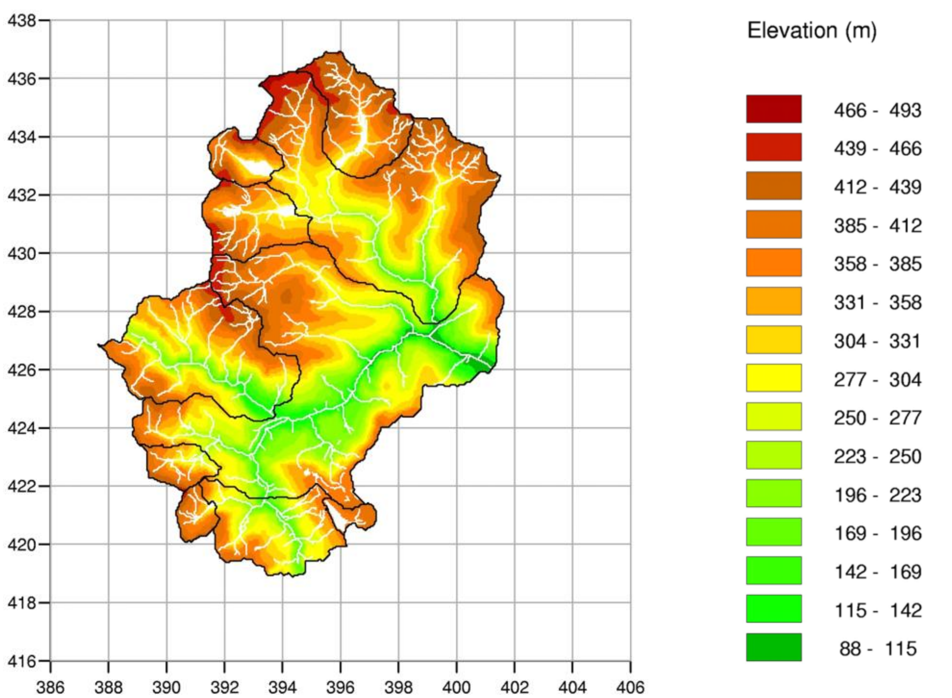

Figure 4.3 Maps of SAAR (1km grid) and relief for the Upper Calder catchment.

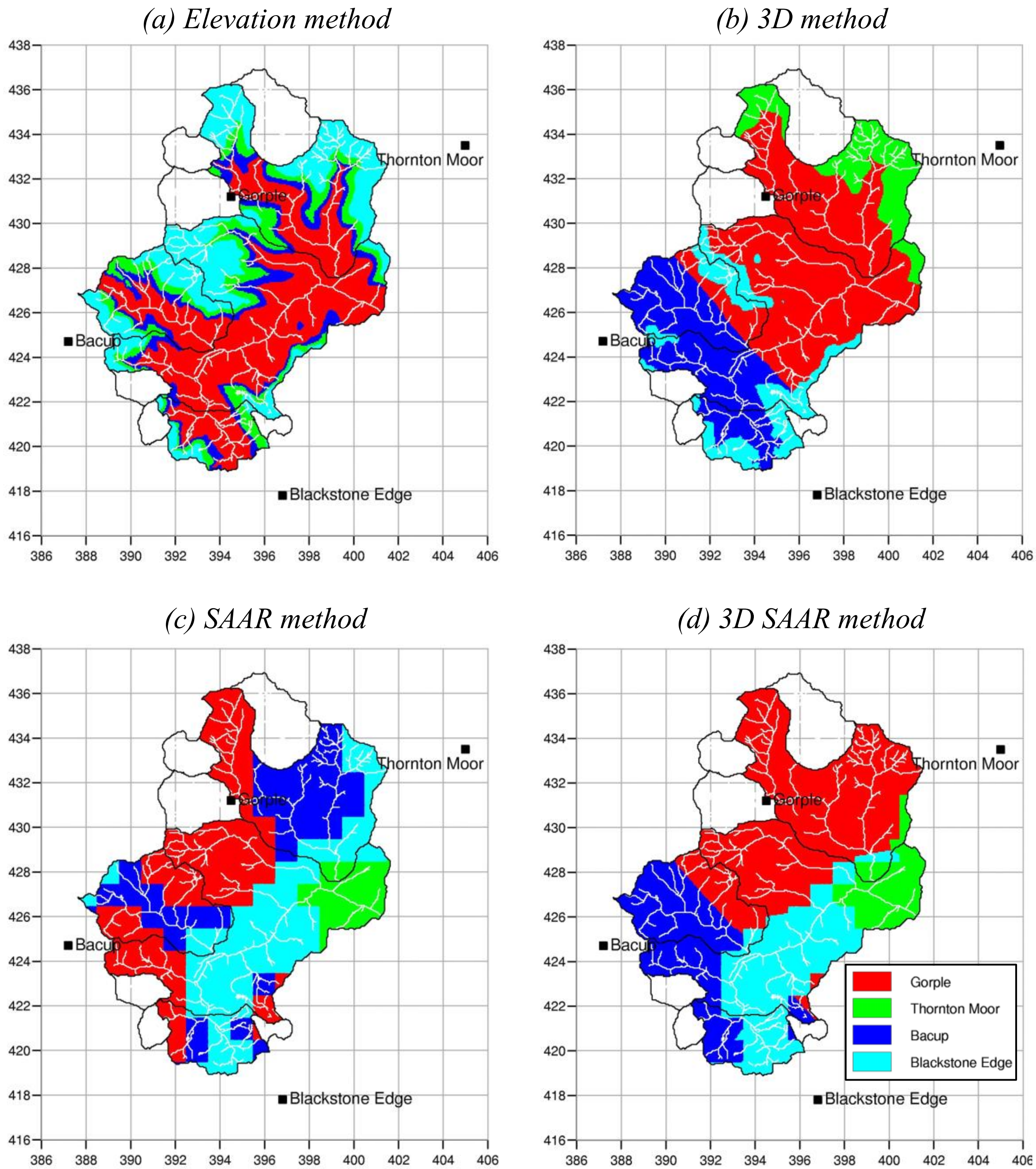

Figure 4.4 Raingauge area allocations for the Mytholmroyd catchment, based on different weighting measures.

(v) 3D SAAR method

Similar to the elevation method, the SAAR method has no knowledge of horizontal distances. This has been rectified along the same lines as the 3D method. The distance measure is defined as:

$$d_{ij} = \sqrt{(x_i - x_j)^2 + (y_i - y_j)^2 + 100(\mathrm{SAAR}(x_i, y_i) - \mathrm{SAAR}(x_j, y_j))^2}$$

which includes a measure of the horizontal distance. The SAAR component has been multiplied by a factor of 100 to increase its influence and to alter the 3D SAAR method sufficiently from the standard Thiessen method. The area allocation derived using this method for the Mytholmroyd catchment, including the Blackstone Edge raingauge, is presented in Figure 4.4 (d) and is seen to sit somewhere between the standard Thiessen allocations (Figure 4.2 (b)) and the SAAR allocations (Figure 4.4 (c)).

From Figures 4.2 and 4.4, the Thiessen, 3D and 3D SAAR methods are seen to give the most sensible area allocations. These three methods form the basis for the suggested raingauges weights to use when calculating the catchment average rainfall. These weights are listed, along with the weights in use by the Environment Agency (where available), in Tables 4.3 to 4.6

Table 4.3 Raingauge weightings for Mytholmroyd catchment
(a) Blackstone edge excluded

Method	Weights (SAAR adjusted weights)		
	Gorple	**Thornton Moor**	**Bacup**
Thiessen	0.631 (0.607)	0.058 (0.063)	0.311 (0.307)
3D	0.569 (0.545)	0.121 (0.136)	0.309 (0.305)
3D SAAR	0.559 (0.547)	0.123 (0.125)	0.318 (0.313)
EA weights	0.79	0.13	0.08
Suggested weights	0.6	0.1	0.3

(b) Blackstone Edge included

Method	Weights (SAAR adjusted weights)			
	Gorple	**Thornton Moor**	**Bacup**	**Blackstone Edge**
Thiessen	0.583 (0.562)	0.058 (0.063)	0.186 (0.186)	0.173 (0.177)
3D	0.517 (0.493)	0.121 (0.136)	0.243 (0.239)	0.119 (0.127)
3D SAAR	0.463 (0.458)	0.092 (0.092)	0.202 (0.204)	0.243 (0.243)
EA weights	-	-	-	-
Suggested weights	0.5	0.1	0.2	0.2

According to Table 4.2, only the Mytholmroyd and Walsden catchments are affected by the inclusion of the Blackstone Edge raingauge. So, for these catchments, there are two tables: one detailing the weights derived including the Blackstone Edge raingauge and the other detailing the weights excluding it. For the remaining catchments, Todmorden and Nutclough, only one table of derived raingauge weights is necessary.

Table 4.4 Raingauge weightings for Walsden catchment
(a) Blackstone Edge excluded

Method	Weights (SAAR adjusted weights)	
	Bacup	Gorple
Thiessen	1.000 (0.980)	-
3D	1.000 (0.980)	-
3D SAAR	1.000 (0.980)	-
EA weights	0.692	0.308
Suggested weights	0.98	-

(b) Blackstone Edge included

Method	Weights (SAAR adjusted weights)		
	Bacup	Blackstone Edge	Gorple
Thiessen	0.083 (0.085)	0.917 (0.959)	-
3D	0.519 (0.504)	0.481 (0.508)	-
3D SAAR	0.421 (0.425)	0.579 (0.594)	-
EA weights	0.275	0.5	0.225
Suggested weights	0.4	0.6	-

Table 4.5 Raingauge weightings for Todmorden catchment

Method	Weightings (SAAR adjusted)	
	Gorple	Bacup
Thiessen	0.341 (0.339)	0.659 (0.655)
3D	0.345 (0.343)	0.655 (0.651)
3D SAAR	0.332 (0.330)	0.668 (0.664)
EA weights	0.4	0.6
Suggested weights	0.34	0.66

Table 4.6 Raingauge weights for Nutclough catchment

Method	Weightings (SAAR adjusted)	
	Gorple	Thornton Moor
Thiessen	0.860 (0.842)	0.140 (0.155)
3D	0.627 (0.612)	0.373 (0.423)
3D SAAR	0.943 (0.924)	0.057 (0.059)
EA weights	0.6	0.4
Suggested weights	0.9	0.1

4.3.2 Model calibration using raingauges

This sub-section discusses the raingauge-based calibration for each catchment. For all catchments the same form of the PDM was used with a cubic baseflow storage, zero soil tension capacity (S_t=0) and a cascade of two unequal linear reservoirs for the routing of the surface runoff. Using 15 minute data between events to maintain a water balance so as to provide initial conditions for the next event, had little effect on model performance. As a consequence, each event was automatically initialised starting from a low period of flow without recent rainfall and with a 24 hour warm-up period discounted from the R^2 statistics.

For each catchment the raingauge-calibrated PDM parameters are listed in Table 4.7 and the corresponding event R^2 statistics are given in Table 4.8. (Tables and figures of results have been grouped together at the end of this Section 4.3.) Analyses of the major peak within each calibration event are given in Table 4.9. Note that this clearly shows the expected temporal structure for events dominated by widespread stratiform rain, with the upstream catchment hydrographs peaking first followed by Mytholmroyd. The hydrographs produced using the raingauge-calibrated PDM for each catchment are presented in Figures 4.6 to 4.10 and are grouped by event.

Mytholmroyd

Mytholmroyd was calibrated first as it is the largest catchment and it should provide a basis for the calibration of its three subcatchments. Although a set of calibrated parameters existed for the Mytholmroyd catchment from the 1997 Calder Report, the rating equation in use has since changed and consequently the calibration was started from scratch. Parameters were initially manually adjusted and then optimised automatically across all five calibration events. The raingauge weightings suggested in Table 4.3(a) proved to be as successful, or more so, than the weightings used by the Environment Agency.

A good fit was found for all events with R^2 statistics varying from 0.770 (Event 5a) to 0.934 (Event 2); see Table 4.8 and Figures 4.6 to 4.10. The lowest R^2 value for Event 5a is mainly due to the occasional overestimation of the flow e.g. around day 9 in Figure 4.9. After these overestimations the model corrects and performs well again. Encouragingly, the major peak of each event was generally very well predicted; see Table 4.9. Even the thunderstorm-driven large flood event during the summer of 2000 (Event 4) was reasonably predicted (see Figure 4.8), although the magnitude was slightly low. Also the timing of the peaks was very successfully modelled.

The simulated baseflow of the calibrated model agrees well with the observed flow confirming that the long-term parameters are reasonable. Only for Event 6, the calibration event with the smallest peak (see Table 3.6), is there a slight disagreement with the simulated baseflow creeping up with time; see Figure 4.10. At first this was conjectured to be a problem associated with the initialisation of the soil stores at the starting point of the event. However, the creeping of the baseflow persisted even when a longer warm-up period was used. Secondly, the potential evaporation (PE) profile used within the PDM was investigated. The standard PE profile used is a sine curve profile; the PE in mm on day n (day 1 is 1 January) is given by

$$E = a(1+\sin(2\pi(n-90)/365))$$

where a is the annual mean daily evaporation (a=1.4 mm is the default setting). Alternatively, the Met Office provides estimates of potential evaporation, over short grass and on a 40km grid, through the MORECS (Met Office Rainfall and Evaporation Calculation System) product. Figure 4.5 compares the standard sine profile with MORECS PE data, available as mean monthly values, for the 40km grid-square coincident with the Upper Calder during the period 1997 to 2004. Reassuringly the PE profiles agree well for a majority of the time: the only noticeable differences are during the summer (maximum) and winter (minimum) times where the sine curve profile is slightly underestimating the PE. However, using the MORECS PE data (rather than the sine curve profile) as input to the PDM had little effect on the simulated flow.

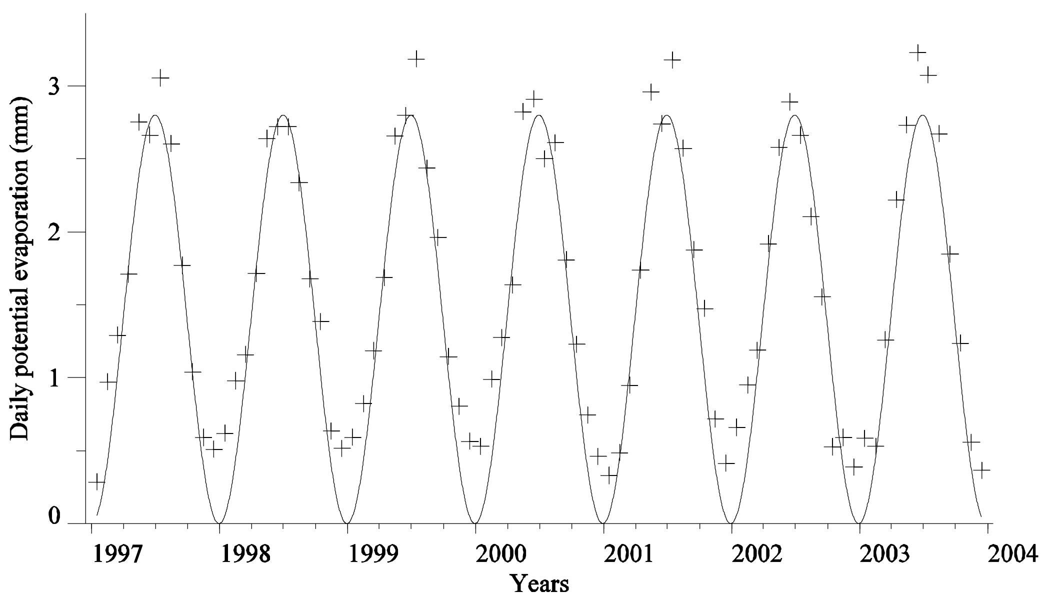

Figure 4.5 Daily potential evaporation estimated by the standard sine curve profile used in the PDM (solid line) and MORECS mean monthly estimates (+).

This confirms that the sine curve profile provides a reasonable estimate of PE in the Upper Calder catchment for use in PDM modelling and that some other factor must be responsible for the slightly high baseflow simulated in Event 6. Further investigations led to the conclusion that the most probable cause is a datum shift in the recorded level rather than any insufficiency in the model. The significant downwards jump, which occurs just prior to Event 6 and is highlighted in Figure 3.8, is a likely candidate.

Todmorden

The calibrated parameters obtained for the Mytholmroyd catchment were used as the starting point for the Todmorden calibration. It was immediately apparent that the observed peak of Event 4 was severely underestimated in comparison to the other calibration events. This meant that automatic calibration performed *including* Event 4 attempted to compensate for this by overestimating the flows in the other events. Clearly this is unsatisfactory and therefore Event 4 was *excluded* from the automatic calibration for Todmorden. Even though the peak of Event 4 is primarily a convective event with spatial variation in rainfall, examination of the peak flow for each event and catchment (see Table 3.6) suggests that the observed peak for Event 4 at Todmorden is too high rather than the result of a poor simulation. The over-prediction of the flow is probably due to the Agency rating equation not being exposed to an event this extreme during its derivation.

Manual adjustment of the parameters, followed by automatic optimisation over the calibration events (other than Event 4), gave a very good fit for the four events with R^2 statistics varying from 0.829 (Event 6) to 0.927 (Event 3); see Table 4.8 and Figures 4.6 to 4.10. The raingauge weightings suggested in Table 4.5 were used. The timings of the simulated peaks were in excellent agreement with the observed peaks and the magnitudes also in very close agreement; see Table 4.9. The worst predicted peak was Event 2 which has the second largest peak of the calibration events. This provides further evidence that the high end of the Agency rating equation could need re-examining.

The simulated baseflow of the calibrated model generally fits the observed flow well but has the same characteristic as Mytholmroyd with the apparent creeping up of the simulated baseflow during Event 6. Investigation of this behaviour indicates that, like at Mytholmroyd, a datum shift during September 2002 is the most likely cause for this difference.

Walsden

Walsden is the smallest catchment of the four and has the lowest peak flows. It contains two reservoirs and has a naturally draining area of approximately 10.4km^2. Walsden's response is typically more flashy than the other catchments and proved the most difficult to calibrate. Initially the calibrated parameters from Mytholmroyd and Todmorden, with only the Bacup raingauge as input, were used as starting points for the Walsden calibration but neither provided satisfactory simulations. A better simulation was obtained using the raingauge weightings used by the Environment Agency (see Table 4.4) which utilises Bacup and Gorple. This is not necessarily surprising since the strategy for deriving raingauge weights, detailed in Section 4.3.2, uses the Thiessen method to select the appropriate subset of raingauges to use and Figure 4.4 (a) shows that the justification for excluding Gorple is marginal. However, the calibration was still not satisfactory: the main difficulty was achieving a sensible baseflow simulation.

As a result, the latest Agency calibration was used as a starting point along with the Agency raingauge weightings. During the calibration process it became clear that a sensible calibration could not be obtained whilst including Event 6 as any attempt to do so led to a significantly over-predicted baseflow for the remaining events. Therefore manual and automatic optimisation were only performed across Events 2 to 5a. Omitting Event 6 is further justified by the poor quality of most of the 2002 Walsden river level data: as highlighted in Table 3.4 and Figure 3.9, the low level values frequently jump. The challenging problems with calibrating the catchment are reflected in the results, with R^2 statistics that range from 0.716 (Event 3) to 0.825 (Event 2); see Table 4.8. This is the poorest performing catchment of the four studied. However, the results are still reasonable given the size of the catchment and the unknown influence of the two reservoirs whose drainage areas account for 24% of the total catchment area.

The different characteristics of the Walsden catchment, relative to the other Upper Calder catchments, are evident in the calibrated parameters (see Table 4.7) and the resulting hydrographs (see Figures 4.6 to 4.10) which show a far more responsive baseflow component. The simulated baseflow is generally good, although it is too low for the uncalibrated Event 6. The peak analysis shows a reasonable peak magnitude prediction; see Table 4.9. There is no evidence of a consistent timing error as the peaks for Events 5a and 6 are predicted just too early whilst there is a slight lag in the timing for the convective Event 4.

Nutclough

Nutclough is the newest river gauging station of the four with data only available from August 2000 onwards. Therefore only Events 5a and 6 were available for calibration. Since the (single part) rating equation was to be re-evaluated within the PDM calibration (see Section 3.5), the period 15 November 2000 to 14 April 2001 was included within the calibration set to expose the rating equation to a wider range of flows. The remaining parameters were based on the Mytholmroyd calibration. These were automatically optimised, along with the rating equation coefficients. The final rating equation parameters are α=16.6, d=-0.186 and β=1.450 in the power law relation $Q = \alpha(h+d)^{\beta}$, where h denotes river stage in metres and Q is flow in m^3s^{-1}. The raingauge weights suggested in Table 4.6 were used.

The simulated baseflow agrees very well with the observed (see Figures 4.9 and 4.10) and the flow simulations yield good R^2 statistics of 0.858 (Event 5a) and 0.843 (Event 6); see Table 4.8. The timing of the simulated peaks is in very good agreement and the peak magnitudes are well predicted; see Table 4.9.

Table 4.7 Comparison of raingauge-calibrated PDM parameters across catchments. The radar-calibrated PDM parameters are identical except for the rainfall factor and time delay which are also listed.

Parameter name	Catchment			
	Mytholmroyd	**Nutclough**	**Todmorden**	**Walsden**
Rainfall factor				
f_c (raingauge)	1.089	1.105	0.982	1.045
f_c (radar)	0.97	1.0	0.80	0.90
Time Delay				
τ_d (raingauge)	1.189	0.985	0.272	0
τ_d (radar)	1.0	1.0	0	0
Soil Moisture				
c_{min}	1.3	1.3	1.3	1.3
c_{max}	23.4	21.1	23.1	117.1
b	0.296	0.321	0.448	3.580
Evaporation function				
b_e	2.5	2.5	2.5	2.5
Recharge function				
k_g	1459	2205	1207	239.3
b_g	2.218	2.334	2.380	1.764
S_t	0	0	0	0
Surface routing				
k_1	7.042	11.12	3.588	7.811
k_2	0.519	0.501	0.322	0.300
Baseflow storage (cubic)				
k_b	133.9	70.3	144.8	108.7

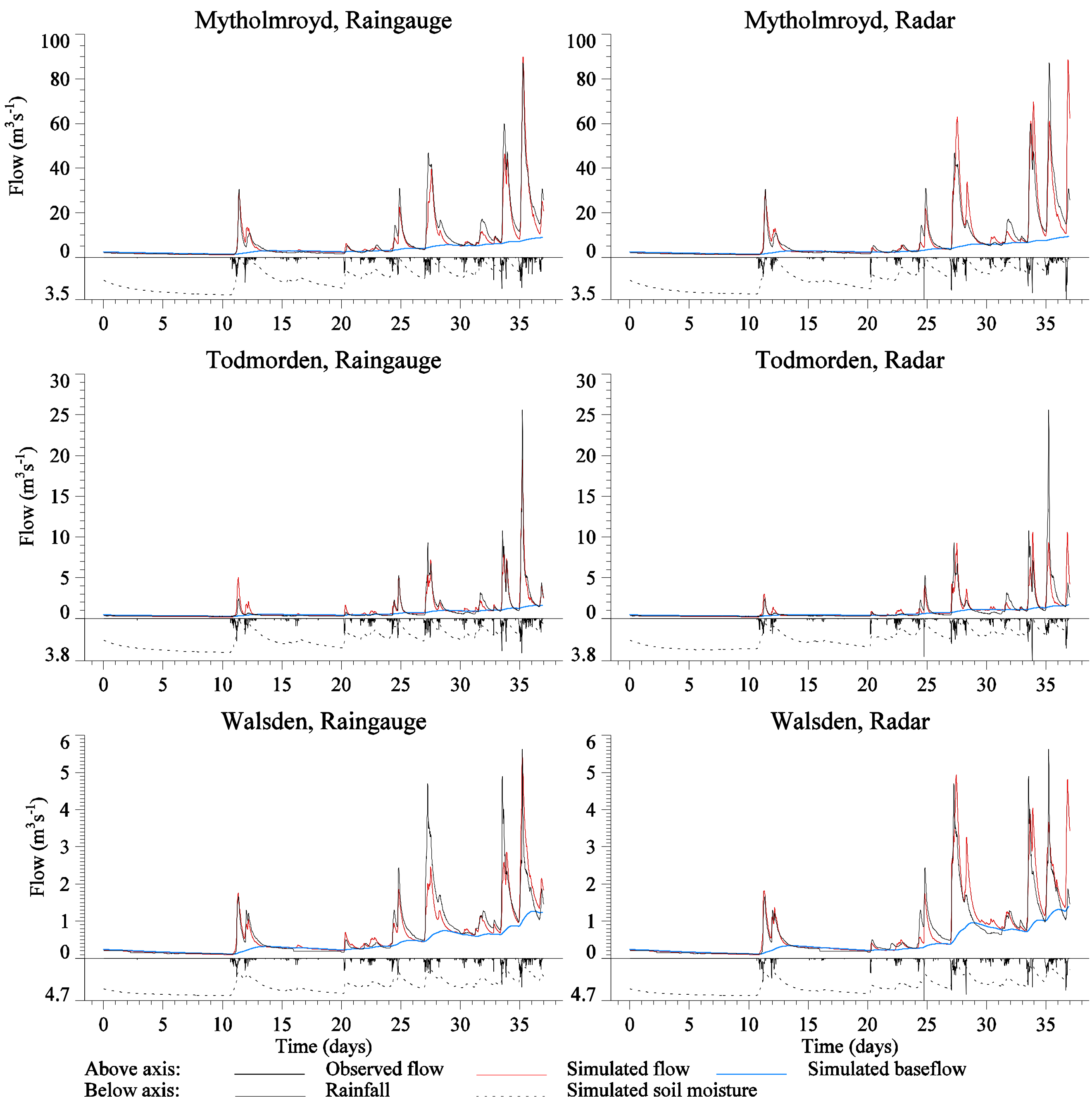

Figure 4.6 Hydrographs for Event 2: 09:00 20 September to 09:00 26 October 1998 (plus 1 day warm-up). The figure below the axis is the maximum rainfall (from either raingauge or 5km radar) for that catchment.

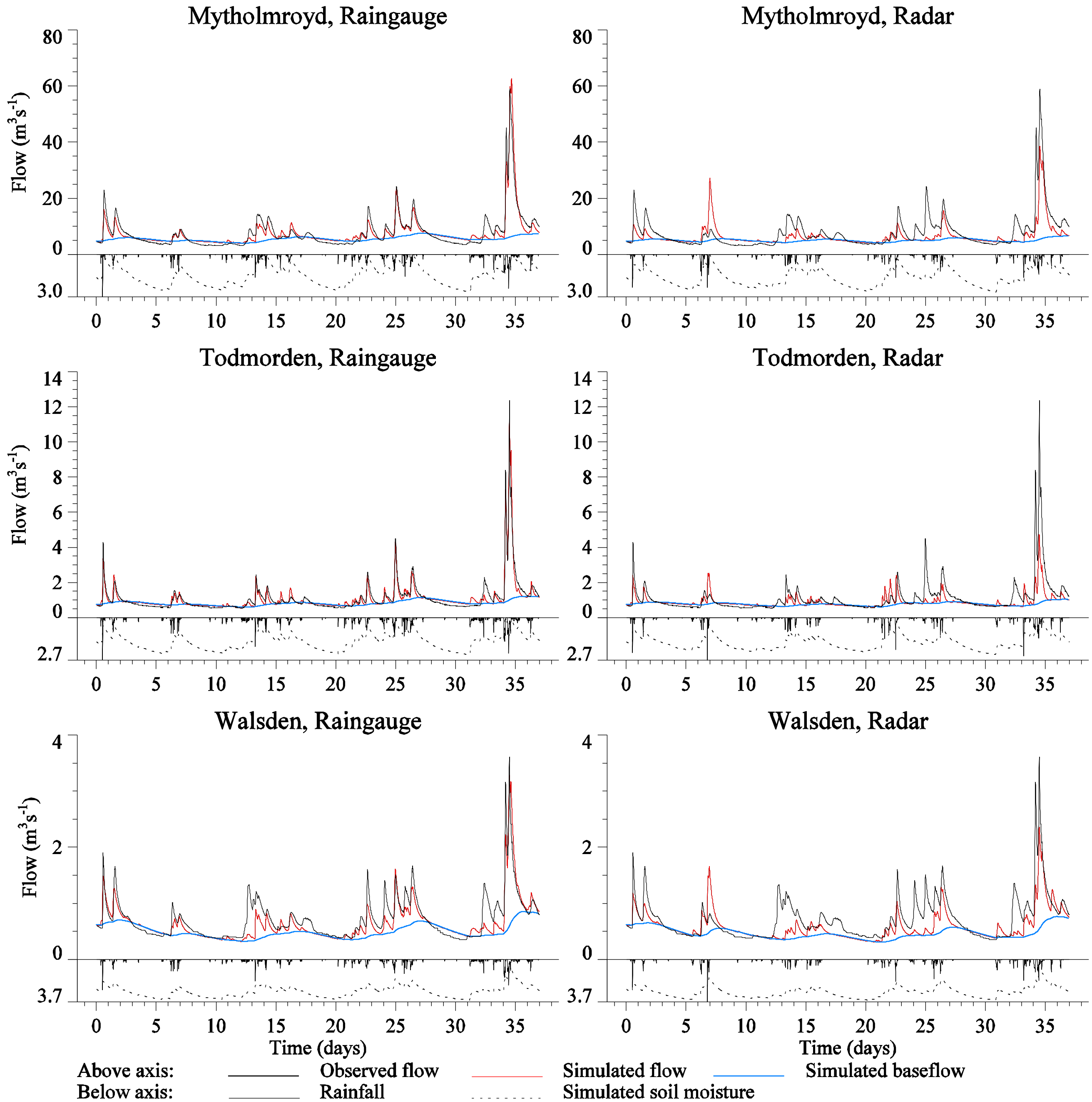

Figure 4.7 Hydrographs for Event 3: 09:00 13 December 1998 to 09:00 18 January 1999 (plus 1 day warm-up). The figure below the axis is the maximum rainfall (from either raingauge or 5km radar) for that catchment.

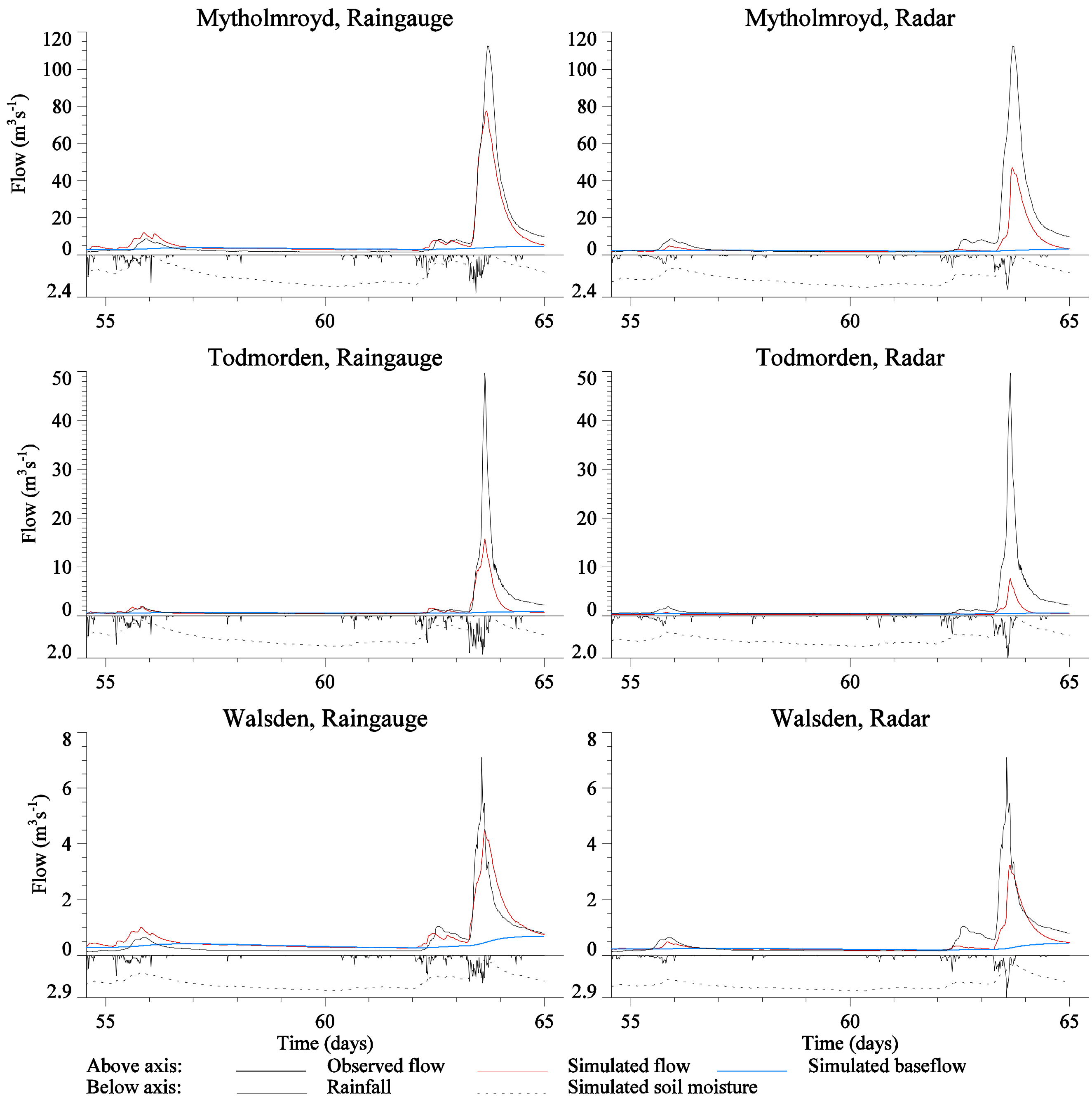

Figure 4.8 Hydrographs for the last ten days of Event 4: 09:00 2 April to 09:00 5 June 2000. The figure below the axis is the maximum rainfall (from either raingauge or 5km radar) for that catchment.

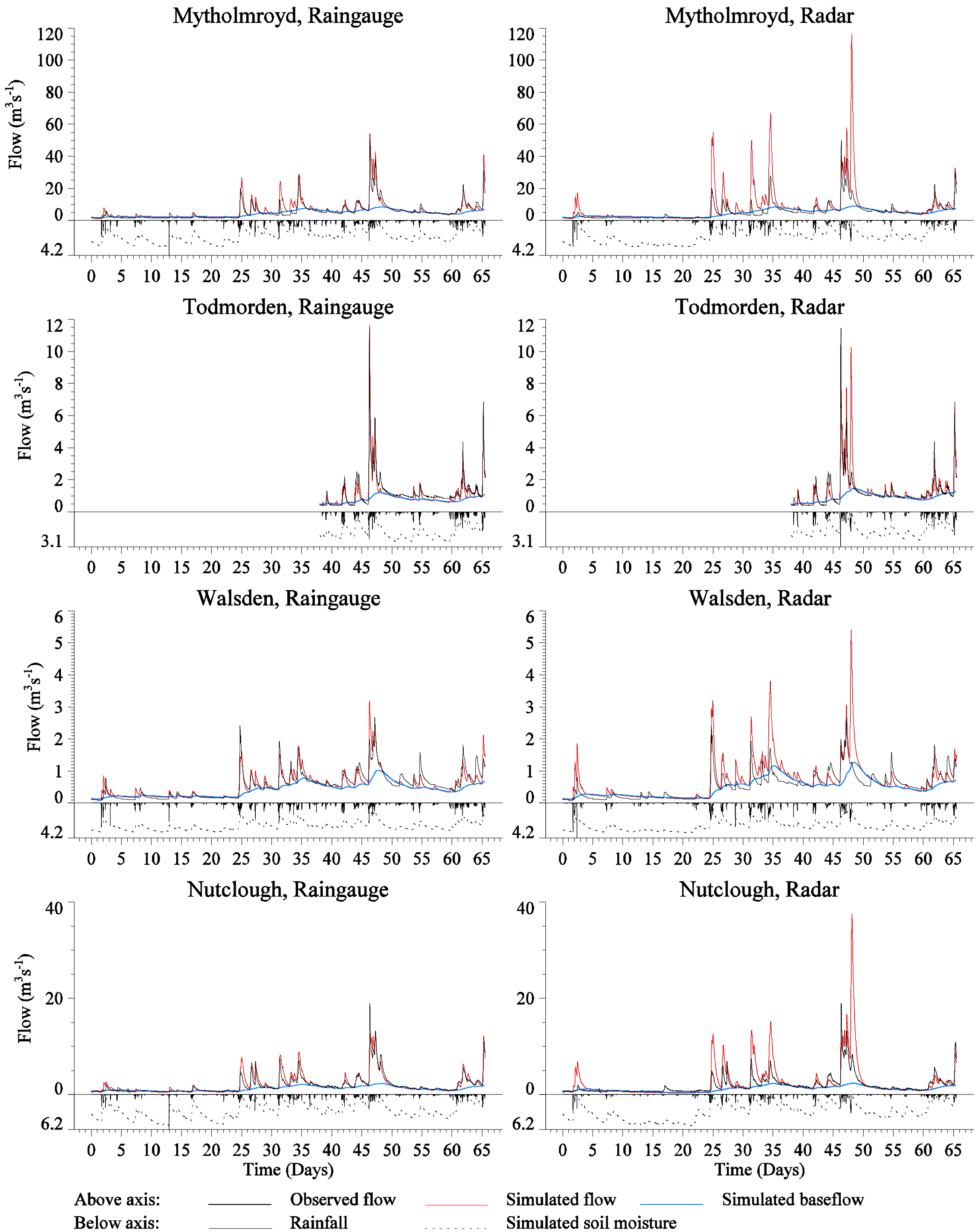

Figure 4.9 Hydrographs for Event 5a: 09:00 25 August to 22:00 28 October 2000 (plus 1 day warm-up). The figure below the axis is the maximum rainfall (from either raingauge or 5km radar) for that catchment.

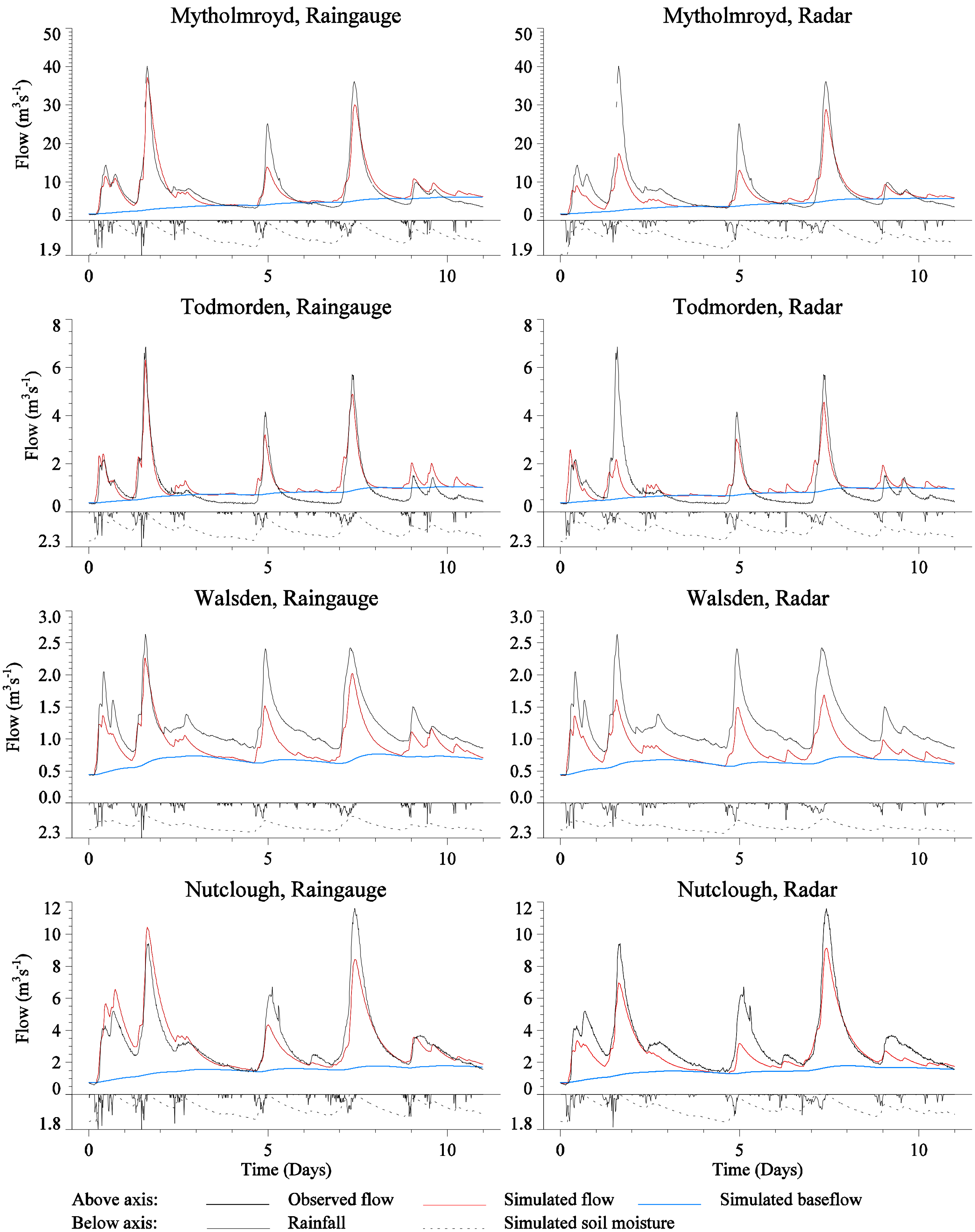

Figure 4.10 Hydrographs for Event 6: 09:00 2 November to 09:00 12 November 2002 (plus 1 day warm-up). The figure below the axis is the maximum rainfall (from either raingauge or 5km radar) for that catchment.

Table 4.8 Calibration performance (R^2 statistic) for each catchment using raingauge and Nimrod 5km analysis rainfall

Event	Rainfall input type	Catchment			
		Mytholmroyd	Nutclough	Todmorden	Walsden
2					
	Raingauge	0.934	N/A	0.922	0.825
	5km analysis	0.742	N/A	0.664	0.757
3					
	Raingauge	0.886	N/A	0.927	0.716
	5km analysis	0.561	N/A	0.460	0.433
4					
	Raingauge	0.894	N/A	0.597*	0.789
	5km analysis	0.449	N/A	0.207	0.594
5a/b					
	Raingauge	0.770	0.858	0.883	0.816
	5km analysis	-1.961	-1.091	0.468	-0.153
6					
	Raingauge	0.881	0.843	0.829	0.305*
	5km analysis	0.688	0.772	0.550	-0.243

** Indicates that the event was not included within the raingauge-based automatic optimisation.*

Table 4.9 Peak analysis for calibration events. Unbracketed terms relate to raingauge calibrations and bracketed terms to radar calibrations.

Event/ Catchment	Observed		Computed		Error	
	Peak	Time	Peak	Time	% peak	Time (h)
Event 2						
Mytholmroyd	87.1	15:15 24 Oct 98	89.8 (61.1)	15:30 24 Oct 98 (16:00 24 Oct 98)	-3.1 (29.9)	-0.25 (-0.75)
Nutclough				N/A		
Todmorden	25.6	14:15 24 Oct 98	19.4 (9.29)	14:15 24 Oct 98 (14:15 24 Oct 98)	24.1 (63.7)	0 (0)
Walsden	5.63	14:15 24 Oct 98	5.52 (3.66)	14:15 24 Oct 98 (14:15 24 Oct 98)	2.0 (34.9)	0 (0)
Event 3						
Mytholmroyd	58.9	22:00 15 Jan 99	59.9 (38.6)	22:15 15 Jan 99 (22:00 15 Jan 99)	-1.8 (34.5)	-0.25 (0)
Nutclough				N/A		
Todmorden	12.4	21:00 15 Jan 99	11.3 (4.73)	21:00 15 Jan 99 (20:30 15 Jan 99)	8.6 (61.7)	0 (0.5)
Walsden	3.61	20:45 15 Jan 99	3.28 (2.35)	20:45 15 Jan 99 (20:45 15 Jan 99)	9.0 (34.7)	0 (0)
Event 4						
Mytholmroyd	113	01:45 4 Jun 00	77 (46.9)	01:15 4 Jun 00 (01:45 4 Jun 00)	31.2 (58.3)	0.5 (0)
Nutclough				N/A		
Todmorden	49.7	00:30 4 Jun 00	15.8 (7.58)	00:30 4 Jun 00 (00:30 4 Jun 00)	68.3 (84.7)	0 (0)
Walsden	7.12	22:45 3 Jun 00	4.54 (3.25)	00:15 4 Jun 00 (00:15 4 Jun 00)	36.2 (54.3)	-1.5 (-1.5)
Event 5						
Mytholmroyd	49.8	17:30 9 Oct 00	54.1 (40.0)	17:15 9 Oct 00 (17:00 9 Oct 00)	-8.5 (19.8)	0.25 (0.5)
Nutclough	19.0	17:00 9 Oct 00	12.7 (10.8)	17:15 9 Oct 00 (17:15 9 Oct 00)	33.2 (43.1)	-0.25 (-0.25)
Todmorden	11.5	15:45 9 Oct 00	11.6 (10.5)	15:45 9 Oct 00 (15:30 9 Oct 00)	-1.6 (8.7)	0 (0.25)
Walsden	1.98	16:00 9 Oct 00	3.18 (1.81)	15:45 9 Oct 00 (15:45 9 Oct 00)	-60.3 (9.3)	0.25 (0.25)
Event 6						
Mytholmroyd	40.2	00:00 3 Nov 02	37.1 (17.4)	00:15 3 Nov 02 (00:15 3 Nov 02)	7.6 (56.7)	-0.25 (-0.25)
Nutclough	9.37	00:15 3 Nov 02	10.4 (6.96)	00:15 3 Nov 02 (23:30 2 Nov 02)	-11.8 (26.2)	0 (0.75)
Todmorden	6.86	23:15 2 Nov 02	6.32 (2.16)	22:45 2 Nov 02 (22:30 2 Nov 02)	7.9 (68.4)	0.5 (0.75)
Walsden*	2.63	23:00 2 Nov 02	2.26 (1.61)	22:45 2 Nov 02 (22:30 2 Nov 02)	14.0 (38.8)	0.25 (0.5)

4.4 Radar-based model calibration

The original intention was to calibrate the PDM with the Nimrod 5km radar data from scratch for the Mytholmroyd catchment and then use this as a basis for calibrating the other three study catchments. Unfortunately this proved to be impractical. The main hindrance was the Nimrod 5km analysis overestimating rainfall during some periods and underestimating rainfall during others. This over/underestimation can be detected in the cumulative rainfall time-series presented in Appendix C. It became most apparent when the catchment average rainfall data, derived form the Nimrod 5km analysis, were used in the modelling. For example, compare the radar- and raingauge-derived rainfall time-series for Event 3 (see Figure 4.7) together with the observed flow: there is an overestimation of radar-derived rainfall around day 6 whilst there is underestimation around day 25. This characteristic of under/overestimation prevented any sensible use of automatic optimisation, effectively making a calibration from scratch, or even from a given starting set of parameters, impossible.

Attempts were made to associate periods of over/underestimation with a particular radar error. This proved difficult to do using the derived Nimrod 5km analysis rather than the raw 2km product, as some effects are 'smeared' out by the coarser resolution. The only obvious source of error is associated with the infill map. This is discussed in Section 3.3.3 and an example is presented in Figure 3.7. Also using raingauges to replace periods of poor Nimrod performance was deemed inappropriate as it is the Nimrod 5km product that is being evaluated.

However, notwithstanding the above problems, progress using radar data for model calibration is still possible. In an ideal situation one can envisage that the raingauge-based and radar-based calibrations would have extremely similar parameter values with the only significant differences relating to parameters influencing the magnitude and timing of the rainfall input. The two relevant parameters are the rainfall factor (f_c) and the time delay (τ_d). In fact the hope would be that a rainfall factor of 1 would be optimal for the radar-based calibration. Using this ideology, the strategy for performing the radar-based calibration was to use the raingauge-based calibration as a starting point and then manually adjust the rainfall factor and time delay parameters whilst being aware that the R^2 statistic can be significantly affected by the periods of over/underestimation. Also the calibration was performed with a slight preference placed on Events 5 and 6 since these events, and the assessment events, post-date the Cyclops upgrade to the radar processing on 1 September 2001.

For each catchment the calibrated values of the rainfall factor and the time delay are given in Table 4.7. The R^2 statistic for each catchment and event has still been calculated in Table 4.8 but this criterion should not be used as the sole judge of model performance. Performance should also be assessed with regard to the peak analysis given in Table 4.9 and the simulated hydrographs produced using the radar-calibrated PDM presented in the right hand columns of Figures 4.6 to 4.10.

Mytholmroyd

After manually adjusting the rainfall factor and time delay, values of 0.97 and 1.0 respectively were found to give the most consistent simulation. Event 5a has the worst R^2 statistic (-1.961) by some margin; see Table 4.8. However, the corresponding hydrograph (see Figure 4.9) indicates that this poor statistic is due to a period of significant rainfall overestimation up to day 35 and a small period of large overestimation around day 38. For the remainder of the event the simulated flow is in good agreement with the observed. During Event 5a, the radar processing was upgraded to Cyclops on 1 September 2000 (day 8) and is the probable cause for the intermittent periods of large overestimation immediately after that date.

The best R^2 statistic is achieved for Event 2 with a value of 0.742. The hydrograph for this event (see Figure 4.6) shows good agreement up to day 34 but with a slight tendency to overestimate. This is followed by a significantly underestimated flow peak around day 35 and then an overestimated flow peak at the end of the event. Both of these departures from the observed flows at the tail end of Event 2 can be attributed to periods where the Nimrod 5km analysis had been infilled with the Nimrod rain-rate analysis (see Table 2.3) by the Met Office.

Prior to calibration, there was some expectation that the Nimrod 5km analysis would provide better flow estimates for the predominantly convective Event 4. However, examination of the catchment average rainfall estimates contained in Figure 4.8 show that the Nimrod 5km analysis predicted less rain than the raingauge–based estimates and this is reflected in a lower simulated peak. Event 3 shows both periods of over- and under-estimation (see Figure 4.7), further highlighting the difficulties encountered with the radar-based calibrations. Event 6 shows the Nimrod 5km analysis initially underestimating for the first 3 days but then performing as well as the raingauge-based model for the remainder of the event; see Figure 4.10.

Encouragingly, the simulated baseflow agrees well with the observed flow, except for the creeping of the simulated baseflow during Event 6 which also occurs for the raingauge-based model, and can recover reasonably quickly from periods of over/underestimated rainfall. The peak analysis (see Table 4.9) shows most of the flow peaks being underestimated but any attempt to correct this through a larger rainfall factor caused the simulated baseflow to become too high and worsened the overall agreement. The timings of the simulated peaks were very similar to those of the raingauge-based model and in general agreed well with the observed.

Overall the radar-based model calibrations were not as consistent as the raingauge-based ones. The primary cause is that possible sources of error in radar-based rainfall estimation have a far greater impact than errors associated with raingauge-based rainfall estimation. Secondly, raingauge measurement techniques have not changed over the period of study whereas Nimrod is clearly an evolving product and system upgrades, such as Cyclops, have the potential to significantly alter radar-based rainfall estimation.

Todmorden

For the Todmorden catchment, a rainfall factor of 0.8 and a time delay of 0 were found to give the best simulation results. The rainfall factor of 0.8 for Todmorden is considerably less than the value of 0.97 used for Mytholmroyd. A likely cause is that the west and south-west parts of the Upper Calder (including the Todmorden catchment) are situated closest to the radar and can be subject to more overestimation than the rest of the area. Possible evidence for this comes from the cumulative rainfall time-series given in Appendix C which compare the Bacup and Gorple raingauges (see Figure 4.4 for their location) with the radar values for the 2 and 5km radar grid-squares coincident with them. These time-series show that generally the radar values over Bacup overestimate significantly more than those over Gorple.

As was the case for Mytholmroyd, the best R^2 statistic of 0.664 (see Table 4.8) is achieved for Event 2 and the poor performance of the final two peaks of the event (see Figure 4.6) can be attributed to use of the Nimrod rain-rate analysis by the Met Office for infilling missing values. The remainder of Event 2 is well modelled. Event 4 has the worst R^2 statistic (0.207), as it did in the raingauge case, and is worsened by the possible problem with the high end of the Agency-derived rating equation. Event 5b is generally well modelled and Todmorden is least affected by the large overestimation of the rainfall that occurs around day 48 (see Figure 4.9). Although Event 3 has an R^2 statistic of only 0.460, the corresponding hydrograph (see Figure 4.7) shows that this is dominated by the underestimation of the major peak at the end of the event. Event 6 shows the same behaviour as observed at Mytholmroyd, with the Nimrod 5km analysis producing similar results to the raingauge-based model beyond day 3 (see Figure 4.10) whilst initially underestimating the rainfall.

Over all the calibration events, the simulated baseflow of the radar-based calibration is very similar to the raingauge-based one and generally agrees well with the observed flow. The only exception is Event 6 which suffers the same problem as the raingauge-based model of a high baseflow; see the raingauge-based calibration for discussion. The peak analysis shows that the timings of the simulated peaks are good but the raingauge-based model results are better. This analysis also indicates that the peak magnitudes are generally under-predicted by the radar-based model but this cannot be remedied by increasing the rainfall factor as this generates too much baseflow. Once again the conclusion is that the raingauge-based models provide a more consistent simulation for Todmorden.

Walsden

A rainfall factor of 0.9 and a time delay of 0 gave the most consistent calibration for the Walsden catchment. The lower value of the rainfall factor, compared to 0.97 for the Mytholmroyd catchment, reflects the proximity of the Walsden catchment to the radar as in the Todmorden case – see the discussion of Todmorden above.

Event 6 has the worst R^2 statistic of -0.243 but this is expected since it was omitted from the automatic optimisation performed in the raingauge-based calibration. Event 5a also has a poor R^2 statistic of -0.153. However, examination of the corresponding hydrograph (see Figure 4.9) shows that this statistic is dominated by the overestimation of the rainfall around day 48 and the general overestimation up to day 40. In fact, other than the mentioned overestimation, the radar-based model performs as well, or better than, the raingauge-based one. In particular, the peak of Event 5b is modelled better by the radar-based model; see Table 4.8.

The best R^2 statistic of 0.757 occurred for Event 2, as in the raingauge-based calibration. The hydrograph (see Figure 4.6) shows evidence of the Nimrod 5km analysis rainfall giving a better flow simulation, up to day 34, than when the model with gauge rainfall is used. After day 34, the data used to infill missing Nimrod 5km analysis rainfalls do not serve so well. During the peak of Event 4, the Nimrod 5km analysis does not predict enough rainfall from the convective storm. As a result, the magnitude of the simulated peak is less than that of both the observed and the raingauge-based model simulation. The hydrograph for Event 3 (see Figure 4.7) shows, like in the case of Mytholmroyd and Todmorden, periods of over- and under-estimation and confirms that the raingauge-based model performs best over this event.

The simulated baseflow of the radar-based model is in good agreement with the observed flow for a majority of the time. As mentioned in the raingauge-based calibration, the calibrated parameters for Walsden differ from those for the other study catchments giving the simulation a more responsive baseflow component. This is visible in the flow hydrographs (see Figures 4.6 to 4.10) and extends the time the model needs to recover from periods of overestimated rainfall. For example, the hydrograph for Event 5a shows a very high simulated baseflow response after the overestimations around days 35 and 48 and it takes the model for Walsden more time to recover than the models for the other catchments. The peak analysis (see Table 4.9) shows that the timing of the simulated peaks is almost identical to those of the raingauge-based models and that there is a general trend of underestimation in the peak magnitudes.

Over all the calibration events the raingauge-based model is still considered to give the best simulations. However, the radar-based model does perform well and actually out-performs the raingauge-based one in some instances, the most notable being up to day 34 of Event 2 and during Event 5a, discounting the periods of overestimation near day 48 and prior to day 40.

Nutclough

Nutclough river level data are only available for Event 5a and Event 6. The radar-based model uses the raingauge-based model parameters including those defining the rating equation. A rainfall factor of 1.0 and a time delay of 1.0 were found to give the best simulation. Both events show that the simulated baseflow has been modelled well and agrees with the observed flow. During Event 5a, the radar-based model for Nutclough behaves similarly to those for the Mytholmroyd and Todmorden catchments with the Nimrod 5km analysis over-predicting the rainfall prior to day 35 and about day 48 whilst elsewhere the simulated flow agrees well with the observed; see Figure 4.9. Event 6 is also very similar: for the first 3 days of the event the flow is under-predicted and then the Nimrod 5km analysis performs almost as well as the gauge estimates of rainfall for the remainder of the event; see Figure 4.10. The peak analysis indicates that the timings of the radar-based model simulated peaks are not as good as the raingauge-based ones and that the magnitudes are underestimated.

Overall the raingauge-based model performs best but the radar-based one can perform as well when the Nimrod 5km analysis allows. Also the radar-based model can recover from periods of large overestimation quite quickly, as illustrated in Figure 4.9.

4.5 Summary

Successful raingauge-based PDM model calibrations were achieved for all catchments. The Walsden catchment was the most difficult to calibrate and this is reflected in the R^2 statistics; see Table 4.8. The strategy for deriving raingauge weights, detailed in Section 4.3.1, used the Thiessen method to select a subset of the raingauges for each catchment and then a suggested weighting (for the subset of gauges) was arrived at by considering the weights derived from the Thiessen, 3D and 3D SAAR methods. These weights were used for all catchments, other than Walsden, and performed at least as well as the Environment Agency weights at deriving the catchment average rainfall needed for modelling. For Walsden, the strategy of Section 4.3.1 suggested only using the Bacup raingauge whereas the Agency use a weighting between Bacup and Gorple raingauges. The latter proved to be the best for modelling purposes and is not necessarily surprising since the justification for excluding Gorple based on the Thiessen method is marginal (see Figure 4.2 (a)). Therefore it is concluded that the strategy of Section 4.3.1 provides a generally good guide for selecting raingauge weights, but if a particular weighting is known to perform well then use it.

The raingauge-based models (apart from Nutclough as data were not available) all underestimated the magnitude of the thunderstorm-driven flood peak during Event 4; see Figure 4.8. The models for Mytholmroyd and Walsden catchments gave reasonable simulations but the extent of underestimation for the Todmorden catchment, and the comparison of the flow peak magnitudes given in Table 3.6, strongly suggest that the high end of the Todmorden rating equation needs to be reassessed.

When attempting the radar-based model calibrations from scratch, it was immediately apparent that there were periods when the Nimrod 5km analysis was either over- or under-estimating the rainfall; this feature is evident in Figures 4.6 to 4.10. Coupled with this, the radar processing was upgraded to Cyclops during the period of calibration causing some differences (hopefully enhancements) in the Nimrod product. Using the automatic optimisation option within the PDM tended to result in the model trying to accommodate an extreme period of overestimation, giving an unsatisfactory calibration. Therefore, performing radar-based model calibrations from scratch was not possible.

To make progress, it was hypothesised that the only noticeable difference between the radar-based and raingauge-based model calibration parameters would relate to the timing and magnitude of the rainfall input. This specifically identifies the rainfall factor (f_c) and the time delay (τ_d) parameters. Therefore the radar-based model calibrations were performed by using the raingauge-based ones as a basis and then manually adjusting the rainfall factor and time delay parameters. During the radar-based model calibrations one must be aware that the periods of over/underestimation can severely affect the R^2 statistic. Also some emphasis was placed on Events 5 and 6 as they occur after the Cyclops upgrade, as do the assessment events. The resulting hydrographs for the radar-based calibrations (see Figures 4.6 to 4.10) highlight the difficulties encountered when trying to select the appropriate rainfall factor, with some events being over-predicted and others under-predicted.

The general conclusion is that the raingauge-based models provide more consistent flow simulations than the radar-based ones. This is mainly due to the consistency of the data sources; the method and equipment used in collecting the raingauge-based data have remained relatively constant over the period of study whereas the Nimrod product has evolved and experienced changes in terms of software and hardware, the most significant being the Cyclops upgrade to the radar processing software and the replacement of the Hameldon Hill magnetron.

Disappointingly, the radar-based models did not out-perform the raingauge-based ones for the thunderstorm-driven peak of Event 4: see Figure 4.8. This is slightly surprising as radar might be expected to be capable of estimating catchment average rainfall for highly spatially-varying convective events more accurately than using the relatively sparse network of raingauges. However, *when* the Nimrod product is performing well it can give similar results to the raingauge-based models and occasionally outperform them, as was the case. up to day 34 of Event 2 for Walsden (see Figure 4.6).

5 MODEL ASSESSMENT AND SENSITIVITY ANALYSIS

The primary concern of this section is to compare the performance of the raingauge- and radar-based models over a set of assessment events not used for model calibration. As discussed in Section 3.6 the selection of the assessment events, by the Met Office and Environment Agency, focussed on spatially-varying storms of convective origin. This resulted in the selection of three short-duration events (Events 7-9). A longer event (Event 10) was also selected by the Met Office and the Agency. However, the magnitudes of these events were relatively small in comparison to the calibration events: see Table 3.6 and 3.7. Therefore, an additional long period, with a substantial flow peak, was selected from early 2002 (Event 11). Table 3.7 lists the dates of the assessment events and are seen to all post-date the Cyclops upgrade on 1 September 2000.

This section also presents a sensitivity test on the use of a Nimrod rainfall forecast in place of the Nimrod rainfall analysis. The rainfall forecast, also at a 5 km resolution, is chosen to have a 1 hour lead-time. The test aims to provide a consistency check on the rainfall-runoff model operation using analysis and forecast rainfall estimates as input. It does not aim to formally assess the performance of Nimrod rainfall forecasts for use in flood forecasting, as then forecasts for each lead-time would be used.

A further sensitivity test is carried out using the higher resolution Nimrod 2 km analysis. This product is available at a 5 minute, rather than 15 minute, time-interval allowing potentially more accurate 15 minute rainfall accumulations to be formed. A third and final sensitivity test concerns the raingauge-based models. This aims to assess the sensitivity of the raingauge-based models for the Walsden and Mytholmroyd catchments to using raingauge weights derived *including* the Blackstone Edge raingauge which is available only for the later events (from 1 February 2001); see Section 4.3.1.

5.1 Model Assessment

This sub-section examines model performance for both raingauge- and radar-based models for each catchment over the prescribed set of assessment events. It has been found to be most revealing to consider each event in turn, allowing comparison of model performance across the four catchments event by event. This serves to focus on how well rainfall is estimated by radar from one event to the next, using rainfall-runoff model performance across the four catchments as an indicator.

The most informative method of assessing model performance is to study the hydrographs produced by the model and to compare these to the observed flows. These hydrographs have been produced for each catchment in event order: see Figures 5.1 to 5.5. The reader is reminded that the assessment events are typically much shorter in duration and smaller in magnitude than the calibration events and this is reflected in the appearance of the hydrographs.

The assessment is aided by the peak analysis which is summarised in Table 5.2. For the calibration events, the peak analysis (see Table 4.9) showed a consistent temporal behaviour with the upstream catchments peaking first before Mytholmroyd. This is not evident in all of the assessment events due to the nature of the spatially-varying convective rain.

The R^2 performance statistic for each catchment and event is listed in Table 5.1 but should be used in conjunction with the hydrographs and peak analysis when assessing a model's performance, especially for the shorter, low-peak events where timing errors can have a drastic affect on the R^2 statistic.

The performance of the models is discussed below on an event by event basis.

Event 7

Event 7 is the second smallest assessment event in terms of magnitude. The hydrographs presented in Figure 5.1 show that it is not, in general, very successfully modelled. Note that the Nutclough river gauging station was suffering an oscillatory error during this event, as discussed in Section 3.4. Over Event 7 the radar-based models perform similarly for all four catchments and significantly underestimate the peak; see Table 5.2. This is reflected in the R^2 statistics for the Nimrod 5km analysis listed in Table 5.1. For the Mytholmroyd and Walsden catchments the raingauge-based models perform marginally better than the radar-based ones: the hydrograph peaks of the raingauge-based simulations are slightly closer to the observed than the radar-based ones but the peak timing of the radar-based simulations are significantly better.

For the Todmorden and Nutclough catchments the only successful flow simulations are achieved by the raingauge-based models, producing R^2 statistics of 0.635 and 0.729 respectively. The corresponding hydrographs show the better peak prediction of the raingauge-based models, relative to the radar-based estimates, although it is still an under-prediction. The peak analysis also indicates that the raingauge-based models predict the timing of the peaks slightly more successfully.

Event 8

As the R^2 statistics suggest, Event 8 is well modelled by both raingauge- and radar-based models with the former giving a slightly better overall fit; see Table 5.1. In particular, the radar-based simulations for Walsden and Todmorden suffer some overestimation near the beginning of the event (Figure 5.2), reducing the respective R^2 statistics.

The peak analysis given in Table 5.2 shows that the timings of the raingauge- and radar-based models are very similar for all catchments except for Walsden where the radar-based model performs markedly better. The magnitude of the peaks are equally well predicted by both forms of model for the Nutclough and Walsden catchments. However, the magnitude of the Mytholmroyd peak is best simulated by the raingauge-based model whilst the radar-based model performs best for the Todmorden peak.

Although the R^2 statistics confirm that raingauge-based models perform most consistently over the entire event, the assessment shows the potential benefits radar can bring when radar is performing well as an estimator of rainfall: for example, the improved peak timing at Walsden and the peak magnitude at Todmorden.

Event 9

Event 9 is the smallest in terms of peak flow magnitude. The R^2 statistics (see Table 5.1) imply that the raingauge-based models (R^2 values range from 0.646 to 0.814) perform far better than the radar-based-ones (R^2 values range from -0.751 to 0.081). Inspection of the simulated hydrographs (see Figure 5.3) confirm this is the case. The general fit and shape of the raingauge-based simulations is very good whereas the stretches of overestimation associated with the Nimrod 5km analysis seriously affect the radar-based simulations. In particular, the radar-based flow simulation for Walsden over-predicts the first two peaks and the simulation for Nutclough seriously over-predicts the second peak.

The superiority of the raingauge-based models is evident in the percentage peak error presented in Table 5.2. Also, the peak analysis shows that this is the poorest simulated assessment event in terms of peak timing errors. The raingauge-based models have the best timing for the Mytholmroyd and Walsden catchments whilst the radar-based model has the best for Nutclough. Overall, Event 9 is simulated best by the raingauge-based models. However, the poor R^2 statistics and visual fit of the simulation for the radar-based model are in part a reflection of the small magnitude of the event.

Event 10

Event 10 covers a period immediately prior to calibration Event 6. This is a longer event (9 days) and the R^2 statistics are a good guide to the models' performance. Table 5.1 indicates that the Mytholmroyd, Todmorden and Walsden catchments have similar signatures of performance during this event with the raingauge-based models performing significantly better than the radar-based ones. The simulated hydrographs (see Figure 5.4) verify this and show the raingauge-based simulations agreeing well with the observed flows after initially overestimating. The radar-based simulations actually outperform the raingauge-based ones for the first few days before overestimating the flow for the remainder of the event. In particular, the badly overestimated final peak of the radar-based simulations seriously affects the R^2 statistics and, as this is the main peak of the event, the peak percentage error. The R^2 statistics for the Nutclough catchment are equally poor for both types of model. The simulated hydrographs show both models overestimating the flow for the entire event. The peak analysis (see Table 5.2) for all catchments shows that the timing errors of both types of model are very similar.

For all catchments other than Nutclough the raingauge-based models perform most consistently, although the first three days of the event are simulated best by the radar-based models whilst the raingauge-based ones perform best for the rest of the event. The observed flow at Nutclough is poorly simulated by both types of model.

Event 11

This event was chosen to broaden the set of assessment events so as to encompass larger peak flows. As the event is of the order of a month long, the R^2 statistic provides a useful measure of performance. Table 5.1 shows that the raingauge-based models perform very well with R^2 statistics ranging from 0.842 for Walsden to 0.954 for Mytholmroyd. The simulated hydrographs (see Figure 5.5) confirm the excellent agreement of the raingauge-based simulations with the observed flows, including good baseflow fits, and is a pleasing verification of the calibration. The peak analysis shows that the timing of the raingauge-based simulated peaks are all within one hour of the observed and that the magnitude is predicted very well by the Mytholmroyd and Todmorden models. The underestimation of the simulated peak at Nutclough is likely to be related to the limited exposure of the rating equation to high flows during calibration. A reassessment of the high end of the rating may be needed.

The R^2 statistics and simulated hydrographs indicate that the radar-based models do not perform as well over Event 11. The hydrographs are particularly informative and imply periods of both over- and under-estimation of rainfall by the Nimrod 5km analysis. The underestimation near day 10 of the event is due, in part, to a days worth of missing radar data on 25 January 2002 (see Table 3.3). The slight overestimation near day 16 for the Nutclough and Mytholmroyd models can be traced back to a noticeable error associated with the (25km radius) infill map (see Section 3.3). Other periods of over- and under-estimation are not easily attributable to a specific radar error. However, the radar-based models can recover fairly quickly from these periods. In fact the radar-based models perform on a par with the raingauge-based ones over the large peak event. The peak analysis shows that both types of model predict the magnitude of the event well with the radar-based model performing noticeably better for the Walsden catchment. Again, the raingauge-based models simulate the peak of the flow to within one hour of the observed whereas the radar-based models are more erratic: in particular, the Walsden peak is predicted 2h 45mins too late.

Overall, this event shows the consistency that can be achieved with the raingauge-based models. It also highlights how the frequent over- and under-estimation of the Nimrod analysis prohibits the radar-based model achieving a similar consistency. However, the fact that the substantial peak of this event is well simulated by the radar-based model provides an indication of what is possible *when* the Nimrod analysis is performing well as an estimator of rainfall. This also suggests that if a more consistent Nimrod product is achieved, then the radar-based models could become as effective, or more so in certain scenarios, as the raingauge-based models at simulating river flows.

Table 5.1 Evaluation performance (R^2 statistic) for each catchment using raingauge, Nimrod 5km analysis, Nimrod 2km analysis and Nimrod 1-hour lead-time forecast rainfalls.

Event	Rainfall input type	Catchment			
		Mytholmroyd	**Nutclough**	**Todmorden**	**Walsden**
7					
	Raingauge	0.154	0.729	0.635	-0.229
	Raingauge 2*	0.132			0.677
	5km analysis	-0.189	0.365	0.336	-0.277
	2km analysis	-0.095	0.293	0.680	-0.117
	5km forecast	-0.944	0.047	-0.975	-1.342
8					
	Raingauge	0.908	0.956	0.776	0.695
	Raingauge 2*	0.930			0.759
	5km analysis	0.717	0.888	0.548	0.105
	2km analysis	0.749	0.894	0.514	0.061
	5km forecast	-0.069	0.369	0.287	-0.268
9					
	Raingauge	0.814	0.646	N/A	0.751
	Raingauge 2*	0.789			-2.610
	5km analysis	0.081	-0.751	N/A	-0.584
	2km analysis	0.258	-1.590	N/A	-0.073
	5km forecast	-0.349	-0.381	N/A	0.203
10					
	Raingauge	0.527	-1.336	0.580	0.668
	Raingauge 2*	0.508			0.260
	5km analysis	-0.078	-1.320	-0.051	0.147
	2km analysis	0.107	-0.888	-0.256	0.513
	5km forecast	0.734	-0.652	0.608	0.604
11					
	Raingauge	0.954	0.936	0.929	0.842
	Raingauge 2*	0.949			0.849
	5km analysis	0.667	0.736	0.503	0.715
	2km analysis	0.794	0.842	0.594	0.805
	5km forecast	0.562	0.676	0.413	0.466

** indicates that Blackstone Edge raingauge data were included*

Table 5.2 Peak analysis for assessment events. Unbracketed terms relate to raingauge calibrations and bracketed terms to radar calibrations.

Event/ Catchment	Observed		Computed		Error	
	Peak	Time	Peak	Time	% peak	Time (h)
Event 7						
Mytholmroyd	13.6	15:15 10 Jun 02	7.5	14:30 10 Jun 02	45.0	0.75
			(6.8)	(15:00 10 Jun 02)	(49.1)	(0.25)
Nutclough	2.66	21:45 10 Jun 02	2.27	21:00 10 Jun 02	14.7	0.75
			(1.46)	(20:45 10 Jun 02)	(45.2)	(1.00)
Todmorden	2.67	12:45 10 Jun 02	1.92	12:45 10 Jun 02	28.1	0
			(1.50)	(12:15 10 Jun 02)	43.6	(-0.5)
Walsden	1.73	16:30 10 Jun 02	0.88	13:30 10 Jun 02	49.1	3.0
			(0.83)	(15:30 10 Jun 02)	(51.8)	(1.0)
Event 8						
Mytholmroyd	24.9	05:00 10 Aug 02	24.8	06:00 10 Aug 02	0.4	-1.0
			(29.7)	(05:45 10 Aug 02)	(-19.3)	(-0.75)
Nutclough	8.81	05:15 10 Aug 02	7.89	05:45 10 Aug 02	10.4	-0.5
			(9.53)	(05:45 10 Aug 02)	(-8.2)	(-0.5)
Todmorden	3.63	02:00 10 Aug 02	2.82	01:45 10 Aug 02	22.3	0.25
			(3.70)	(01:30 10 Aug 02)	(-1.9)	(0.5)
Walsden	1.31	09:15 10 Aug 02	1.39	05:00 10 Aug 02	-6.1	4.25
			(1.35)	(08:00 10 Aug 02)	(-3.4)	(1.25)
Event 9						
Mytholmroyd	8.92	05:30 10 Sep 02	8.74	03:45 10 Sep 02	2.1	1.75
			(10.7)	(00:30 10 Sep 02)	(-20.0)	(5.00)
Nutclough	2.47	00:45 10 Sep 02	2.32	03:45 10 Sep 02	6.2	-3.00
			(3.77)	(01:15 10 Sep 02)	(-52.8)	(-0.5)
Todmorden				N/A		
Walsden	1.05	04:00 10 Sep 02	0.96	03:00 10 Sep 02	7.9	1.0
			(1.11)	(01:00 10 Sep 02)	(-6.2)	(3.0)
Event 10						
Mytholmroyd	29.2	14:30 27 Oct 02	25.6	14:45 27 Oct 02	12.3	-0.25
			(48.8)	(14:45 27 Oct 02)	(-67.2)	(-0.25)
Nutclough	6.47	14:00 27 Oct 02	8.28	14:30 27 Oct 02	-28.1	-0.5
			(10.5)	(14:45 27 Oct 02)	(-61.6)	(-0.75)
Todmorden	4.23	13:30 27 Oct 02	3.77	13:15 27 Oct 02	10.8	0.25
			(8.71)	(13:15 27 Oct 02)	(-106.0)	(0.25)
Walsden	2.39	13:45 27 Oct 02	1.96	13:15 27 Oct 02	18.0	0.5
			(3.72)	(13:30 27 Oct 02)	(-55.6)	(0.25)
Event 11						
Mytholmroyd	81.2	03:45 11 Feb 02	84.1	04:15 11 Feb 02	-3.6	-0.5
			(82.8)	(04:15 11 Feb 02)	(-2.0)	(-0.5)
Nutclough	30.0	03:30 11 Feb 02	23.1	04:15 11 Feb 02	23.1	-0.75
			(23.4)	(05:00 11 Feb 02)	(22.0)	(-1.5)
Todmorden	12.2	02:00 11 Feb 02	12.4	02:15 11 Feb 02	-1.7	-0.25
			(12.7)	(01:15 11 Feb 02)	(-4.2)	(0.75)
Walsden	4.78	01:15 11 Feb 02	3.65	02:00 11 Feb 02	23.6	-0.75
			(4.30)	(04:00 11 Feb 02)	(10.1)	(-2.75)

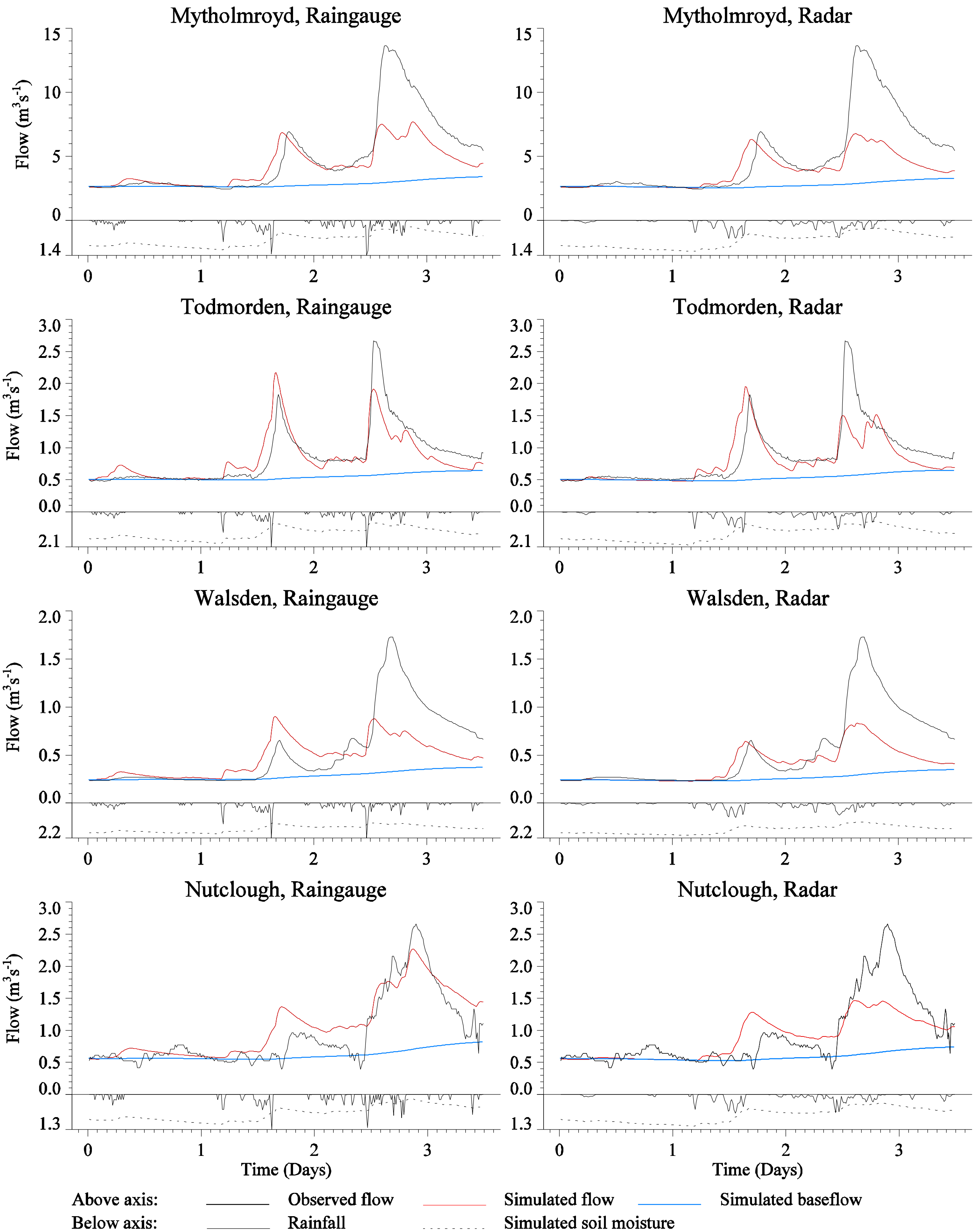

Figure 5.1 Hydrographs for Event 7: 00:00 10 June to 12:00 11 June 2002 (plus 2 day warm-up). The figure below the axis is the maximum rainfall (from either raingauge or 5km radar) for that catchment.

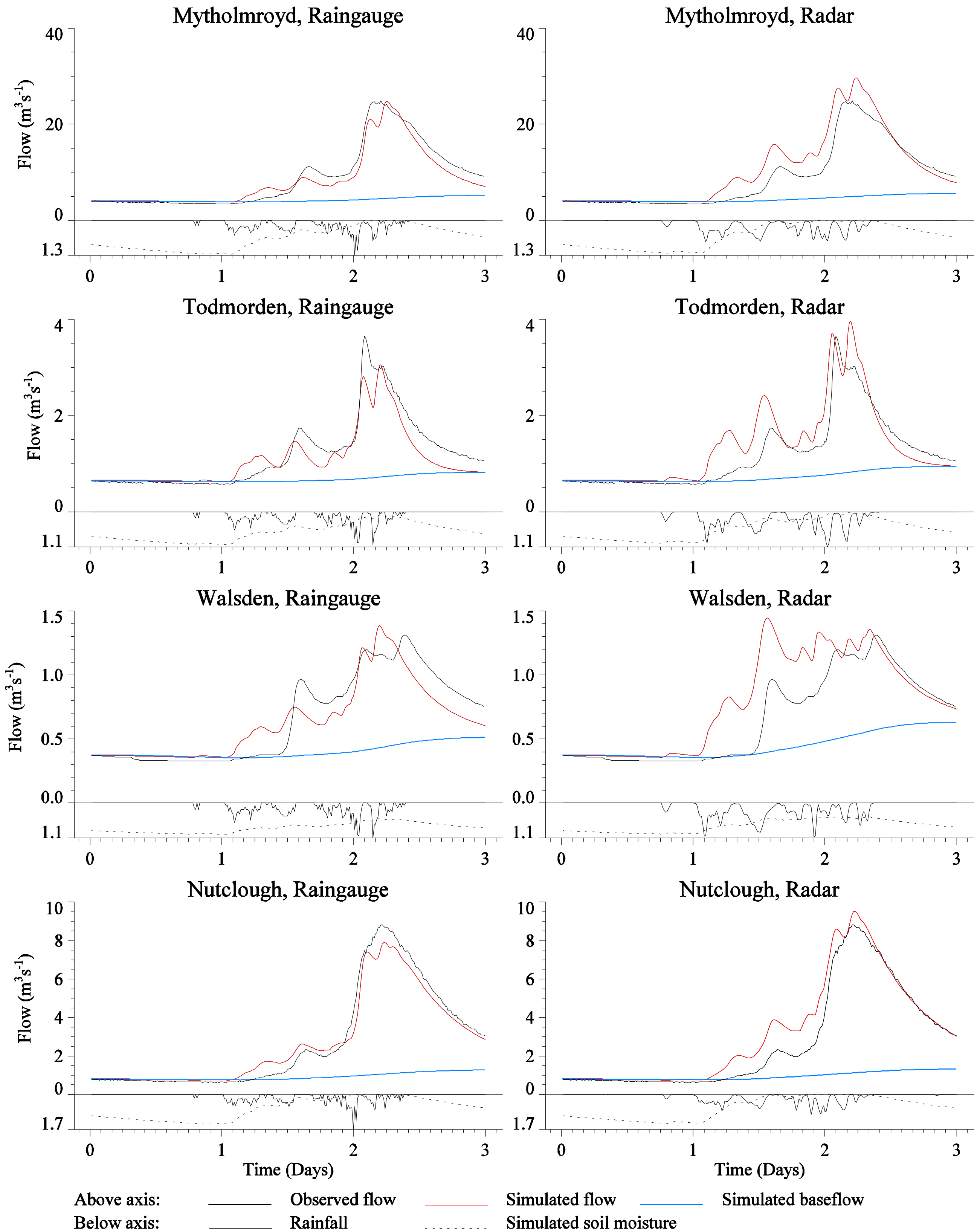

Figure 5.2 Hydrographs for Event 8: 00:00 9 August to 00:00 11 August 2002 (plus 1 day warm-up). The figure below the axis is the maximum rainfall (from either raingauge or 5km radar) for that catchment.

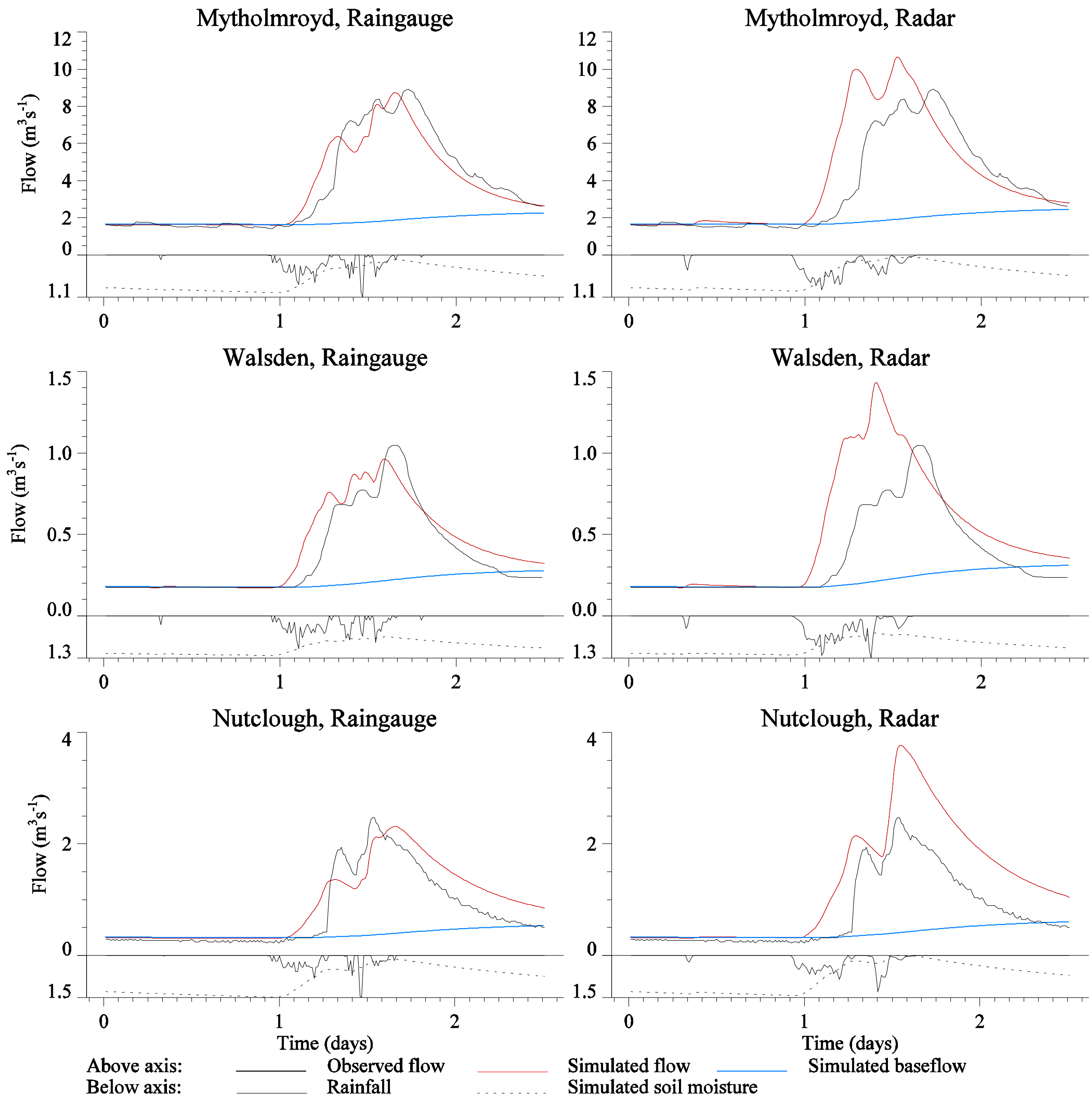

Figure 5.3 Hydrographs for Event 9: 12:00 9 September to 00:00 11 September 2002 (plus 1 day warm-up). The figure below the axis is the maximum rainfall (from either raingauge or 5km radar) for that catchment.

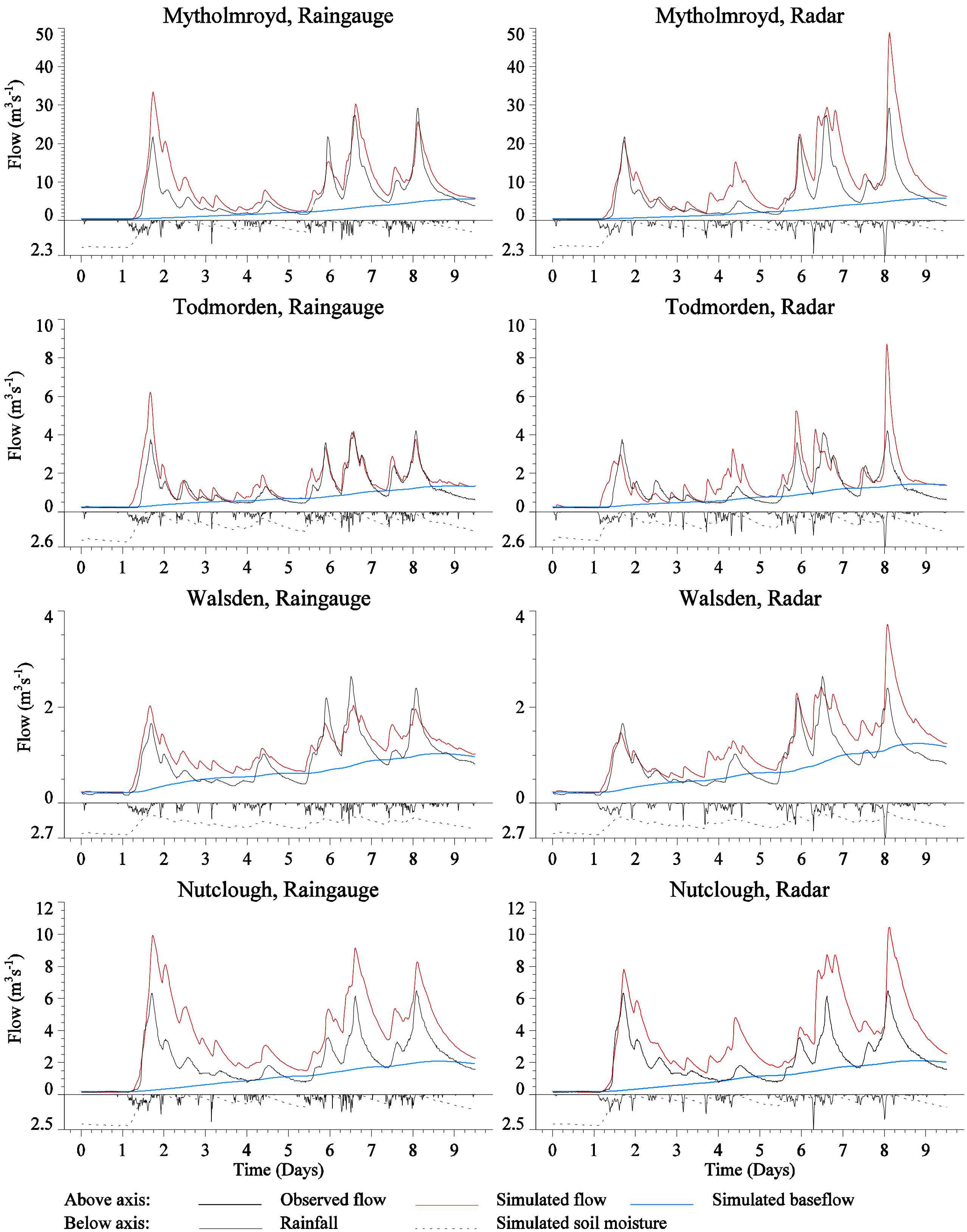

Figure 5.4 Hydrographs for Event 10: 12:00 20 October to 00:00 29 October 2002 (plus 1 day warm-up). The figure below the axis is the maximum rainfall (from either raingauge or 5km radar) for that catchment.

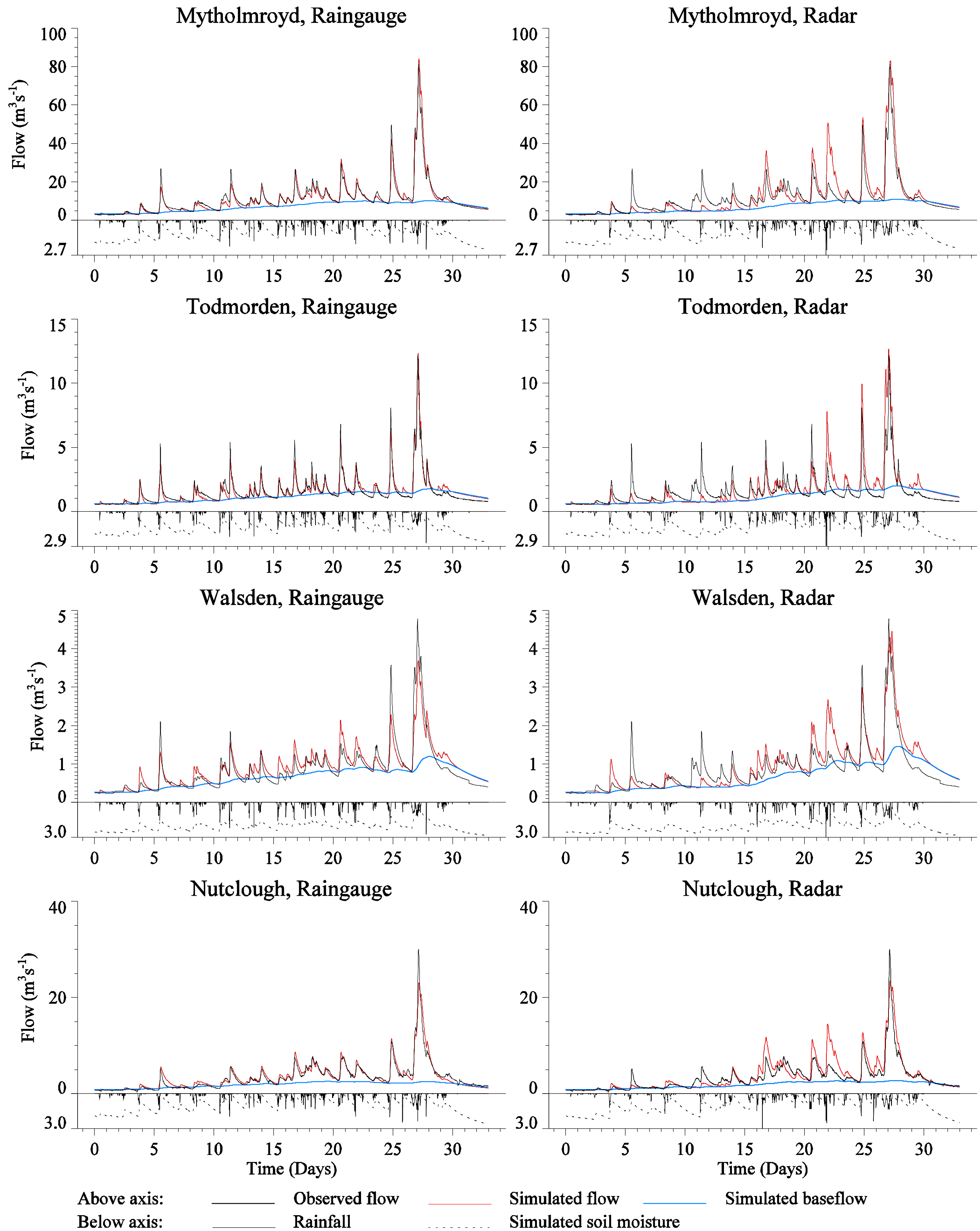

Figure 5.5 Hydrographs for Event 11: 00:00 16 January to 00:00 17 February 2002 (plus 1 day warm up). The figure below the axis is the maximum rainfall (from either raingauge or 5km radar) for that catchment.

5.2 Sensitivity Analysis

5.2.1 Radar-based sensitivity analyses

The radar-based sensitivity analyses aim to examine the response of the radar-based rainfall-runoff models to using different Nimrod estimates of catchment average rainfall as input. Two Nimrod products are tested: the Nimrod 2km analysis and the Nimrod one-hour lead-time forecast. The Nimrod 2km analysis product was chosen to assess the models' response to a finer spatial resolution product. It also has a higher delivery frequency of 5 minutes, compared to 15 minutes for the Nimrod 5km analysis. Therefore, the 15 minute rainfall accumulations are better defined as the average of four instantaneous values of rain-rate rather than just two. This could be particularly beneficial for rainfall estimation during convective storms. The averaging procedure used weights of 1/6, 1/3, 1/3 and 1/6.

The Nimrod rain-rate forecast product is available at a 5km resolution every 30 minutes and provides forecasts at 15 minute intervals up to 6 hours. A forecast lead-time of one hour was selected for the sensitivity analysis A long lead time was seen as inappropriate for convective rainfall events whilst a too short one would not differ significantly enough from the Nimrod 5km analysis. The main purpose of this sensitivity analysis is to test the consistency of rainfall-runoff model performance when Nimrod analysis and forecast estimates of rainfall are used as inputs. It does not aim to formally assess the Nimrod forecasts for use in rainfall-runoff models when forecasts for a sequence of lead-times would be used. The 1-hour ahead 15 minute rainfall accumulation forecasts were obtained from the 30 minute update frequency 15 minute interval rain-rate forecasts as follows. With t denoting the time of the forecast origin, the accumulation at time $t+60$ is calculated by averaging the rain-rates at $t+45$ and $t+60$ in the normal way. For the intervening time-step, the rainfall accumulation at $t+75$ is calculated from the forecast rain-rates at $t+60$ and $t+75$.

To help assess the sensitivity of the radar-based models, the R^2 statistics derived using both the Nimrod 2km analysis and the Nimrod forecast products are presented together in Table 5.1 for each event and catchment. To avoid a proliferation of figures, only the simulated hydrographs for Mytholmroyd are presented. Figures 5.6 to 5.7 show the simulations using the Nimrod 2km and forecast products for events 8 to 11; to aid comparison, the raingauge-based and Nimrod 5km simulations are presented as well. Event 7 is not displayed as the performance is poor for all types of rainfall input.

Nimrod 2km Analysis

The R^2 statistics in Table 5.1 indicate that generally the Nimrod 2km analysis rainfall estimate provides slightly better performance than the 5km analysis. This is confirmed by inspection the simulated hydrographs. The model simulations obtained using the 2km analysis rainfall estimates for Mytholmroyd are presented in Figures 5.6 to 5.7, where they can also be compared with those from using the 5km analysis and the raingauge-based models. The simulations for Event 8 and Event 9 (see Figure 5.6) show that using the 2km analysis provides marginally lower rainfall estimates which are reflected in the simulated flows. The reduced magnitudes of the simulated flows bring them closer to the observed and accounts for the improved R^2 statistic.

The simulations for Event 10 (see Figure 5.7) for the Mytholmroyd catchment show the 2km analysis rainfall estimates generally result in a better fit to the observed flow than when the 5km analysis estimates are used, although the first peak is simulated more successfully using the 5km analysis rainfalls. In particular, the overestimation of the final flow peak is less when using the 2km analysis rainfalls and is the main reason for the better R^2 statistic. Event 11 is a long event (34 days) and shows the simulations using the 2 and 5km analysis rainfalls are similar up to about day 15. Beyond day 15, the 2km analysis rainfalls give a better flow simulation, resulting in a better R^2 statistic. This improvement for Event 11 was evident for all catchment models.

Overall, this sensitivity analysis suggests that some improvement in flow simulation can be achieved using the higher resolution Nimrod 2km analysis rainfall estimates. Additional calibration using the Nimrod 2km analysis product could improve the simulations further. *A priori*, one would expect a higher spatial resolution product to give a better result as proved the case here. However, the degree to which the improvement is due to the increased spatial resolution or the increased temporal sampling is unclear.

Nimrod 5km one-hour lead-time forecasts

The R^2 statistics presented in Table 5.1 do not suggest an overall trend of improvement, or decline in the model performance, when using the Nimrod forecast product instead of the Nimrod 5km analysis. In fact the results indicate that the improvements or declines are event specific.

The simulations using the Nimrod forecast rainfalls for the Mytholmroyd catchment are present in Figures 5.6 to 5.7, where they can also be compared with simulations using raingauge and Nimrod 2 and 5km analysis estimates of rainfall. The simulations for Event 8 and Event 9 (see Figure 5.6) show that the forecast predicts the rain event but overestimates the rainfall considerably more than the other simulations.

The simulations for Event 10 (see Figure 5.7) for the Mytholmroyd catchment show the forecast-based simulation underestimating the peaks around days 2 and 6 and the 5km analysis rainfalls providing a better simulation of these peaks. However, for the remainder of the event the forecast-based simulation performs far better than the 5km analysis giving a better overall fit and R^2 statistic. This improvement occurs for all catchments. In fact, because the raingauge-based simulations overestimate the first peak by so much, the forecast-based simulations give the best R^2 statistic of all models for all catchments apart from Walsden (where the raingauge-based simulation is still best).

The simulations for Event 11 (see Figure 5.7) show the forecast-based simulations severely underestimating the flow at Mytholmroyd for the entire event and this is reflected in the low R^2 statistics. On the plus side, the peak of the event is reasonably well predicted.

In summary, the sensitivity analysis reveals that simulations using the Nimrod forecast product can be variable. For example, the simulations for Event 8 and Event 9 over-predict the observed flow whilst Event 11 is seriously under-estimated. However, the peaks of Events 8 to 11 are reasonably simulated although the raingauge-based and Nimrod analysis based models generally perform better. In general, the Nimrod forecasts appear to perform in a consistent way when used in the radar-based models calibrated using Nimrod 5 km analysis rainfall estimates. The deterioration in performance overall is what might be expected from the use of a rainfall forecast at one-hour lead time in place of a Nimrod analysis rainfall estimate . The comparability of raingauge- and radar -calibrated models has previously been noted. This suggests that, once sensible account has been taken of any differences in rainfall factor and time delay parameters, that raingauge-calibrated models may be used with radar-based rainfall forecasts, such as those provided by Nimrod, to extend the lead-time of flood forecasts and warnings.

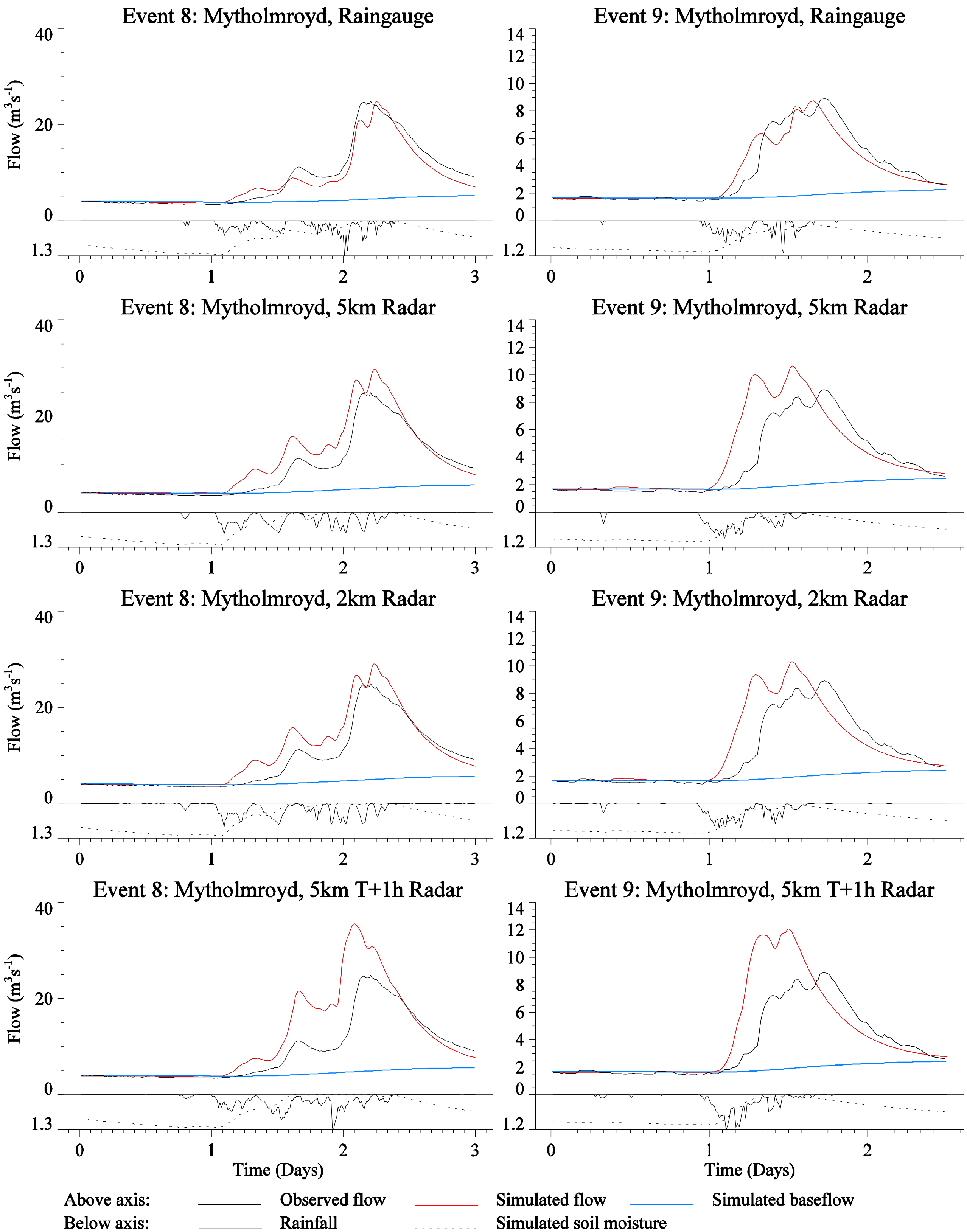

Figure 5.6 Hydrographs for Event 8: 00:00 9 August to 00:00 11 August 2002 and Event 9: 12:00 9 September to 00:00 11 September 2002 (plus 1 day warm up). The figure below the axis is the maximum rainfall (from any rainfall source) for that event.

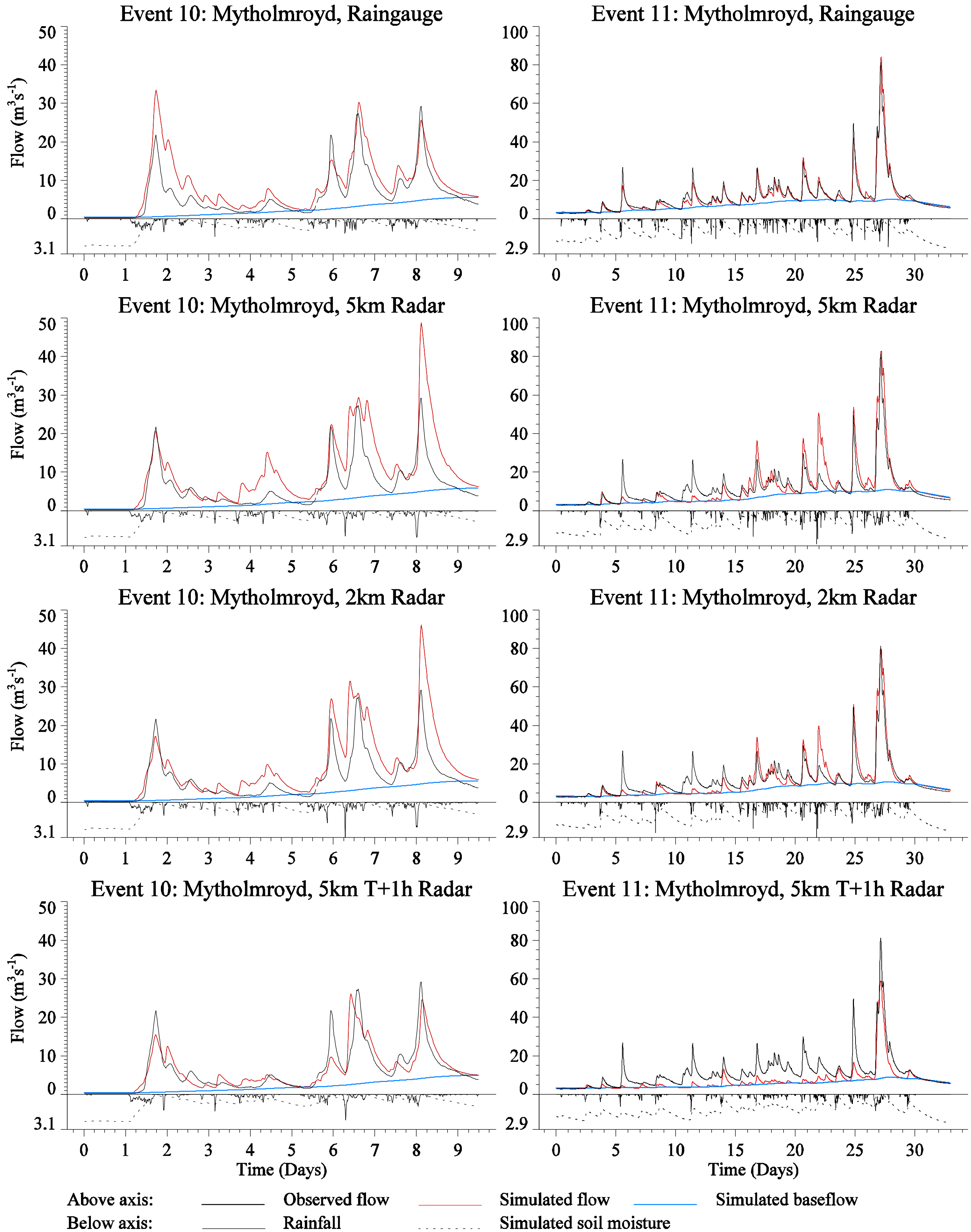

Figure 5.7 Hydrographs for Event 10: 12:00 20 Oct - 00:00 29 Oct 2002 and Event 11: 00:00 16 Jan - 00:00 17 Feb 2002 (plus 1 day warm up). The figure below the axis is the maximum rainfall (from any rainfall source) for that event.

5.2.2 Raingauge-based sensitivity analysis

The sensitivity analysis for the raingauge-based models aims to assess the effect of including the Blackstone Edge raingauge when calculating catchment average rainfall. As discussed in Section 4.3.2, this raingauge is the newest addition to the network with data only available from 1 February 2001. The strategy for selecting raingauge weights was performed with and without the Blackstone Edge raingauge. Including the raingauge was only found to affect the raingauge weights for two catchments, Mytholmroyd and Walsden; the weights are listed in Tables 4.3 and 4.4 respectively.

The sensitivity analysis was performed using the same PDM rainfall-runoff model parameters as were derived for the raingauge-based models *excluding* the Blackstone Edge raingauge. This included using the rainfall factor. In reality this factor is likely to be different for each set of raingauge weights used. However, using the same factor is reasonable for the purposes of the sensitivity analysis.

To aid the analysis, the R^2 statistics of the simulations including the Blackstone Edge raingauge have been calculated for each assessment event for both the Mytholmroyd and Walsden catchments; see Table 5.1. The statistics immediately indicate that the flow simulations for Mytholmroyd change little when Blackstone Edge raingauge is included: this is to be expected since the weightings do not change drastically by including the gauge (see Table 4.3). This confirms that the strategy detailed in Section 4.3.2 can result in good raingauge weightings.

Conversely, Table 5.1 indicates that the flow simulations for Walsden change noticeably as a result of including Blackstone Edge raingauge. Recall that the calibrated raingauge-based model uses the Environment Agency's weightings of 0.692 for Bacup and 0.308 for Gorple whilst the weightings in the sensitivity analysis are 0.4 for Bacup and 0.6 for Blackstone Edge. It is therefore not unexpected that the flow simulations are noticeably different. The simulations at Walsden for both sets of raingauge weights are presented in Figure 5.8 for events 7, 9, 10 and 11. Event 8 is omitted as there is little difference between the two simulations. The performance using the new set of weights is mixed. There is a substantial improvement in simulating the peak of Event 7 and this is reflected in the R^2 statistic improving from -0.229 to 0.677. Also the month-long Event 11 shows that the new weighting including Blackstone Edge can work well over a long period and performs marginally better than the old. On the other hand, the performance over Event 9 and Event 10 is worsened by using the new weight. In particular, Event 9 is extremely overestimated, but made more visually apparent by the low magnitude of the event. All in all, the new raingauge weighting for Walsden is as valid as the original and could be improved further by additional calibration.

Overall, the sensitivity analysis for the raingauge-based models confirms that the strategy for selecting raingauge weights (see Section 4.3.2) is generally good and that there is potential benefit in including the Blackstone Edge raingauge for the Mytholmroyd and Walsden catchments.

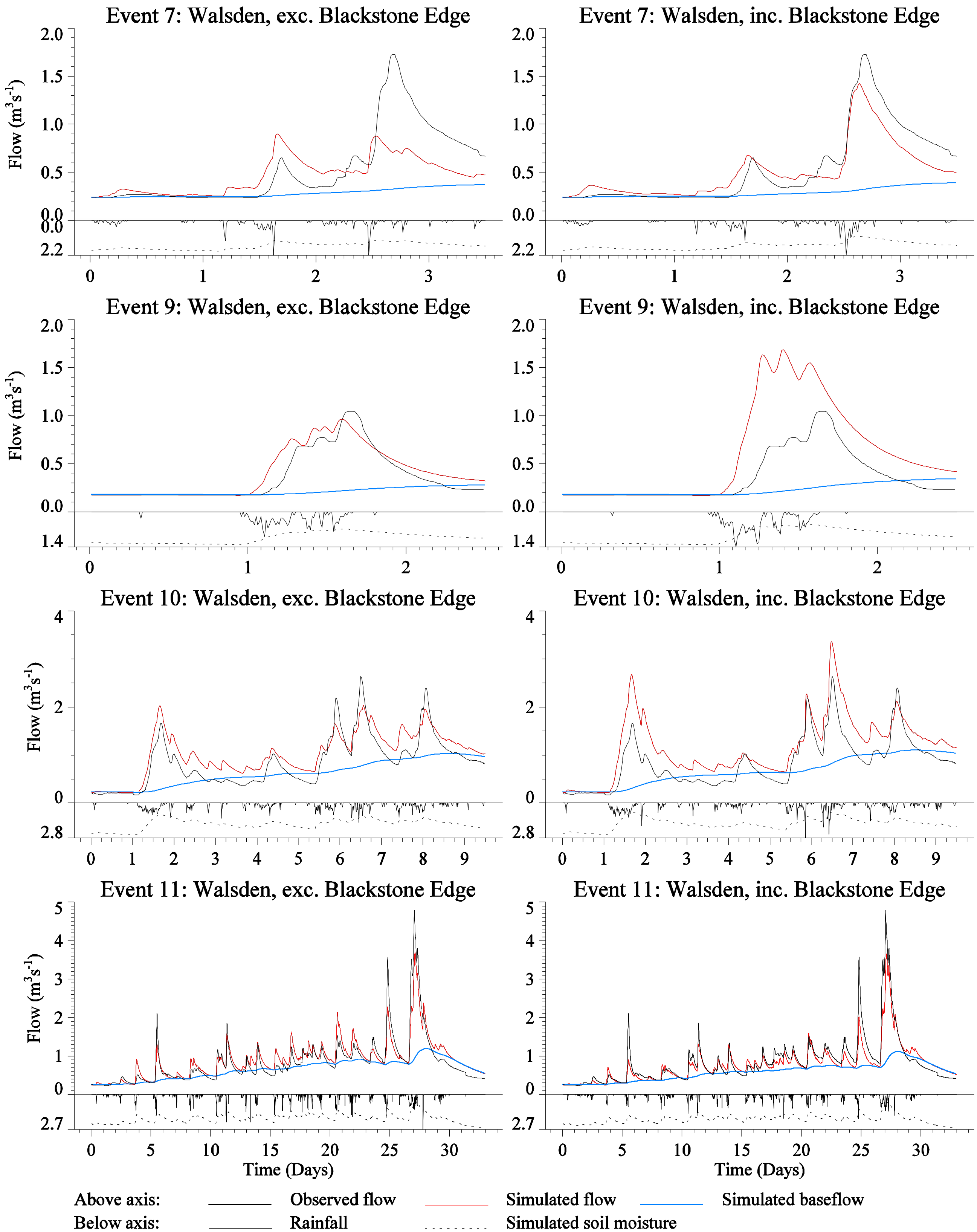

Figure 5.8 Hydrographs for a selection of assessment events at Walsden. Two different raingauge weights are used: one excluding the Blackstone Edge raingauge (left-hand column) and one including it (right-hand column).

5.3 Summary

The assessment of the raingauge- and radar-based PDM rainfall-runoff models detailed in Section 5.1 confirms that, as in model calibration, the raingauge-based models perform most consistently. This includes the short convective events (events 7, 8 and 9) where radar may have been expected to capture the spatial-variation of the rain and more accurately estimate the catchment average rainfall. The raingauge-based simulations are generally good for all events, the only noticeable exceptions being the Nutclough simulation overestimating the flow for Event 10 and the Mytholmroyd and Walsden simulations underestimating the flow for Event 7 where the disagreements are visually heightened by the low magnitude of the event. The raingauge-based models perform well for all catchments during Event 11, which is the longest event, and illustrate the success of the model calibrations.

The assessment of radar-based models again identifies periods of over- and under-estimation of the rainfall by the Nimrod 5km analysis. For example, the simulations for Event 11 show an underestimate near day 5 followed by overestimates near days 16 and 22. The inconsistency in the Nimrod analysis product is reflected in the simulations and the R^2 statistics; see Figures 5.1 to 5.5 and Table 5.1. For Event 7 and Event 9, which are short convective events, the radar-based models do not perform well, under- and over-estimating the flow respectively. For these events, the raingauge-based models easily outperform the radar-based ones. For events 8, 10 and 11 the Nimrod 5km analysis rainfall estimates perform reasonably well. In fact the radar-based simulations at Mytholmroyd and Nutclough for Event 8 are arguably as good as the raingauge-based ones. Event 11 also confirms that the radar-based models can recover from periods of over- or under-estimation and the peak of this event is particularly well simulated. However, there is little evidence of the radar-based models out-performing the raingauge-based ones, perhaps the only noticeable sign being the occasional improvement in the simulated peaks of the radar-based simulations.

The sensitivity analysis of the radar-based models to using different Nimrod products shows that the higher spatial resolution and temporal sampling of the Nimrod 2km analysis rainfalls improves the simulations slightly. However, whether the improvement is due to the finer spatial resolution or the more frequent temporal sampling of the 2km product is not determined. Sensitivity analysis using the Nimrod 5km one-hour lead-time forecast does not indicate an overall improvement or decline in the simulations. In fact the results are event specific. For example, the simulated flow for Event 11 consistently underestimates the observed whilst the simulations for Event 8 and Event 9 overestimate the observed flow. However, the peaks of events 8 to 11, some of which include convective rain storms, are still reasonably simulated by the Nimrod forecast-based model. There is no evidence that the Nimrod forecast product is inconsistent with the analysis product and that the same radar-based rainfall-runoff model cannot be used for both. Further, the comparable nature of raingauge- and radar-based models suggests that use of the raingauge-model with Nimrod rainfall forecasts will be consistent, provided some consideration is given to the rainfall factor, and to a lesser extent the time-delay parameter.

For the raingauge-based models, a sensitivity analysis was performed to assess the effect of including data from a more recently installed raingauge - at Blackstone Edge - when calculating catchment average rainfall. The inclusion of the raingauge only affected the rainfall estimates for the Mytholmroyd and Walsden catchments. The new set of weights for Mytholmroyd only differ marginally from the old and this is reflected in very similar simulations being produced with either weighting. For the Walsden catchment, the original Environment Agency raingauge weighting uses Bacup (0.692) and Gorple (0.308) whilst the new one is significantly different and involves Bacup (0.4) and Blackstone Edge (0.6). Therefore, the simulations using the new weighting are noticeably different with improvements for some events and deterioration for others. Overall, the new raingauge weighting for Walsden is as valid as the original and reinforces the view that the weight selection strategy given in Section 4.3.2 generally produces good results.

6 SUMMARY, CONCLUSIONS AND RECOMMENDATIONS

A summary of the report, including conclusions and recommendations, is presented here under the following thematic headings: catchment characteristics, data quality and availability, model calibration, model assessment, sensitivity analysis, improvements to Project design if repeated, and proposed model calibration procedure for Environment Agency use.

Catchment characteristics

(i) Reservoir influences*:* The influence of reservoirs on the natural flow regime of the modelled catchments in the Upper Calder cannot be ignored. For modelling purposes, reservoir drainage areas have been excluded from the total catchment drainage area to derive the natural drainage area required for rainfall-runoff modelling. Models in operational use by the Agency use a mix of total and naturally draining catchment areas. The natural catchment boundaries, excluding the reservoir-drained areas, should be made available to the Environment Agency for calculation of catchment average rainfall from Nimrod products.

More knowledge of reservoir management and releases could potentially lead to improvements in modelling. This applies in particular to Walsden which is the smallest catchment and currently the least well modelled.

Data quality and availability

(ii) Data archive problems. Pre-2001 radar data were retrieved by the Met Office from their Radar Data Archive. The archive was found to be surprisingly incomplete. Infilling of the missing periods using different Nimrod products proved time consuming.

Data for 2002 were originally to be provided by the Met Office but periods of data were irretrievably lost during the relocation to Exeter. Comparison of the available Met Office data with that held in archive at CEH showed the Met Office data to be less complete. Therefore all 2002 data were retrieved from CEH. Although some infill of missing data was required, this was far less than needed for the Met Office supplied data.

(iii) Data quality control. The quality control process for the radar data was time consuming relative to that required for the flow and raingauge data. The Met Office performed their own analysis on the data they provided. CEH created rainfall accumulation maps to expose areas of anomaly, rainfall accumulation time-series comparing values from a raingauge with the coincident radar grid-square values, and time-series of catchment average rainfall. The individual frames were viewed through Hyrad and assessed in conjunction with the Met Office Daily Weather Reports. This exposed the anomalous influence of the infill map for Hameldon Hill radar, where a higher beam is used within a 25km radius of the radar. Occasionally the beam infill causes a discontinuity in the Nimrod image and can give anomalous radar rainfall values across the Upper Calder catchment. The analysis of the raingauge data confirmed that the raingauge at Gorple, previously thought to under-record, is now recording correctly.

(iv) Significant radar upgrades. Two major upgrades affecting the Hameldon Hill radar occurred during the study period: the processing software upgrade to Cyclops on 1 September 2000 and the magnetron replacement on 23 August 2001. Between the end of the study period and the writing of this report (August 2004), further changes have occurred: the radar receiver unit was upgraded on 11 December 2002 and Cyclops was upgraded to version 5.0 on 19 February 2003. Also the upgrade to RadarnetIV is imminent. In contrast to these changes to the radar data source, the method of raingauge estimation of rainfall has remained constant with the only major change being the extension of the raingauge network to include Blackstone Edge from 1 September 2001.

(v) Problems with river level recording. Occasional problems with recorded river levels have been identified during their quality control. The recorder at Walsden appears unreliable at low levels with sporadic jumps in level being common. During 2002, river levels recorded at both Nutclough and Mytholmroyd suffer oscillations. A noticeable jump (downwards) occurred for both Mytholmroyd and Todmorden during September 2002. No cause has been ascribed but it is possible that datum shifts have occurred during maintenance work at these stations.

Model Calibration

(vi) Raingauge weighting strategy. A strategy for selecting raingauge weights for use in calculating catchment average rainfall from network raingauge data has been developed using new 3D and 3D SAAR weighting methods.

(vii) New raingauge-based model calibrations. Although existing raingauge-based model calibrations existed for some catchments, new calibrations were developed from scratch. Good results were achieved for all events. The upper end of the model-derived rating (stage-discharge relation) for Todmorden may need to be reassessed with the benefit of more extensive calibration data. This applies to a lesser extent to Nutclough. Event 6 for the Mytholmroyd and Todmorden catchments proved difficult to model. This event post-dates the jumps in level that occurred during September 2002 and could be linked to datum changes at these sites, since other causes (for example, potential evaporation) were investigated and discounted.

(viii) Radar-based model calibration. Data quality control of the radar data indicated that the Nimrod 5km analysis product occasionally over- and under-estimated the rainfall. However, this became most apparent when attempting to calibrate the radar-based models. Coupled with this difficulty affecting model calibration, the radar processing was upgraded to Cyclops during the calibration period causing some differences in the Nimrod product. As a consequence, use of automatic optimisation for model parameter calibration was not a viable option and it proved difficult to start calibration of the radar-based model from scratch. Progress was made by hypothesising that the only major differences between the raingauge- and radar-based model parameters would relate to the timing and magnitude of the rainfall input. This directed the focus of radar-based model calibration at the rainfall factor and time delay parameters. Using the raingauge-based model parameters and optimising the rainfall factor and time delay manually resulted in reasonable radar-based model calibrations. The radar-based model was found to recover reasonably quickly from over- and under-estimation of rainfall, implying that a particular period of radar error did not affect the consequent simulation. However, this may not be the case for other types of catchment where water storage and depletion effects are more influential and long-lasting.

(ix) Conclusions drawn from the model calibration. In general, the raingauge-based models provide more consistent flow simulations than the radar-based ones. This reflects the consistency of the data sources as outlined above. This is seen as a major finding of the study.

Radar-based flow simulations did occasionally perform best for the Walsden catchment. This is probably due to the size of the Walsden catchment (10.4 km^2 natural drainage area) and that no raingauges lie within the catchment. The nearest raingauge is Blackstone Edge and is 2km away. The implication is that, for such a small catchment, capturing the spatial-distribution of rainfall within the Upper Calder catchment (121 km^2 natural drainage area) becomes particularly important. This leads to the conjecture that some threshold of catchment-size to nearest-gauge exists which controls the relative superiority of radar and raingauge estimates of catchment average rainfall for input to rainfall-runoff models.

Model Assessment

(x) Conclusions drawn from the model assessment. An assessment of events not used for calibration, again revealed that raingauge-based models perform best. This was the case even for the convective, spatially-varying rainfall events. The consistency in performance from calibration to assessment events suggests the recommended practice of selecting calibration events which contain both stratiform widespread and convective spatially-varying rain events is effective.

The radar-based models were found to over- and under-estimate, as was the case for model calibration, but did perform well for some events. Although the magnitude of the simulated peaks never seriously outperformed the raingauge-based simulations, the timing was occasionally significantly better using radar rainfall.

Sensitivity Analysis

(xi) Effect of increased spatial resolution of radar data. There was a general (minor) improvement of the radar-based models using the Nimrod 2km analysis rainfall in place of the Nimrod 5 km analysis rainfall. Since the 2 km product was available at a better temporal frequency (5 minutes rather than 15), the improvement could be attributed to a combination of higher spatial resolution and increased temporal sampling.

(xii) Consistency of Nimrod rainfall forecasts. The effect of using the Nimrod forecast product as input to the radar-based model was event specific, improving some simulations and worsening others. This demonstrated the relative consistency of the forecast and analysis Nimrod radar products when used in a radar-based model.

(**xiii) Sensitivity to inclusion of an additional raingauge.** Raingauge weights derived *including* the Blackstone Edge raingauge were equally valid to those used in calibration which *excluded* it. This outcome suggests that the raingauge weight selection strategy provides a good guide to combining raingauge values to estimate catchment average rainfall. Note that the rainfall factor model parameter is expected to be different for different raingauge weightings. Thus, explicit calibration of this parameter for the model *including* the Blackstone Edge raingauge should further improve model performance.

Improvements to Project design if repeated

(ix) Nimrod 2km analysis product. Ideally the Nimrod 2km analysis product (or the Nimrod 1 km analysis available for more recent events and catchments within 50 km range of a radar), available every 5mins, should be used for model calibration.

(x) Stable Nimrod Product period. The period of study should only date back to the most recent significant change in the Nimrod product: for example, the Cyclops or RadarnetIV upgrades.

(xi) Radar-raingauge merging. Evidence from previous studies has indicated the clear benefits of merging radar and raingauge estimates of radar for flood forecasting. The prescriptive nature of the present study has meant that this obvious and straightforward path to exploit the full benefit of weather radar has not been pursued.

(xii) Improved handling of reservoirs. More information about reservoir management and controlled releases could improve modelling.

(xiii) Hydrometric changes. Details of any changes relating to the river gauging stations need to be considered in relation to their impact on modelling. For example, datum shifts, major maintenance and changes to rating equations can have serious consequences to model performance.

(xiv) Grid-based rainfall-runoff models. A future investigation could investigate the potential benefits of using a grid-based rainfall-runoff model spatially-configured on the weather radar grid.

Proposed model calibration procedure for Environment Agency use

The proposed procedure for model calibration is set down separately for raingauge- and radar-based calibrations and is appropriate for both stratiform and convective spatially-varying rainfall. If a good raingauge-based calibration already exists for a catchment then this should be used, only carrying out the radar-based model calibration.

Raingauge-based model calibration

Before embarking on a raingauge-based calibration, one must be aware of any hydrometric changes that have occurred and their possible impact on rainfall-runoff modelling. Factors such as datum shifts and major maintenance need to be considered.

Step 1: Event selection
Select a variety of calibration events encompassing a mix of stratiform widespread and convective spatially-varying rainfall periods. Generally it is good practice to select more recent events but not so recent that the data have not been checked.

Step 2: Data Quality Control
Quality control of the data should be performed across the whole period of study (i.e. not just the calibration events), noting any periods of missing or suspect data. If an event is affected, it should be removed from the calibration set. The main forms of quality control are listed below.

Raingauge data:

- Compare cumulative rainfall time-series, over periods of 1-3 month, for all 15 minute tipping bucket raingauges in the vicinity.
- Compare these with daily totals if available.

Level/flow data:

- If a stage-discharge relation is known for the catchment, convert levels to flows and examine hydrographs produced over periods of 1-3 months duration. Comparison with hydrographs from different catchments in the vicinity can be useful for identifying suspect periods.
- If a stage-discharge relation is **not** known for the catchment, examine the stage hydrographs over 1-3 month periods. The stage-discharge equation should then be derived within the PDM calibration. It is not advisable to base it on other stage-discharge equations used in encompassing or neighbouring catchments.

Step 3: Raingauge weights
Derive raingauge weights using the strategy outlined in Section 4.3.1 (unless a good set of weights are already known).

Step 4: Model calibration
Perform model calibration, either from scratch or starting from a previous calibration. This can involve investigation of which raingauge weights perform best.

Radar-based model calibration

As for the raingauge-based model calibration, one must be aware of any hydrometric changes and their possible impact on modelling. In addition, one must also be aware of any significant radar upgrades that have occurred and when. For example, the processing software upgrade to Cyclops on 1 September 2000.

Step 1: Event selection.
Select a variety of calibration events to include stratiform widespread and convective spatially-varying rainfall. Events should be selected as recently as possible to avoid capturing different versions of Nimrod products.

Step 2: Data retrieval and calculating catchment average rainfall
Two options are available for obtaining radar-derived catchment average rainfall for the calibration events, the preferred source being 2km (and/or 1 km) data.

(i) In some regions of the Environment Agency (for example, Northeast), time-series of catchment average rainfalls are calculated in real time through Hyrad and archived.

(ii) Hyrad can be used to calculate catchment average rainfalls retrospectively, from archived radar data, for a given event.

(This project has shown that, over the events in 2002, the Nimrod 2km and 5km analysis and 5km forecast data were reasonably complete in the CEH archive. This uses the same datafeed from the Met Office as the Agency employs. Surprisingly, the CEH archive was found to be more complete than the Met Office for these Nimrod products, although this may not be the case for more recent data.)
Consider using a merged radar-raingauge rainfall estimate if available.

Step 3: Data Quality Control

Radar data:
Other than noting missing periods of radar data, quality control procedures can be time consuming. In fact, using the model calibration procedure to identify suspect periods of radar data proves to be the quickest way of performing quality control, circumventing the need to analyse each radar image in detail. However, viewing the event through Hyrad can be informative to identify the type of rainfall event. Using Hyrad to obtain rainfall accumulation maps and time-series (for catchments and grid-squares containing raingauges) can also highlight spatial and temporal anomalies.

Level/flow data:
As for raingauge-based model calibration.

Step 4: Model calibration

- Ideally, attempt to carry out a radar-based model calibration from scratch across all calibration events.
- If automatic optimisation proves unsatisfactory, then retry removing any obviously over- or under-estimated events.
- If automatic optimisation of the reduced set of calibration events still proves unsatisfactory, then use the raingauge-based calibration parameters and manually optimise the rainfall factor and time delay parameters.

7 REFERENCES

Austin, R.M., Bell, V.A., Jones, D.A., Moore, R.J. (1997) *River Calder Flood Warning Improvements RFFS Model Network*. Contract Report to The Environment Agency, November 1997, 39pp.

Bell, V.A., Carrington, D.S., Moore, R.J. (2001) *Comparison of rainfall-runoff models for flood forecasting. Part 2: Calibration and evaluation of models.* Environment Agency R&D Technical Report W242, Research Contractor: Institute of Hydrology, September 2001, Environment Agency, 239pp.

CEH Wallingford (2001) PDM Rainfall-Runoff Model. Version 2.1, September 2001. (Incorporates: Practical User Guide, Guide, Practical User Guide to the Calibration Shell, User Manual, Training Exercises).

Collier, G.C. (1989) *Applications of weather radar systems.* Ellis Horwood.

Gill, P.E., Murray, W. and Wright, M.H. (1981) *Practical Optimisation*, Academic Press.

Golding, B.W. (1998) Nimrod: A system for generating automated very short range forecasts. *Meteorol. Appl*. **5**, 1-16.

Harrison, D.L., Driscoll, S.J. and Kitchen, M. (2000). Improving precipitation estimates from weather radar using quality control and correction techniques. *Meteorol. Appl*. 6, 135-144.

Moore, R.J. (1999) Rainfall and flow forecasting using weather radar. In: R. Casale and C. Margottini (eds.), *Floods and landslides: Integrated Risk Assessment*, Chapter 6, 83-100, Springer.

Moore, R.J., Austin, R.M., Carrington, D.S. (1993) *Evaluation of FRONTIERS and Local Radar Rainfall Forecasts for use in Flood Forecasting Models.* R&D Note 225, Research Contractor: Institute of Hydrology, National Rivers Authority, 156pp.

Moore, R.J., Bell, V.A. & Carrington, D.S. (2000). Intercomparison of rainfall-runoff models for flood forecasting. In: M. Lees and P. Walsh (eds.), *Flood forecasting: what does current research offer the practitioner?* Occasional Paper No. 12, British Hydrological Society, 69-76.

Nelder, J.A. and Mead, R. (1965) A simplex method for function minimisation*,* *Computer Journal,* 7, 308-313.

O'Connor, K.M. (1982) Derivation of discretely coincident forms of continuous linear time-invariant models using the transfer function approach, *J. Hydrology*, 59, 1-48.

Sauvageot, H. (1992) *Radar Metoerology.* Artech House

Thiessen, A.H. (1911) Precipitation for large areas. *Monthly Weather Review*, 39, 1082-1084.

APPENDIX A SYNOPTIC CONDITIONS FOR THE PEAK RAINFALL PERIODS

Appendix A provides brief synoptic descriptions of the peak rainfall periods within each of the events used in this study. The Meteorological Office Daily Weather Summary, the Royal Meteorological Society monthly weather log and the Journal of Meteorology have been used as sources of information. A surface pressure chart for each period, taken from the Meteorological Office Daily Weather Summary, is included. Typical radar images, produced from the Nimrod products by the Hyrad display client, are included to aid visualisation of the peak rainfall period and its relation to the Upper Calder study area.

Event 2: 24 October 1998

The day started dry, apart from a few showers in the Outer Hebrides and Northern Isles. Rain, heavy at times, spread into all places southwest of a line from Glasgow to the Isle of Wight by dawn, while showers still peppered Lewis and the Northern Isles. During the morning a depression moved in from the west with its centre passing over Northern Ireland. The associated rain moved east over the morning period, reaching across all parts of Britain by midday. Meanwhile, the rain had turned to showers in Northern Ireland. The wind also increased with the advance of the rain.

The afternoon saw the rain continue but with a change to showers from the west with time. By dusk the rain was mostly confined to East Anglia, southeast England and the Northern Isles. The showers were fast moving in the strong wind. Soon after dark the rain cleared to the east, leaving a mixture of very blustery showers across the whole country. The showers were most frequent in the west and in northern Scotland, where they merged into more persistent rain. Temperatures were around, or a little above, normal in most parts of the country.

The first radar image in Figure A.2, at 12:30, is for the Nimrod 5km rain-rate analysis and is why, as opposed to the single site radar data, the image fills the area. This image shows the widespread rain affecting the catchment (outlined on the image). The later radar image, at 19:45, is for the Nimrod 5km analysis and shows the showers that had developed by the evening.

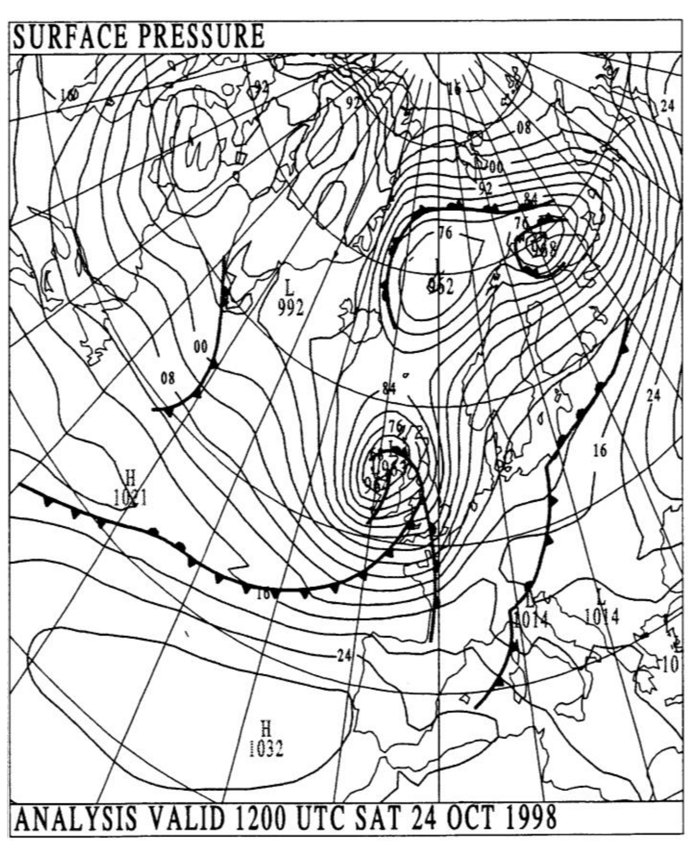

Figure A.1 Surface pressure chart at 12:00 24 October 1998

12:30 24 October 1998 **19:45 24 October 1998**

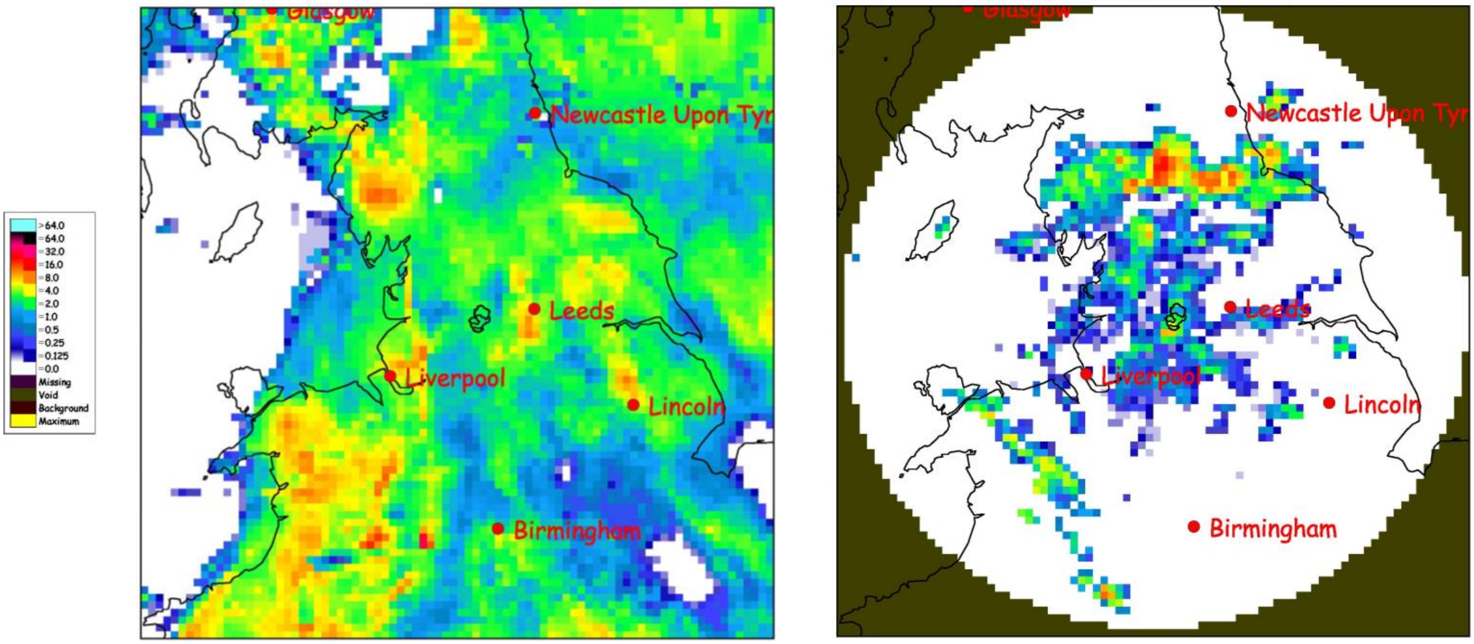

Figure A.2 Nimrod 5km rain-rate analysis (12:30) and Nimrod 5km analysis (19:45) on 15 January 1999

10:00 15 January 1999 **19:30 15 January 1999**

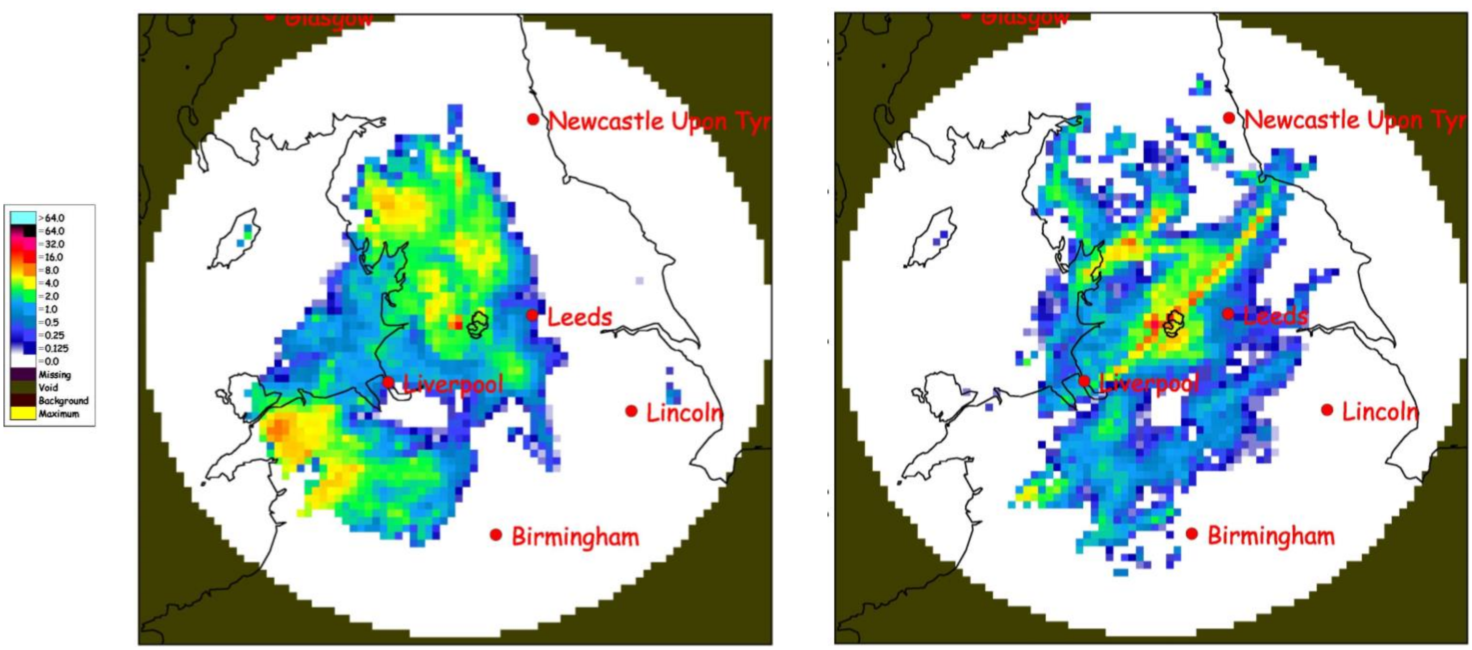

Figure A.3 Nimrod 5km analysis at 10:00 and 19:30 15 January 1999

Event 3: 15 January 1999

Most of England and Wales had a dry night. Northern Ireland had a wet day with some heavy rain associated with a depression centred northwest of Scotland (see Figure A.4). The rain spread across remaining parts of Scotland, Wales and western parts of England through the morning. Through the afternoon the rain pushed east across the rest of England. For much of the day the heaviest rain was over western and especially south-western parts of England. It was a windy day generally, especially so in the west and north. Most places were mild or very mild but temperatures were close to normal in the far north.

Two radar images are given, using the Nimrod 5km analysis, in Figure A.3 with the Upper Calder catchment overlain. The first image, for 10:00, shows largely stratiform rain associated with the passing of the warm front. Note the high rain-rates situated to the east of the catchment: these are caused by the Hameldon Hill radar overestimating rain-rate in its immediate vicinity. Later in the day the cold fronts move across the Upper Calder bringing more spatially-variable rain. The second radar image in Figure A.3, for 19:30, shows convective rainfall affecting the Upper Calder catchment as the second cold front passes through.

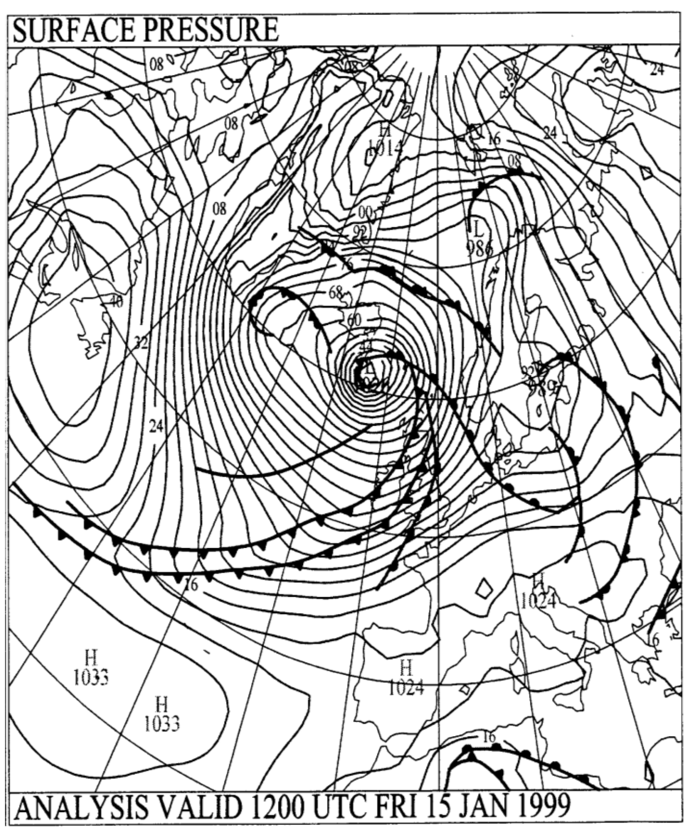

Figure A.4 Surface pressure chart at 12:00 15 January 1999

Event 4: 3-4 June 2000

A complex low pressure system controlled the weather over this period: see Figure A.5. In the early hours of the 3rd, rain persisted in a band extending from the south-west approaches across southern Ireland and into the Scottish Borders. Mist and fog did spread across central England and into East Anglia. The mist was slow to clear western parts with rain and drizzle persisting and becoming moderate, at times extending into the Pennines. It was bright with sunshine in the southeast with the back edge of the rain slowly spreading north. Late on, a band of thundery showers ran up through western Hampshire and across into the east Midlands. Suffolk also experienced thunder just before midnight.

Overnight on the 3rd/4th, heavy rain affected northern England and southern Scotland with localised thundery downpours. Thunderstorms were reported across Lincolnshire and Yorkshire into the early hours of the 4th. During the day, rain affected much of northern England, Northern Ireland and southern and central Scotland, although it turned lighter and more intermittent with time. During the evening, outbreaks of rain continued over northern England, Northern Ireland and southern and central Scotland.

Both images in Figure A.6 are for the Nimrod 5km analysis at 23:15 3 June. The first image shows the localised thundery downpours affecting northern England. The second image is an enlarged view of the Upper Calder emphasising the spatial variation over the study catchments.

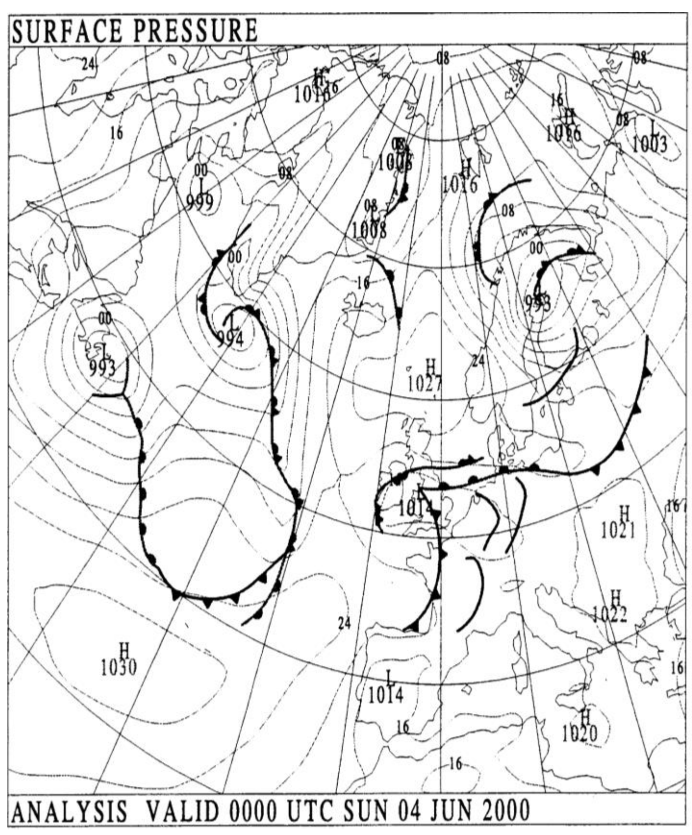

Figure A.5 Surface pressure chart at 00:00 4 June 2000

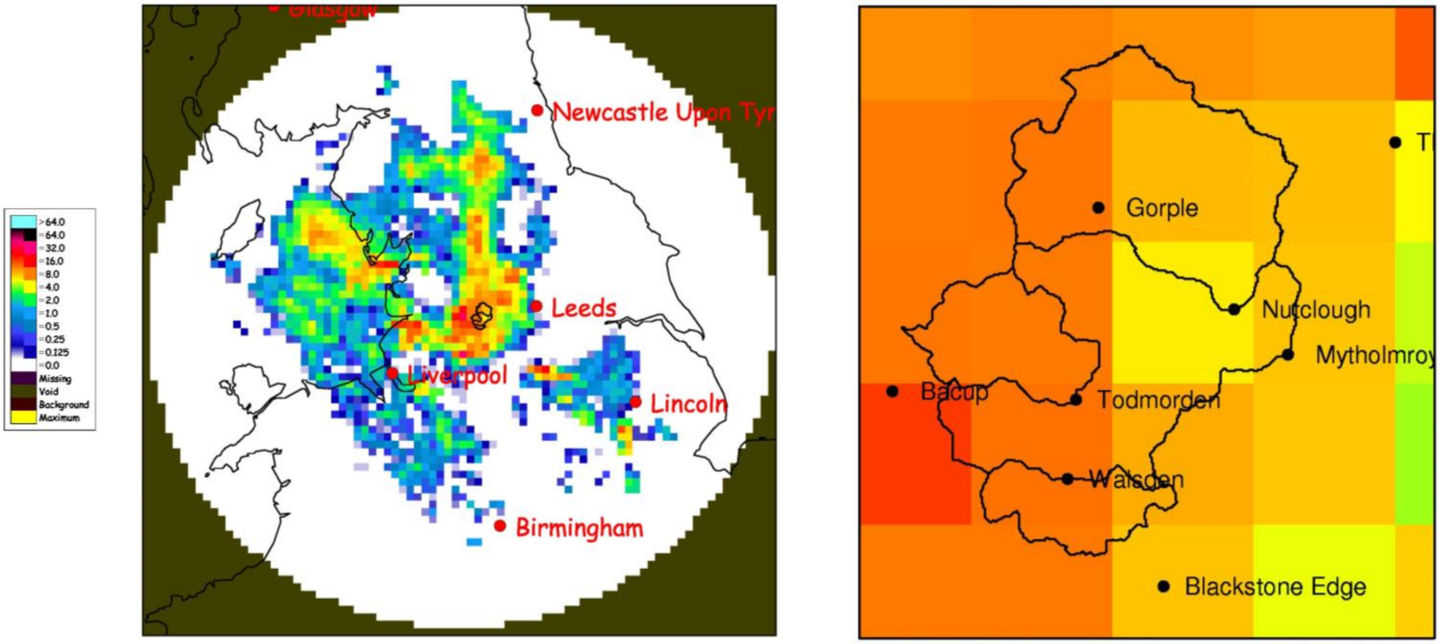

Figure A.6 Nimrod 5km analysis at 23:15 3 June 2000

10:45 9 October 2000 **14:15 9 October 2000**

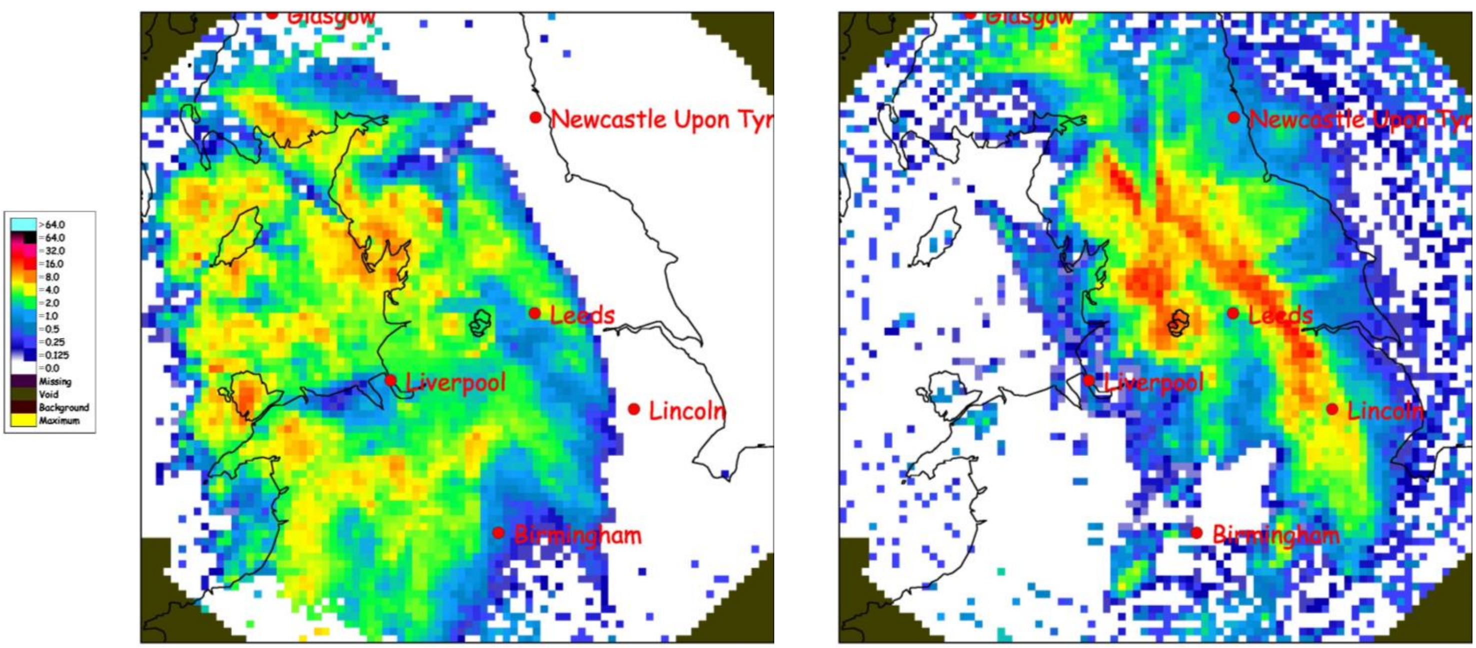

Figure A.7 Nimrod 5km analysis at 10:45 and 14:15 9 October 2000

Event 5: 9 October 2000

The night started mostly dry with some variable cloud and clear spells, some scattered showers across western areas, but with cloudier skies and rain already into Southwest England and South Wales. By dawn, this rain had pushed into Northern Ireland, Wales and further into western parts of England.

During the daytime, the rain extended north and east across the whole of the UK, associated with a low pressure system whose centre tracked slowly northeast across Ireland and into southern Scotland by the evening. The rain was heavy in places and came accompanied with strong southerly winds, with gales along the Welsh and English coasts. By evening, the rain had cleared from the southwest of the UK, with scattered heavy showers instead, some with thunder. By the end of the evening, the rain band was curling back from East Anglia and Southeast England, across Scotland and back through Northern Ireland, into Northwest England. Elsewhere, cloud was more broken with scattered showers, these mainly in the west.

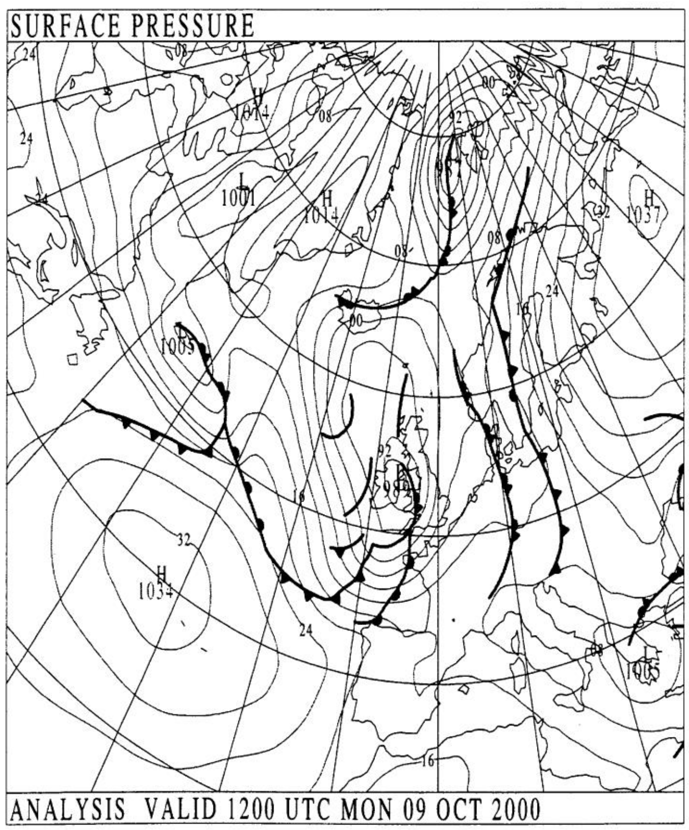

Figure A.8 Surface pressure chart at 12:00 9October 2000

Both images in Figure A.7 are for the Nimrod 5km analysis. Note that during September 2000 the new Met Office radar control and data processing software package, called Cyclops, was implemented at Hameldon Hill. This provided many improvements including the increase in range of the 5km radar grid from 210 to 250km. Clearly, over this peak rainfall period which is just after the upgrade, the radar images show anomalous readings in the previously unattainable long ranges. These anomalies are due to initial calibration issues of the new software which were eventually resolved.

The first radar image, for 10:45, shows the band of rain after it had just reached the Upper Calder catchment. The second, for 14:45, shows the back of the band, which is more intense, passing over the catchment.

Event 6: 2 November 2002

The first few days of November were dominated by south-westerly winds, with depressions moving between Scotland and Iceland and active fronts frequently crossing the UK. In the early hours of the 2nd, Scotland had some outbreaks of rain with this becoming confined to the northeast later. Northern Ireland had a cloudy day and rain spread across the Province in the morning, clearing again by late afternoon. Most of Scotland was also cloudy. There was further rain and drizzle in the northeast. Heavier rain covered the south by mid afternoon, spreading all over the mainland by the evening. The heaviest rain was in the southwest where it became drier by late evening. It was a particularly wet day over most of the UK with at least 25mm recorded widely over western Britain and Northern Ireland.

Examination of the Nimrod 5km analysis shows a stratiform band of rain passing over the Upper Calder from the south-west followed by some localised rain. The first radar image in Figure A.11, at 20:15, shows the localised rain affecting the Upper Calder.

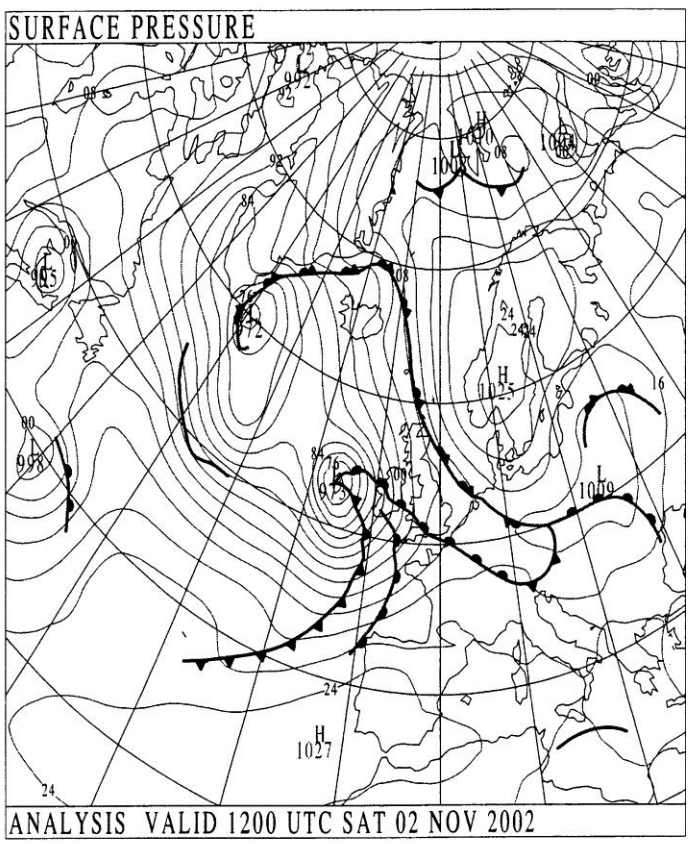

Figure A.9 Surface pressure chart at 12:00 2 November 2002

Event 6: 8 November 2002

The weather on the 8th was dominated by a low pressure system whose centre tracked quickly eastwards across Scotland. It was a cloudy day across the UK, although much of Scotland saw some sunshine. It was also a wet and quite windy day over much of the country. Many places in England and Wales had at least 10mm of rain with quite a few, mainly in Wales and the north, having at least 15mm. (40.4mm at Capel Curig, in the Welsh mountains, from 09:00 to 21:00 hrs.) During the evening the remnant of the rain was still over Northern Ireland, North Wales, the Midlands and East Anglia, moving southwest in the evening over England to reach southeast England later. Clearer weather followed into the north of England and East Anglia later, joining southern Scotland in having a clear end to the day.

The Nimrod 5km analysis shows a band of stratiform rain moving in from the North-West. The second radar image in Figure A.11 shows the band of rain passing over the Upper Calder.

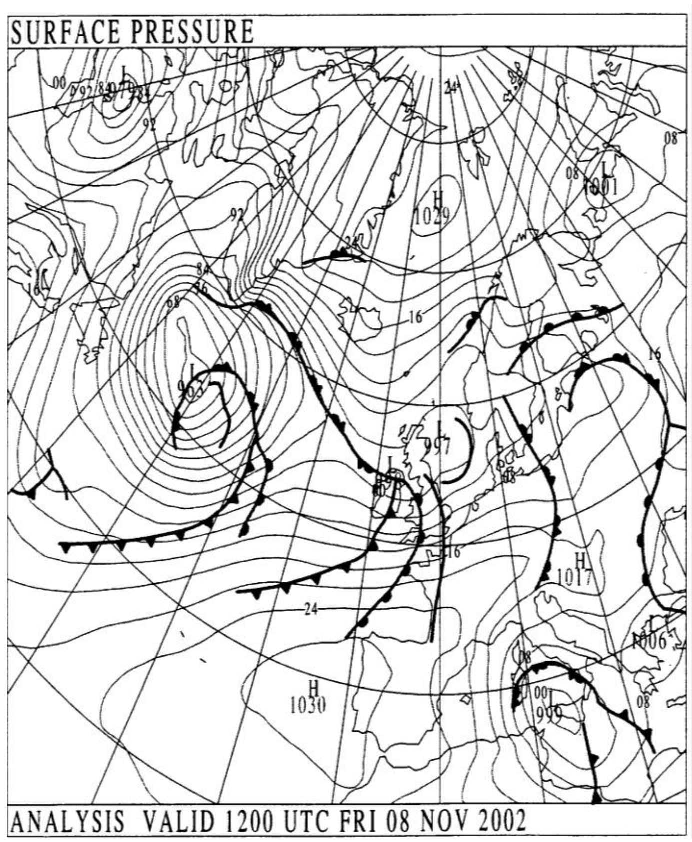

Figure A.10 Surface pressure chart at 12:00 8 November 2002

20:15 2 November 2002 **09:15 8 November 2002**

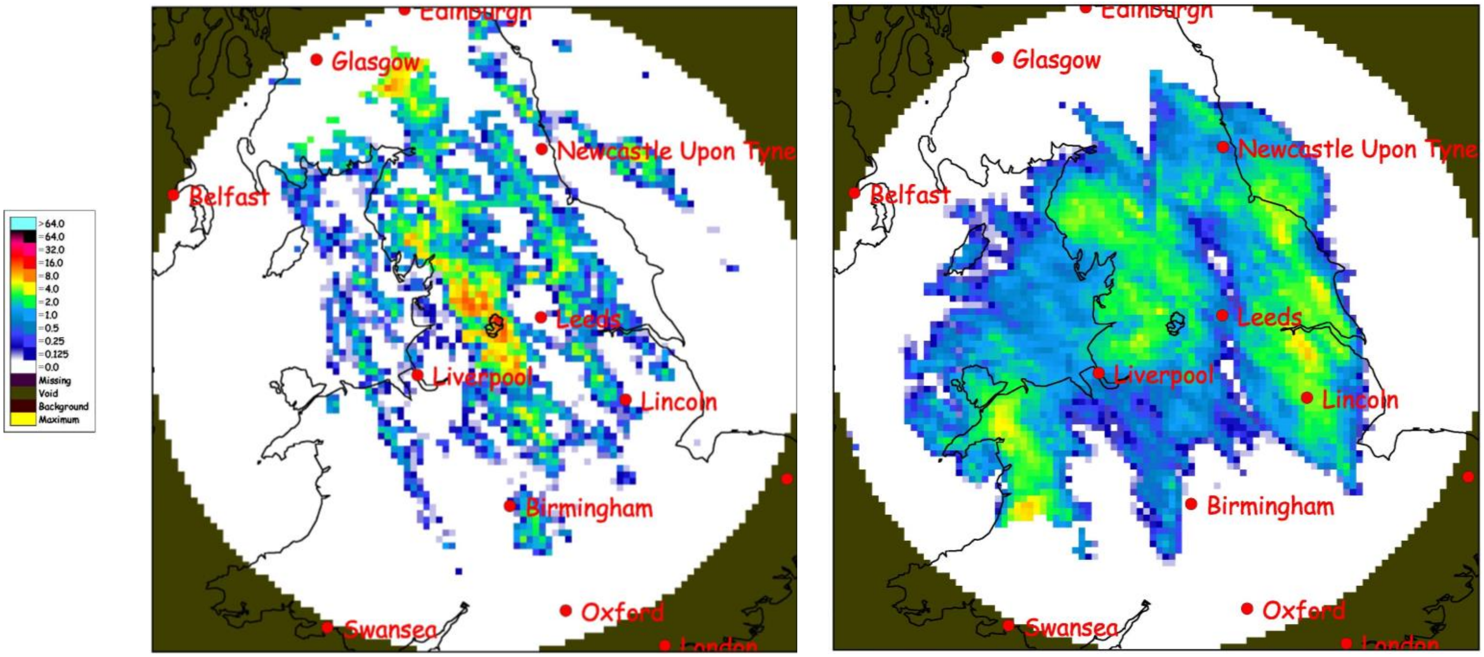

Figure A.11 Nimrod 5km analysis for two times in November 2002

5km **2km**

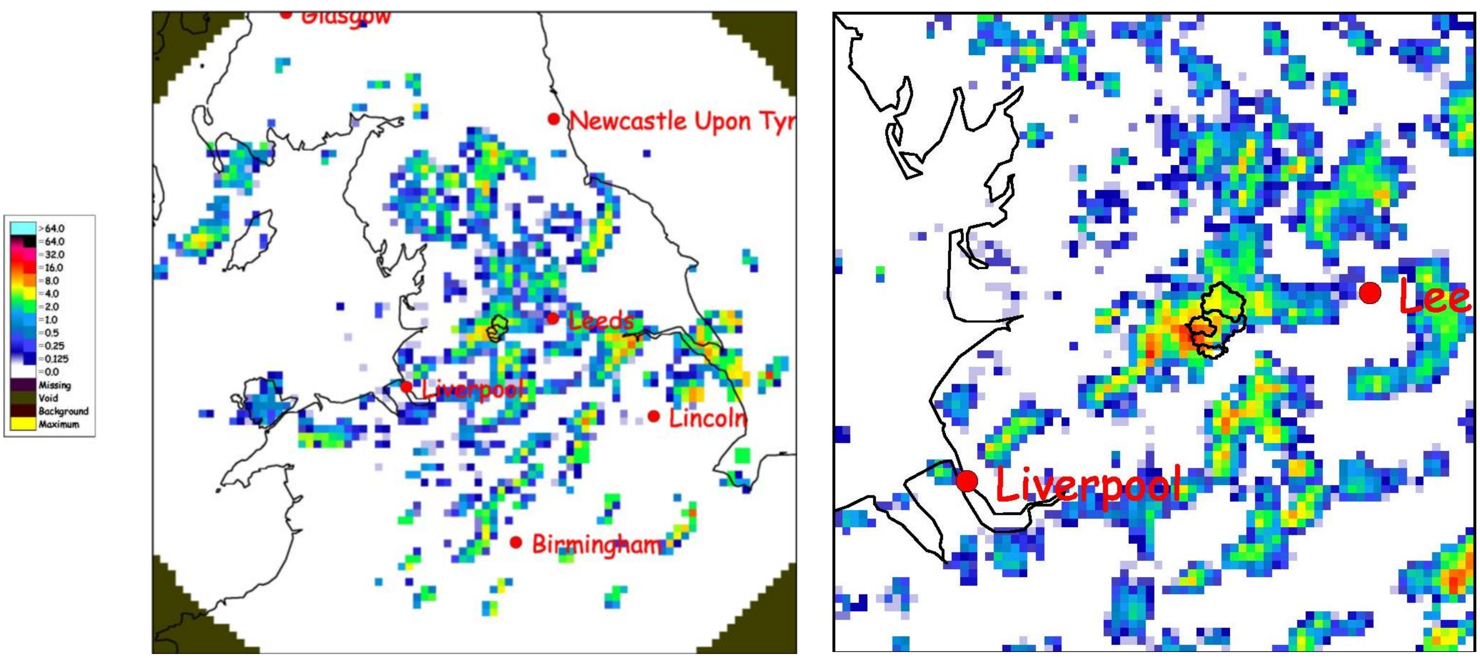

Figure A.12 Nimrod 5km and 2km analysis at 11:15 10 June 2002

Event 7: 10 June 2002

A low pressure system, whose centre lingered off the west coast of Scotland, brought disturbed south westerlies and frequent rain during the 10th. The night of the 9th/10th was mostly cloudy over Scotland and northeast England with outbreaks of rain, although the rain turned more showery in the morning with lengthening clear, then sunny spells. England, Wales and Northern Ireland had clear intervals and showers, the showers mainly in the west and north.

During the day, most parts of the country had a mixture of sunshine and showers, heavy in places. During the evening, showers continued across northern and western Britain, but became scattered in the east and the south. Most parts of the country had a rather cool day.

The Nimrod analysis shows the localised showers crossing the Upper Calder from the west. The showers were heavy at times: an example is given in Figure A.12. The Nimrod 2km analysis again picks up the finer details of the localised showers.

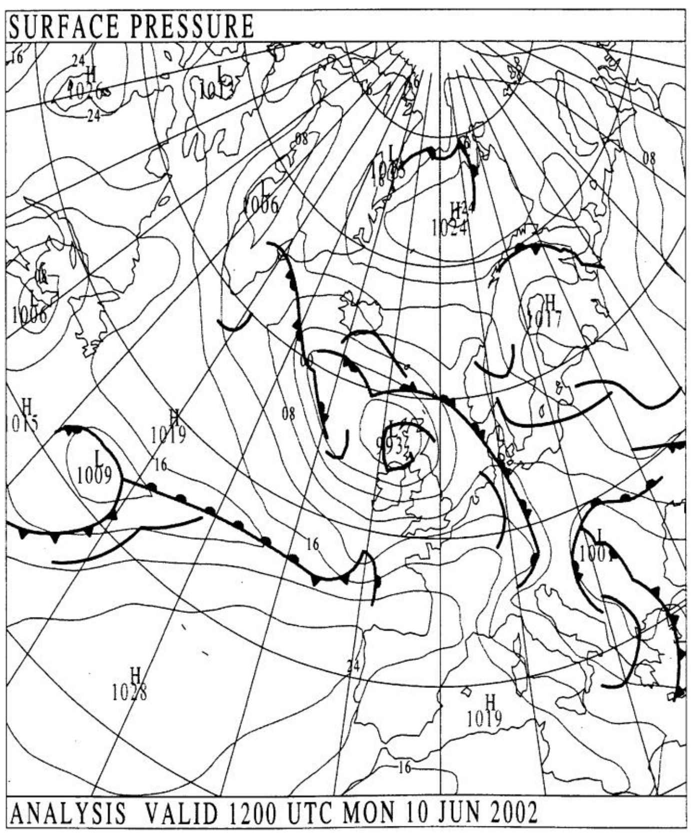

Figure A.13 Surface pressure chart at 12:00 10 June 2002

Event 8: 9-10 August 2002

The weather over this period was dominated by a low pressure system whose centre slowly tracked eastwards across the southern coast of England and into France. Over the night of 8th/9th a band of rain across Wales, central and southern parts of England moved north and east reaching Lancashire, Yorkshire and East Anglia by dawn. There was also some rain across central Scotland and showers over southwest England. During the morning of the 9th, the rain over northern England moved only slowly north whilst that over East Anglia turned showery. During the afternoon, outbreaks of rain affected parts of central and eastern Scotland. The rain over northern England remained slow moving and thundery showers continued across central and southern England. There was little general change in the evening.

Over the night of 9th/10th, the band of slow-moving and occasionally heavy rain continued over the north, primarily affecting Yorkshire and Lancashire. During the morning the rain over northern England tended to peter out, although heavy rain persisted for a while across North Yorkshire.

The Nimrod analysis shows stratiform rain across the Upper Calder during the day of the 9th. An example 2km radar image at 12:00 is given in Figure A.15. This was followed by localised rain during the night of the 9th/10th. An example 2km radar image at 23:20 is given in Figure A.15

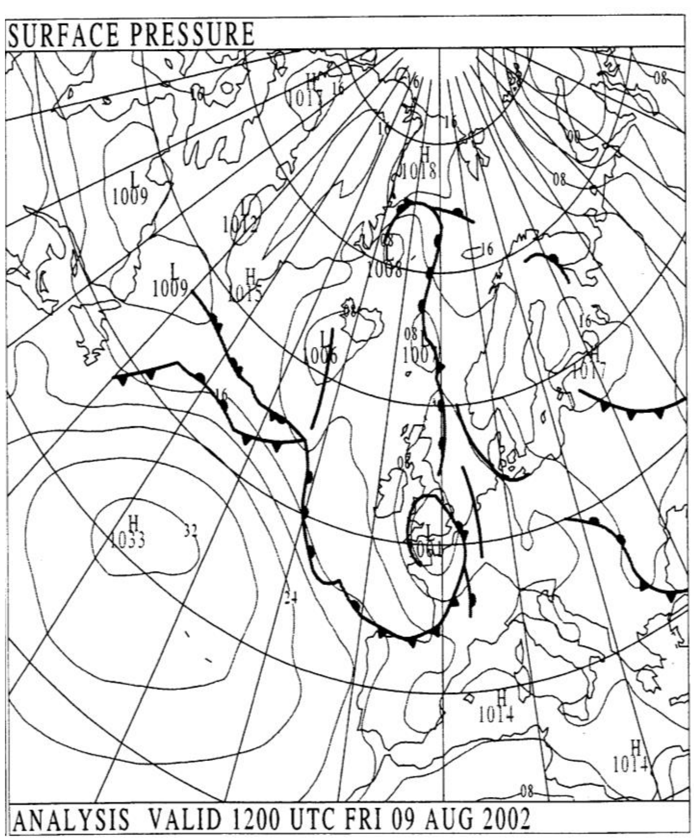

Figure A.14 Surface pressure chart at 12:00 9 August 2002

12:00 9 August 2002 | 23:20 9 August 2002

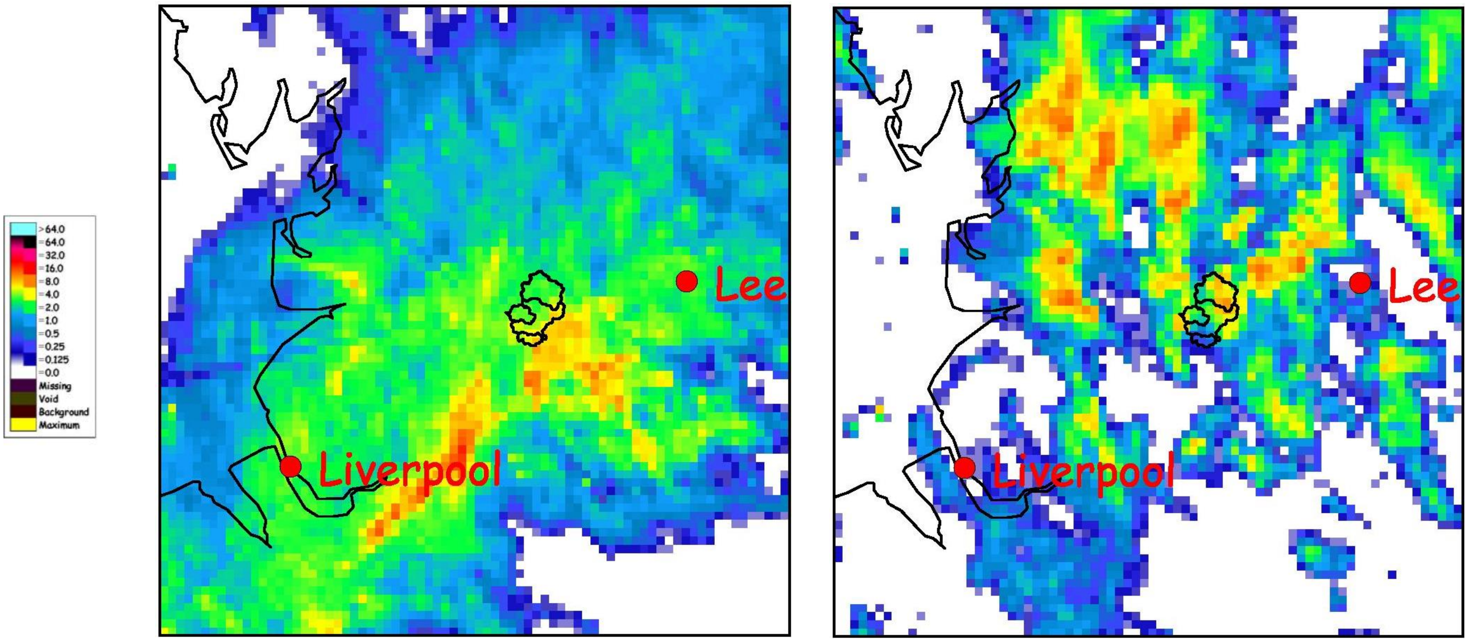

Figure A.15 Nimrod 2km analysis at 12:00 and 23:20 9 August 2002

5km | 2km

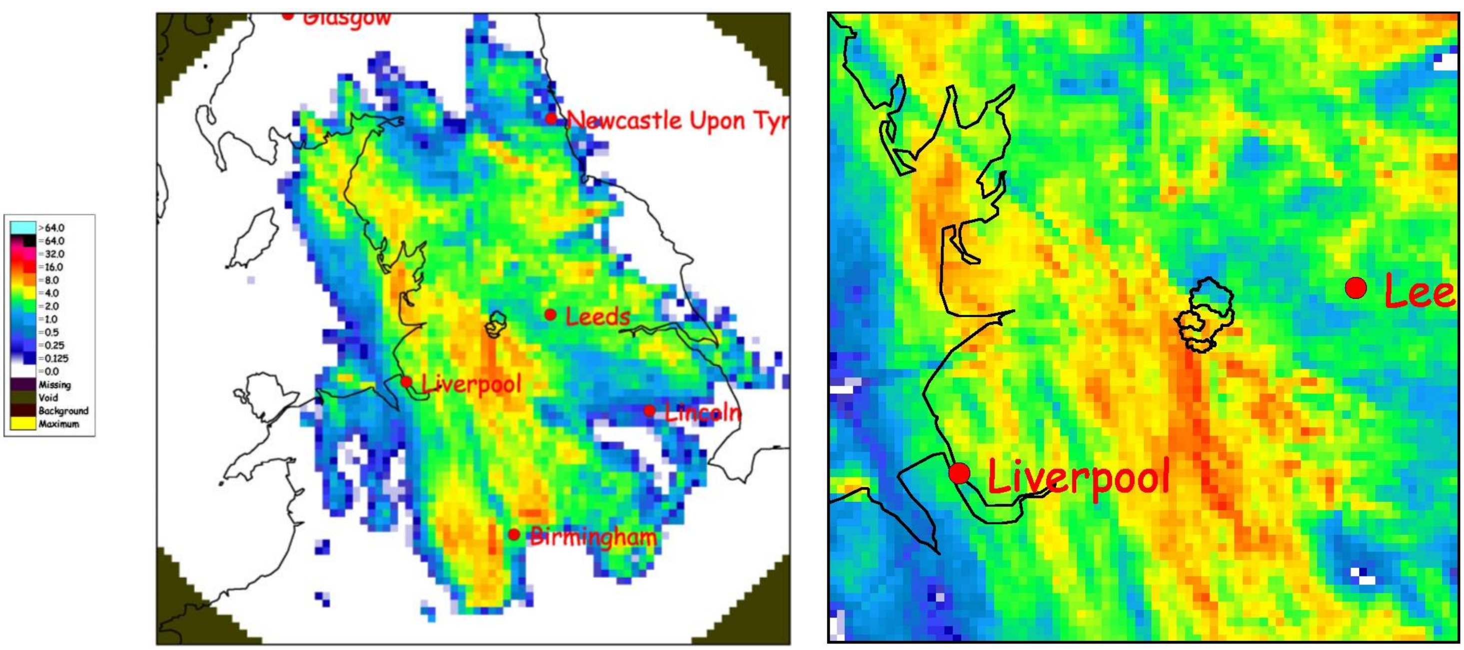

Figure A.16 Nimrod 5km and 2km analysis at 14:15 9 September 2002

Event 9: 9 September 2002

A depression developing over France moved north and then north-west across the British Isles. With this depression came a band of heavy rain which moved north to affect southern England and East Anglia by soon after dawn. It moved quickly north to most of England and Wales by early afternoon. By late afternoon the band had moved northwest to affect much of Scotland (except the north) and then Northern Ireland through the evening. The rain cleared much of the eastern parts of the UK during the afternoon and evening but was still over much of Wales and Northern Ireland by midnight.

Nimrod 5km and 2km images are shown in Figure A.16, for 14:15. This shows the band of heavy rain affecting most of northern England with a more intense part affecting the southern parts of the Upper Calder catchment. The Nimrod 2km image shows the finer resolution detecting smaller features of the rain.

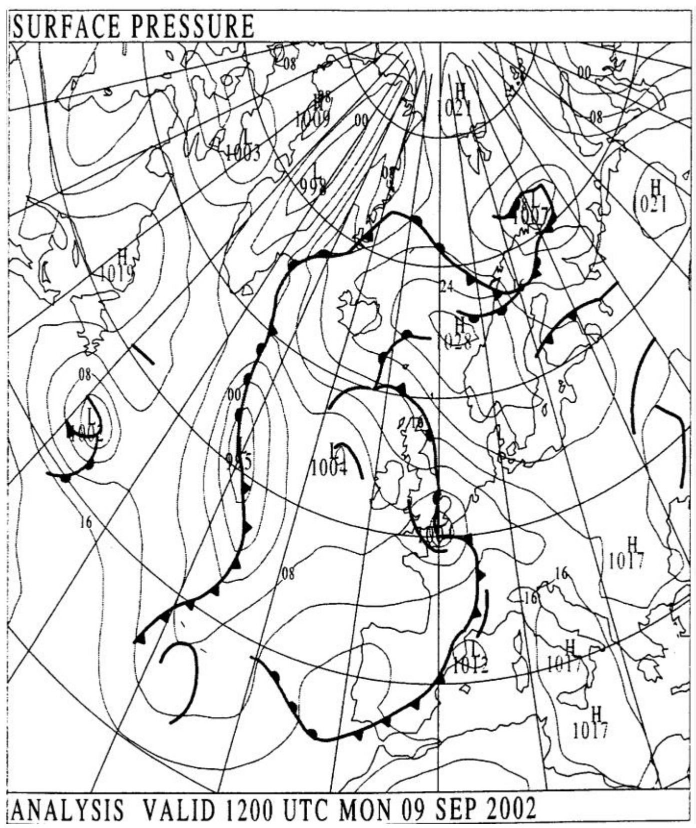

Figure A.17 Surface pressure chart at 12:00 9 September 2002

Event 10: 25-27 October 2002

Over this period, the weather was dominated by successive depressions whose centres tracked north-east across Northern Ireland and then northern England/southern Scotland. The first depression tracked slowly whilst the second sped across the British Isles. Two sample pressure charts are given in Figure A.18.

Over the night of 24th/25th showers, heavy in places, affected many western areas overnight, with heavier and more persistent rain evident later. Many eastern counties were dry for a time before showers arrived towards daybreak. Extensive heavy rain in the west edged eastwards before clearing the east coast by mid-afternoon. Showers, mainly heavy, some thundery and of hail, followed on behind and lingered well into the evening.

In the early hours of the 26th , there was rain over Northern Ireland, Southern Scotland and northern England which petered out during the morning as it moved slowly south. During the afternoon, the sunshine became hazier with thicker cloud and rain arriving by late afternoon over southwest England and west Wales. This then spread steadily north and east to affect much of southern England, Wales and Northern Ireland by the early evening. The rest of England and most of Scotland were affected by the end of the day, with some heavier bursts in places.

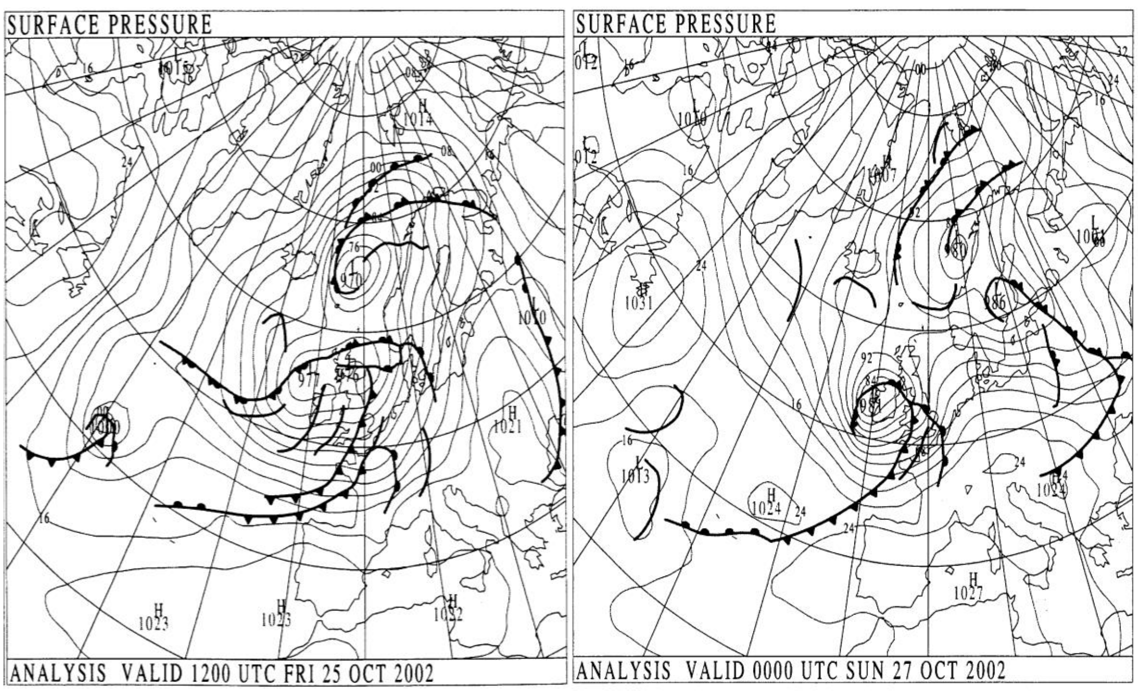

Figure A.18 Surface pressure charts at 12:00 25 October 2002 and 00:00 27 October 2002

During the early hours of the 27th, a deep depression crossed Northern Ireland into the Irish Sea pushing rain quickly across southern parts. Across the north, the rain moved slower with snow at times across the northern highlands. By mid-morning, the low had transferred into the North Sea off Northumberland with a line of heavy and persistent rain curving through eastern and southwest Scotland, the Isle of Man to North Wales. As the low moved away, the rain cleared and blustery showers followed.

The Nimrod analysis shows several broken bands of rain crossing the Upper Calder, predominantly from the west. Occasionally these were localised and intense in places. An example of intense rain over the Upper Calder is given in Figure A.19. The enlarged image shows the detail over the Upper Calder catchment.

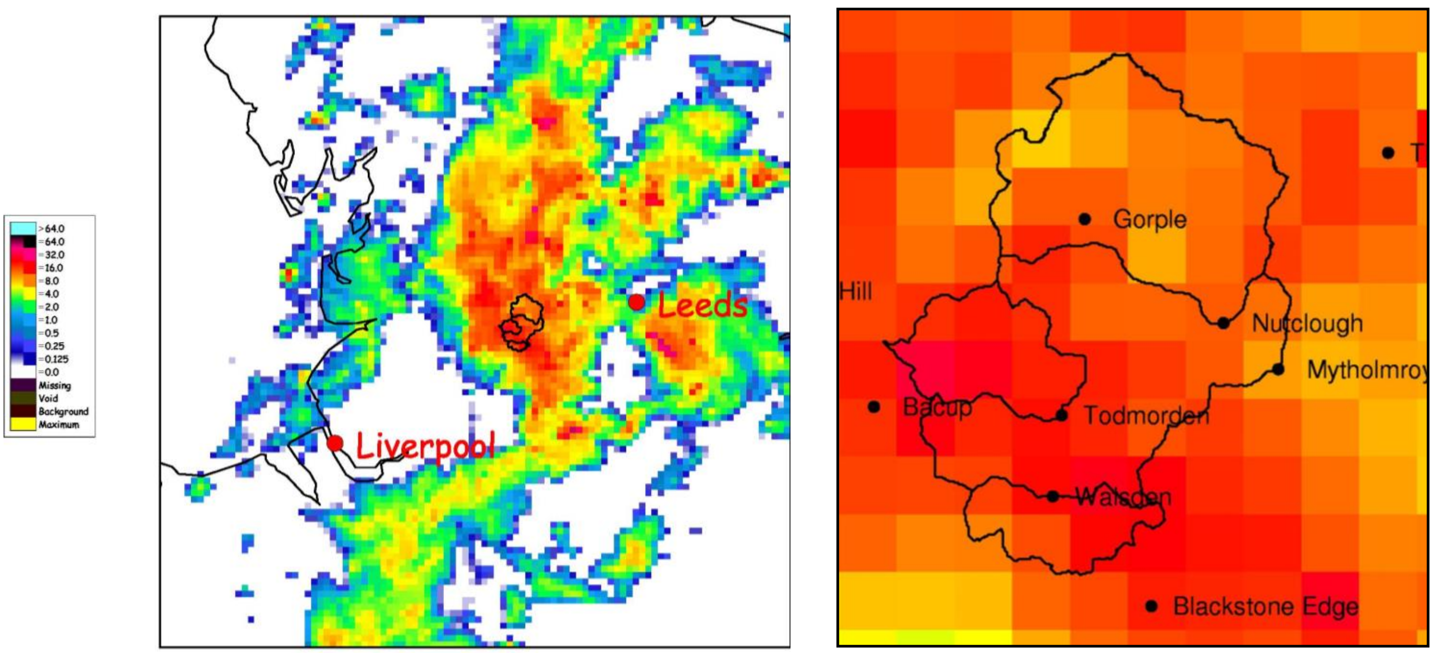

Figure A.19 Nimrod 2km analysis at 18:50 25 October 2002

Event 11: 10-11 February 2002

During the morning of the 10th, a spell of persistent and at times heavy rain spread into Northern Ireland, Wales and western parts of England and Scotland. Through the afternoon the rain became more patchy over Scotland and it was Wales and northwest England that took the brunt of the rain. Rain returned to Northern Ireland and western Scotland during the evening with outbreaks of rain working their way into East Anglia and southern England. However, it was western parts of England and Wales that saw persistent heavy rain again, with a daily total of 91mm recorded at Capel Curig.

The night of the 11th started cloudy over most of the country with outbreaks of rain. Rain was heaviest over the hills and mountains of Wales and western England. The far north of Scotland was dry and clear for a while with a touch of frost in places. Clearer weather, with scattered showers, spread to Northern Ireland in the early hours, and to western Scotland and much of northern England by the morning.

The Nimrod 2km analysis shows a band of stratiform rain moving in from the west during the last 12 hours of the 10th (see the first radar image of Figure A.22), followed by a brief spell of more spatially-varying rain on the morning of the 11th (see the second radar image of Figure A.22).

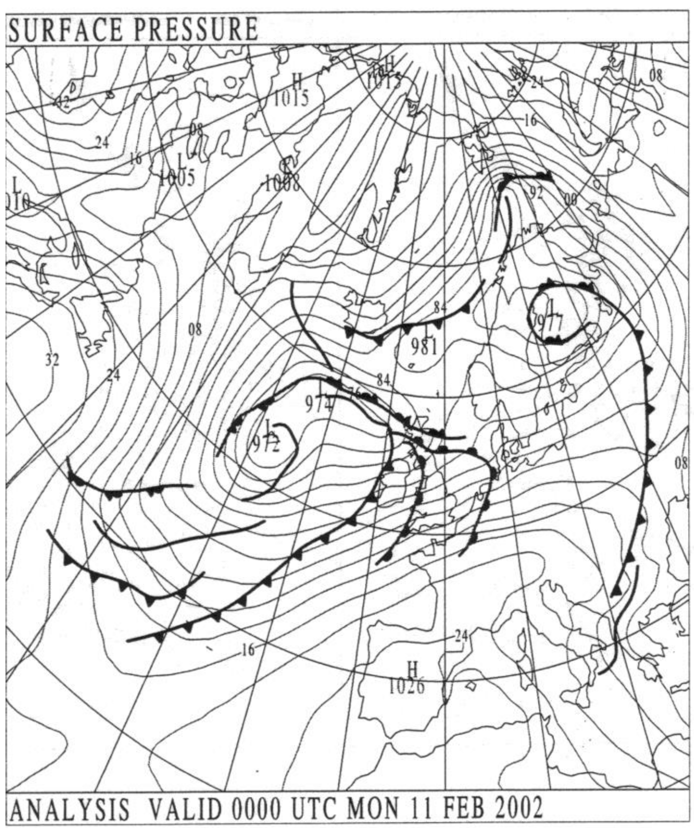

Figure A.21 Surface pressure chart at 00:00 11 February 2002

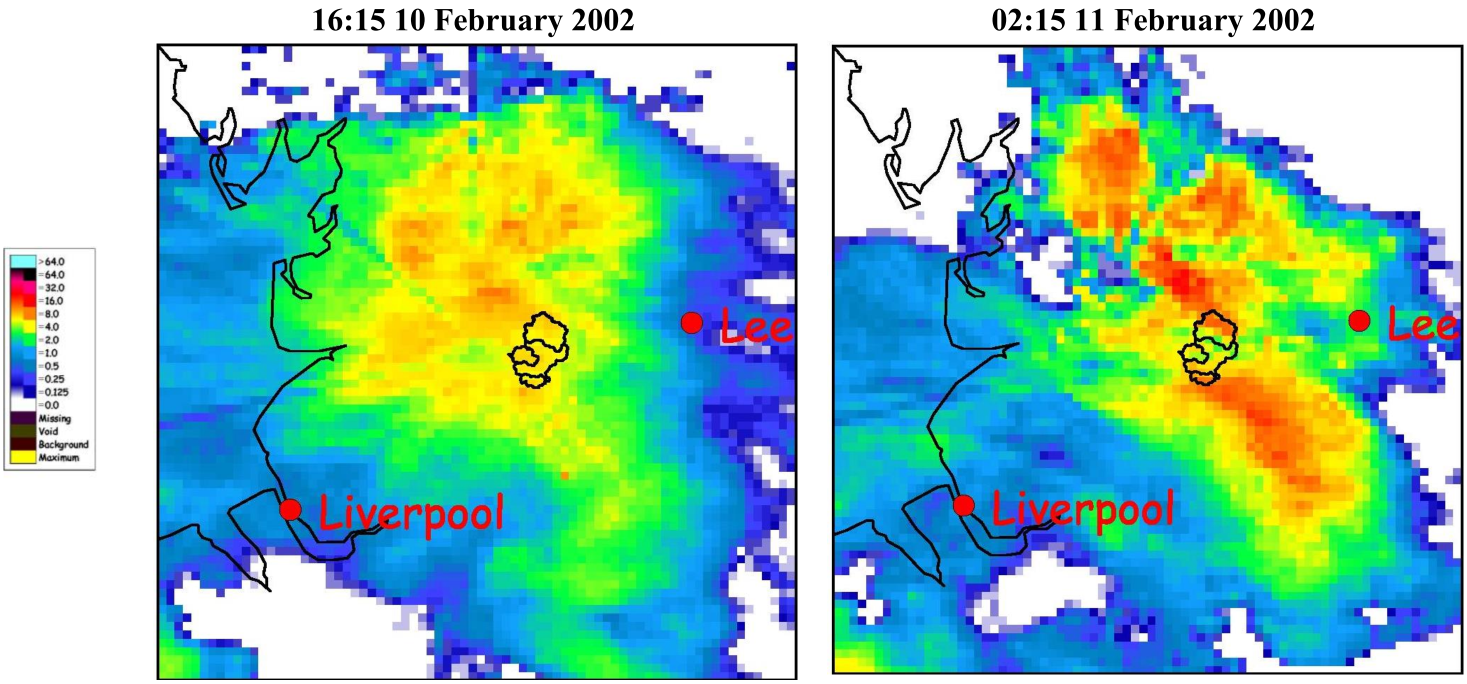

Figure A.22 Nimrod 2km analysis for two times in February 2002

APPENDIX B RADAR RAINFALL ACCUMULATION MAPS

Appendix B details for the Nimrod products the rainfall accumulation maps over the event periods. These accumulation maps were calculated and displayed using the Hyrad software and show the entire Hameldon Hill radar coverage area and a magnified view over the Upper Calder catchment. Note that the figures presented show total rainfall accumulations and therefore a separate scaling is used for each figure (see legends).

Event 2

Figure B.1 shows the rainfall accumulation for Event 2 over 38 days. This highlights several features of the radar image discussed in Section 2.5 such as the radial 'spikes' caused by ground clutter or occultation and the attenuation of the radar signal. For this autumn period, of just over a month, the accumulation shows that the orographic-enhanced rain over the Pennines and Snowdonia dominate. Further examination identified that the region in the immediate vicinity of the radar (that is no more than 5km) was providing over-estimates of the rain. This can be seen in the four grid-squares surrounding the radar in Figure B.1. Indeed, the grid-square containing Hameldon Hill accumulated 172cm of rainfall which is clearly wrong. Outside of this region of overestimation, there is a region of slight under-estimation which can be seen as a "ring" of lower values about the radar which slightly affects the Upper Calder catchment.

Over the Upper Calder catchment there are larger accumulations to the south. The largest accumulation (just) affected is the grid-square containing the Blackstone Edge raingauge with 37.1cm, whilst the smallest is 24cm in the southwest of the catchment.

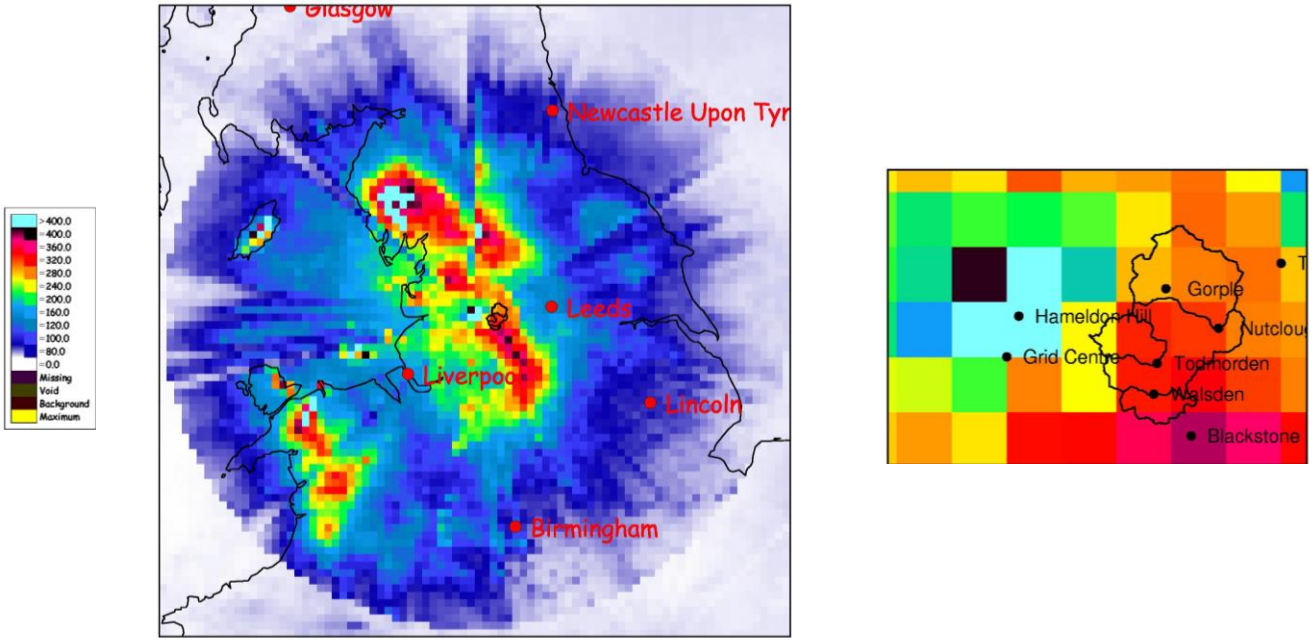

Figure B.1 Rainfall accumulation, using Nimrod 5km analysis, for Event 2; 38 days to 27 October 1998

Event 3

Figure B.2 shows the rainfall accumulation for Event 3 over 38 days. This rainfall accumulation is very similar qualitatively to that for Event 2 with the orographic-enhanced rain over the Pennines and Snowdonia dominating (although the southern Pennines is not as pronounced). The rings of over- and under-estimation surrounding the radar are again evident with the grid-square containing Hameldon Hill accumulating 94cm of rainfall. The southern parts of the Upper Calder have largest accumulations with 21cm over the grid-square containing Blackstone Edge. The grid-square containing the Thornton Moor raingauge had the smallest accumulation affecting the catchment with 15.7cm.

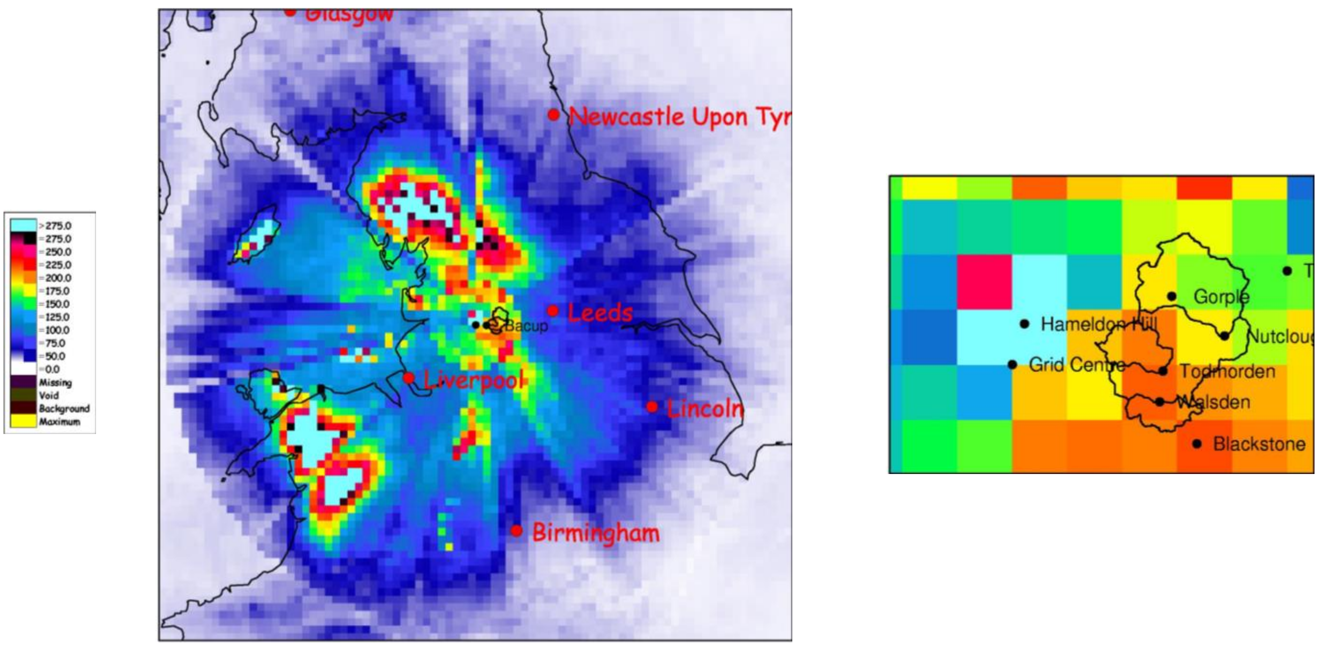

Figure B.2 Rainfall accumulation, using Nimrod 5km analysis, for Event 3; 38 days to 18 January 1999

Event 4

Figure B.3 shows the rainfall accumulation for Event 4 over 69 days during the spring/summer of 2000. The orographic signature of the mid and southern Pennines is evident but the rainfall over this period is generally more evenly distributed. The rainfall near the radar is overestimated once more with the grid-square over Hameldon Hill accumulating 104cm of rainfall; there is no evidence of an outer ring of underestimation. The southern part of the catchment received most rain with 32cm in the southwest. The northwest received the least rainfall of 23cm.

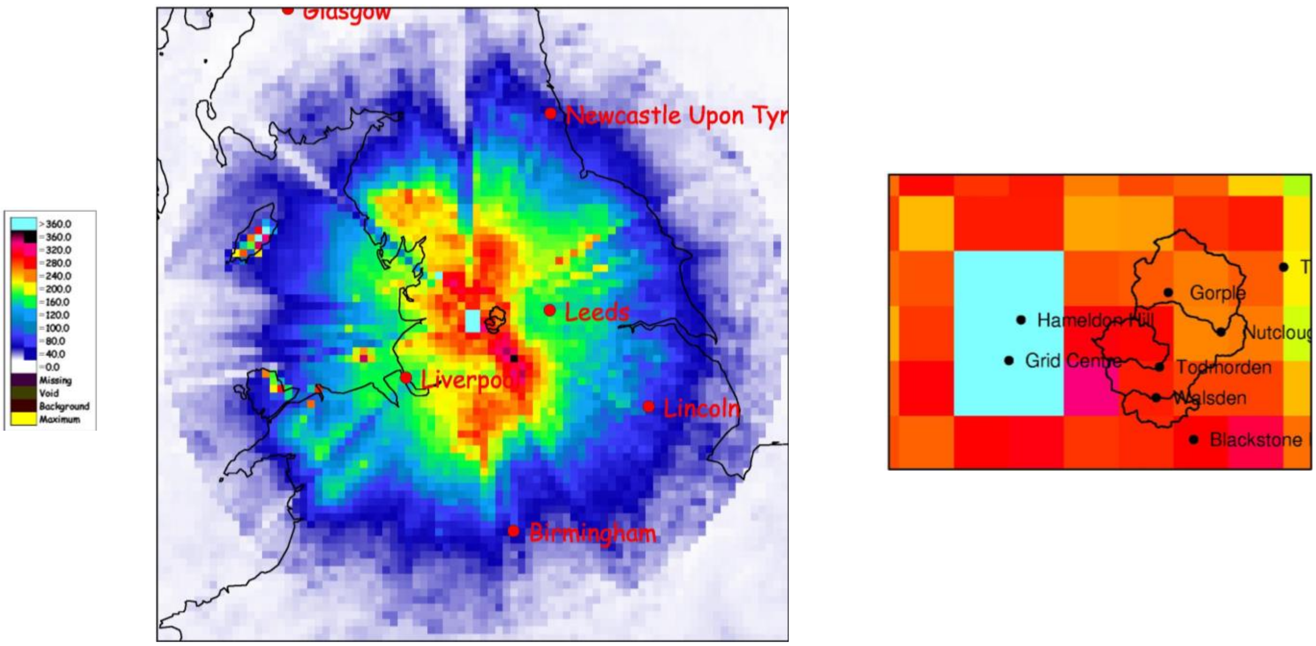

Figure B.3 Rainfall accumulation, using Nimrod 5km analysis, for Event 4; 69 days to 6 June 2000

Event 5

Figure B.4 shows the rainfall accumulation for Event 5 over 66 days during the summer/autumn of 2000. The accumulation clearly shows orographically enhanced rainfall. There is no evidence of severe overestimation near the radar (the accumulation in the grid-square over Hameldon Hill being a far more realistic 68cm) or the ring of underestimation seen in earlier events. This improvement in the near-range characteristics of the radar is due to the upgraded processing software (Cyclops) introduced during the event in September 2000. However, comparison with the raingauge data (see Figure C.5) shows that after the upgrade the radar appears to have been initially overestimating. For example, the grid-square containing the Gorple raingauge accumulated 59cm of rainfall whilst the raingauge only accumulated 38cm; this is presented in Figure C.5 (b). Over the Upper Calder catchment the west experienced most rain with 60cm in the grid-square west of centre, whilst the least rain fell on the far eastern side with only 45cm.

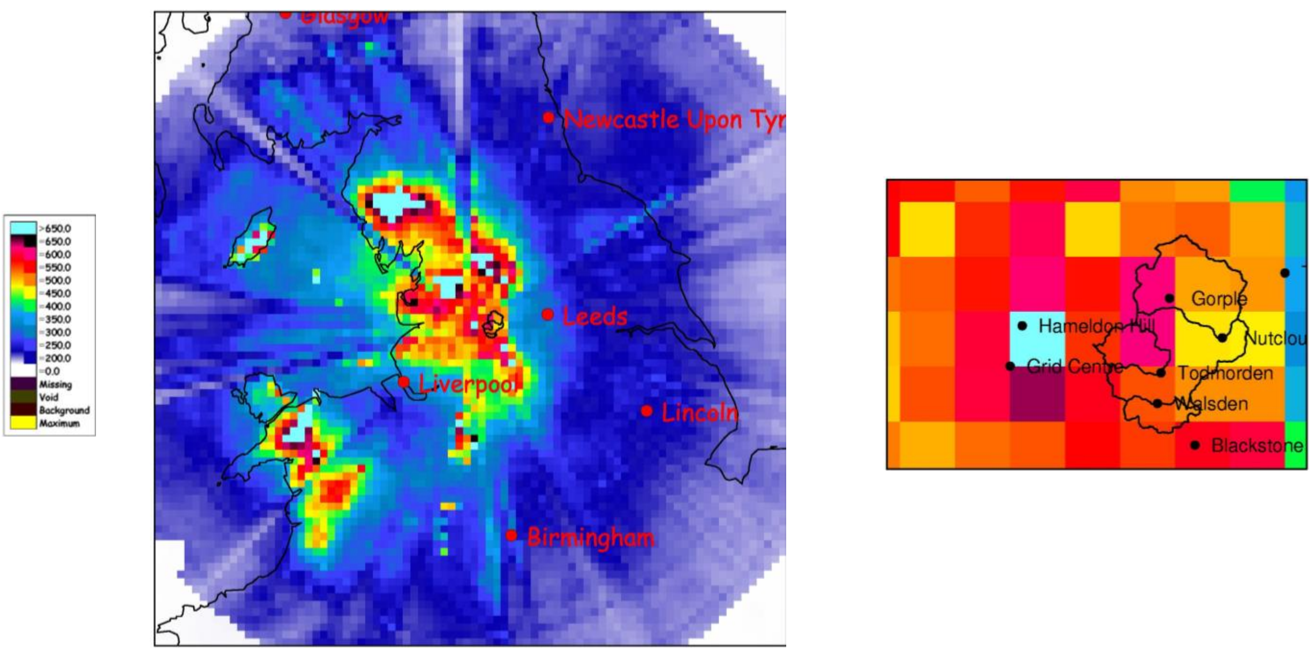

Figure B.4 Rainfall accumulation, using Nimrod 5km analysis, for Event 5; 66 days to 28 October 2000

Event 6

Figure B.5 presents the rainfall accumulation for Event 6 over 11 days. Since Event 6 is in 2002, the Nimrod 2km data were available so these have also been shown. There is clear orographic-enhanced rain over the northern Pennines. The two circled regions highlight anomalous areas of high accumulation values but these are well away from the Upper Calder catchment. In the immediate vicinity of the radar, values now appear to be far more realistic with no evidence of significant under- or over-estimation. The 2km analysis and 5km analysis are in very close agreement.

There is a reasonable range of accumulations over the Upper Calder catchment. For the 5km analysis, the grid-square over the Bacup raingauge had the greatest accumulation of 11.5cm and the north of the catchment accumulated the least rainfall of 7.4cm. For the 2km analysis, the greatest rainfall accumulated in the orange grid-square (13.4cm) whilst the east of the catchment received the least (7.0cm).

Event 7

Figure B.6 shows the rainfall accumulations for Event 7 over 24 hours using both Nimrod 2km and 5km analysis products. This event is characterised by localised showers and, because the event is only a day in length, the traces of the heaviest showers are evident in Figure B.6. Clearly there are some differences between the 2km and 5km accumulations due to the smoothing effects of spatial resolution. Differences are also likely to be in part due to temporal sampling effects, the Nimrod 2km analysis being available every five minutes (as opposed to every 15 minutes for the 5km analysis) which is particularly important for localised convection-driven rain. The 2km accumulations also show a discontinuity at a range of approximately 25km. This is due to the area where a higher beam is used to infill the surface beam and is discussed in Section 3.3. The infill area also affects the 5km accumulation but a sharp discontinuity is not evident because of the coarser resolution used.

The differences between the two products affect the rainfall over the Upper Calder; see Figure B.6. The greatest accumulation was 1.7cm for the 5km analysis and 2.2cm for the 2km analysis, both in the west of the catchment. The least accumulation was 0.8cm for the 5km analysis and 0.6cm for the 2km analysis, both in the northeast of the catchment.

(a) Nimrod 5km analysis

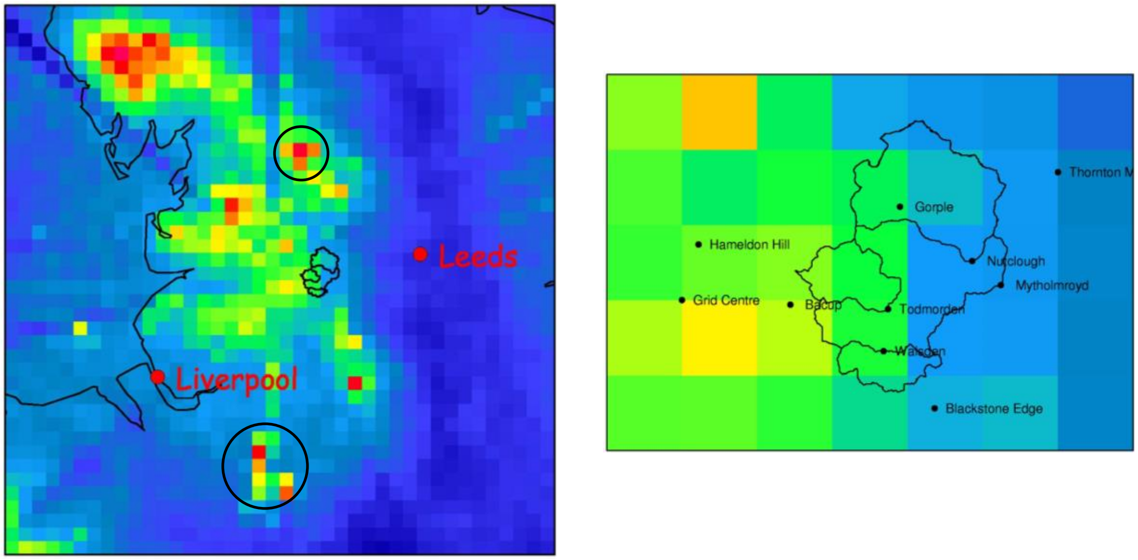

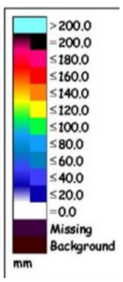

(b) Nimrod 2km analysis

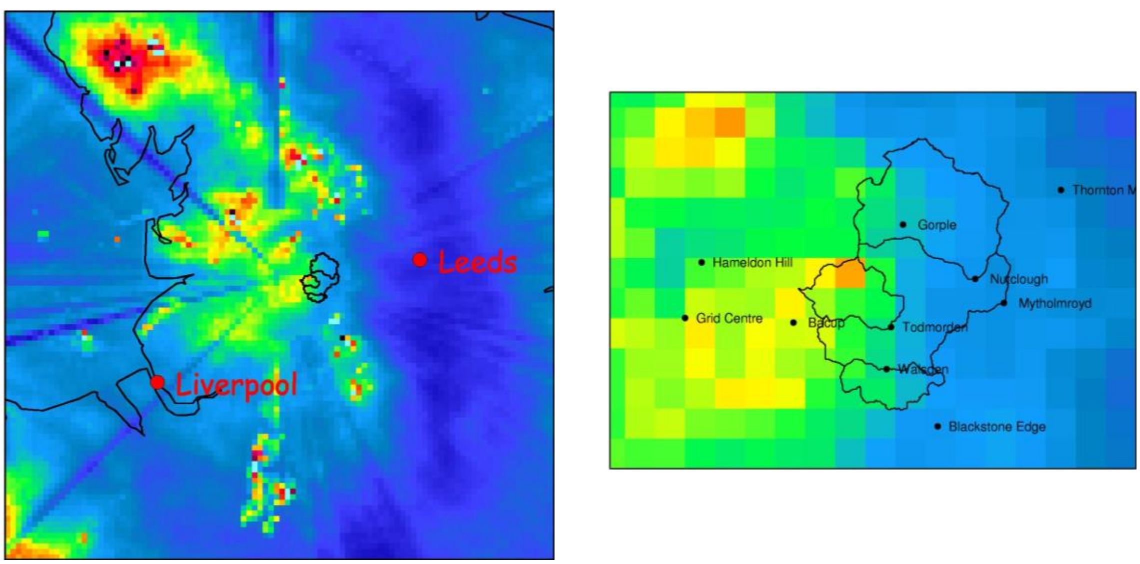

Figure B.5 Rainfall accumulation, using Nimrod 5km and 2km analysis, for Event 6; 11 days to 12 November 2002

(a) Nimrod 5km analysis

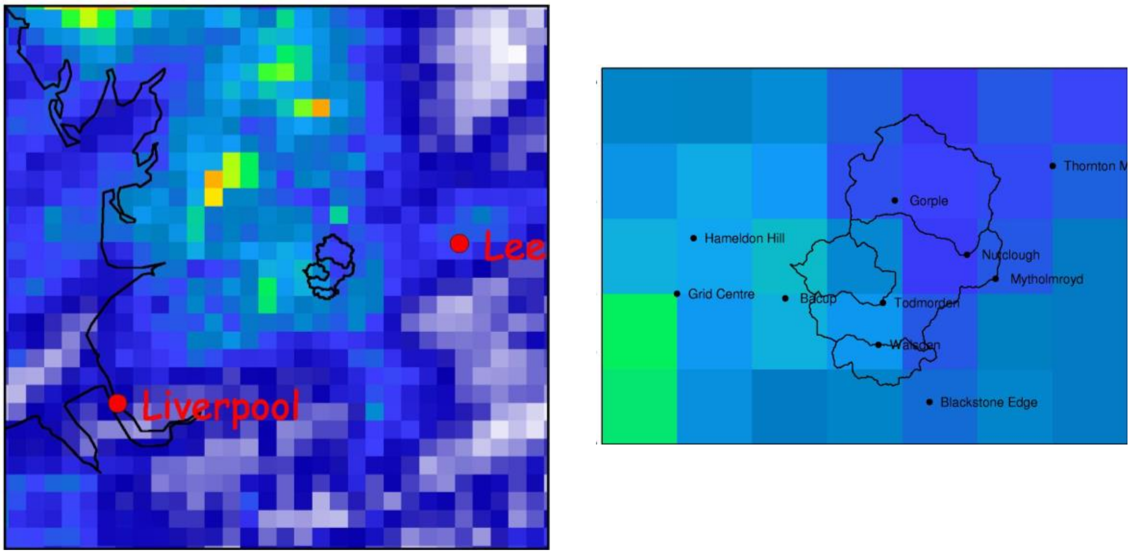

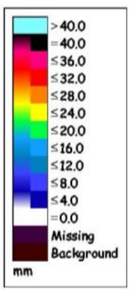

(b) Nimrod 2km analysis

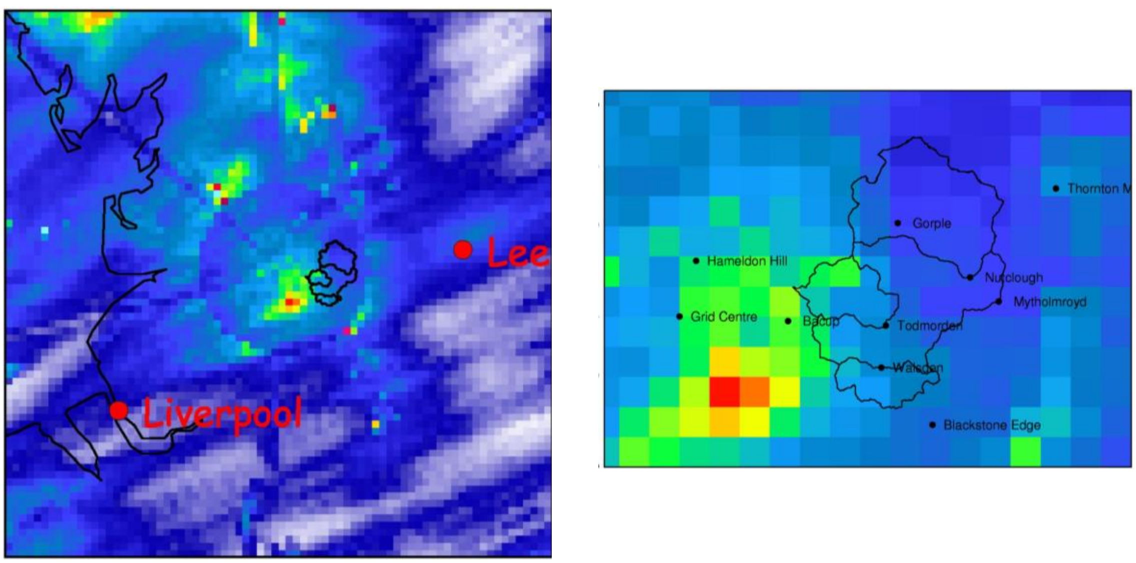

Figure B.6 Rainfall accumulation, using Nimrod 5km and 2km analysis, for Event 7; 24 hours to 00:00 11 June 2002.

Event 8

The 2km and 5km Nimrod rainfall accumulations over the 36 hour period for Event 8 are shown in Figure B.7. There is no evidence of discontinuity at a range of 25km in the 2km accumulations or over/underestimation near the radar site. The 2km and 5km images are very similar. The greatest accumulation was 4.6cm for the 5km analysis and 5.0cm for the 2km analysis, both occurring just north of the Bacup raingauge. The least accumulation was 3.8cm for the 5km analysis and 3.6cm for the 2km analysis, both occurring just east of the Gorple raingauge.

Event 9

Rainfall accumulations from the 2km and 5km Nimrod products for Event 9 over 12hours are shown in Figure B.8. These show the effect of the heavy band of rain which crossed the North of England and affected the Upper Calder catchment, although the heaviest rainfall was experienced south and west of the catchment. The accumulations show no evidence of over/underestimation near the radar or of a discontinuity at a range of 25km.

The Nimrod 2km accumulations have the greatest rainfall of 2.6cm in the southwest of the Upper Calder catchment and the lowest accumulation of 1.4cm in the centre. The Nimrod 5km accumulations show a similar distribution over the catchment with the greatest accumulation of 3.1cm in the south and the least of 1.3cm in the north.

(a) Nimrod 5km analysis

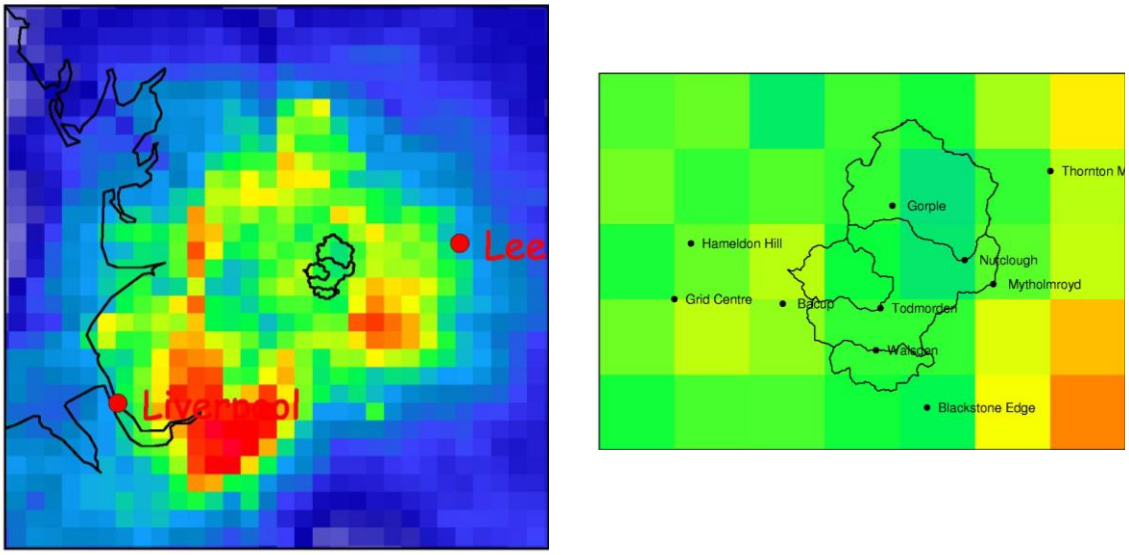

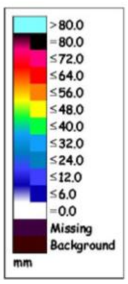

(b) Nimrod 2km analysis

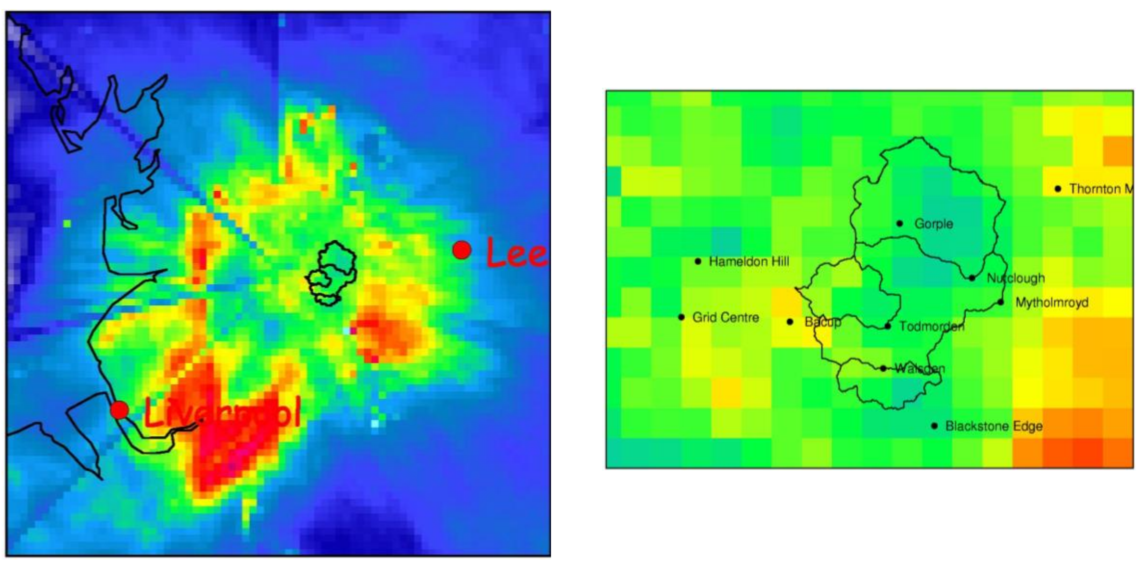

Figure B.7 Rainfall accumulation, using Nimrod 5km and 2km analysis, for Event 8; 36 hours to 12:00 10 August 2002.

(a) Nimrod 5km analysis

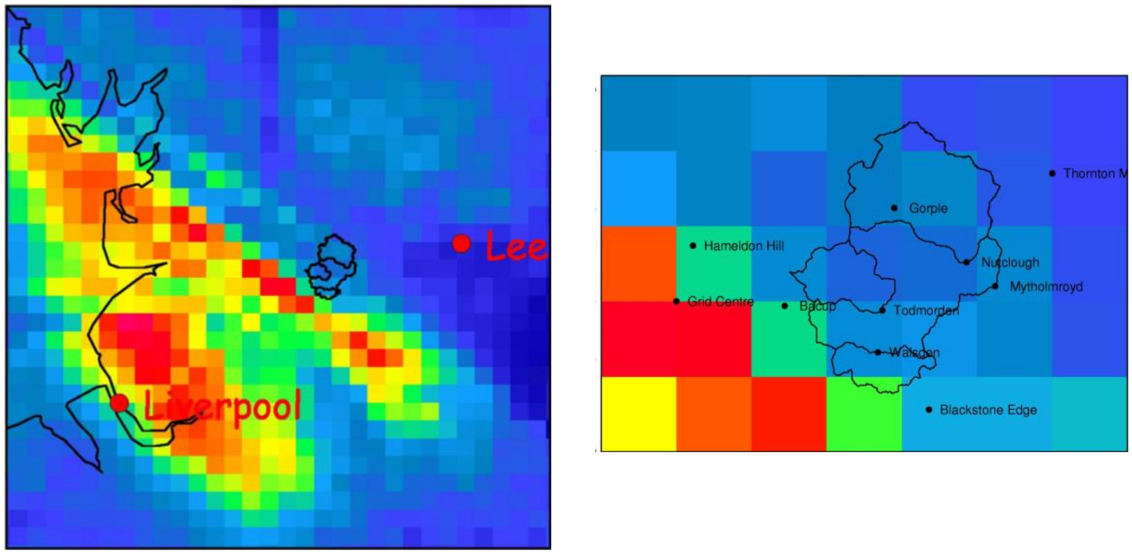

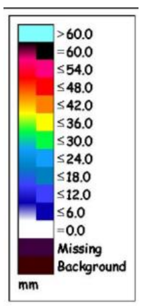

(b) Nimrod 2km analysis

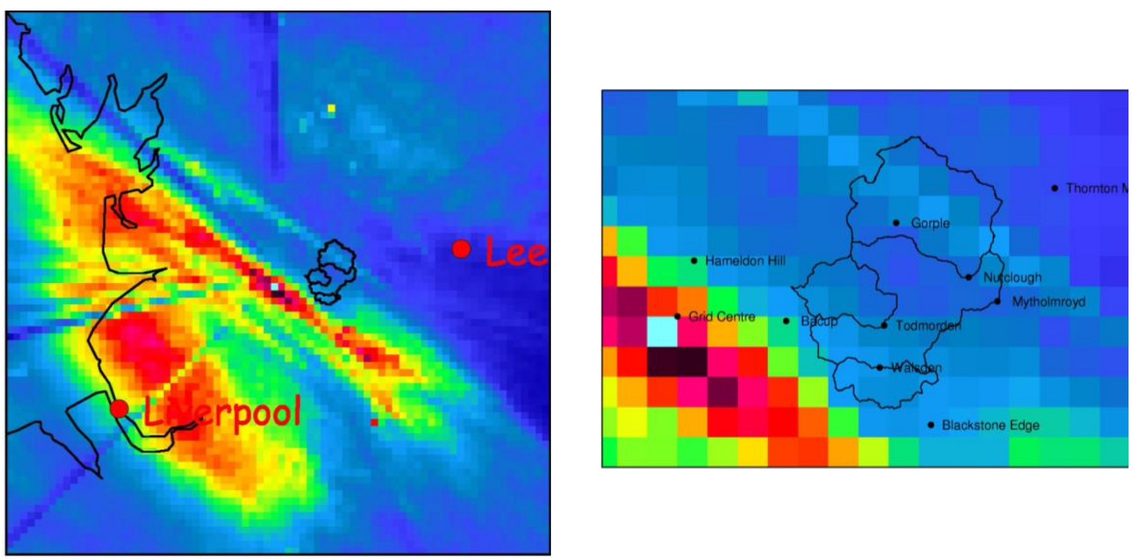

Figure B.8 Rainfall accumulation, using Nimrod 5km and 2km analysis, for Event 9; 12 hours to 00:00 10 September 2002.

Event 10

The 2km and 5km Nimrod rainfall accumulations for Event 10 over 9 days are shown in Figure B.9. A faint echo of the beam infill area can be detected in the 2km accumulations at 25km range.

The 2km and 5km images are similar and show orographic enhancement over the Pennines and Snowdonia. Across the Upper Calder catchment, the greatest 2km accumulation was 16.2cm two grid-squares northeast of the Bacup raingauge and the lowest accumulation was 10.0cm one grid-square northeast of river gauging station at Nutclough. For the 5km analysis, the greatest accumulation of 16.9cm occurred in the grid-square containing the Bacup raingauge and the lowest accumulation of 10.9cm occurred in the grid-square containing the Thornton Moor raingauge.

Event 11

The 2km and 5km Nimrod rainfall accumulations for Event 11 over 33 days are shown in Figure B.10. The beam infill area can be detected in the 2km accumulations at 25km range, particularly in the northern direction.

The 2km and 5km images are similar and show orographic enhancement over the Pennines. Across the Upper Calder catchment, the greatest 2km accumulation was 33.8cm two grid-squares northeast of the Bacup raingauge and the lowest accumulation was 23.4cm one grid-square east of the river gauging station at Nutclough. For the 5km analysis, the greatest accumulation of 33.6cm occurred in the grid-square north of the Bacup raingauge and the lowest accumulation of 27.6cm occurred in the grid-square containing the river gauging station at Mytholmroyd. Over this event the Nimrod 2km analysis appears to be estimating slightly less rainfall than the 5km analysis.

(a) Nimrod 5km analysis

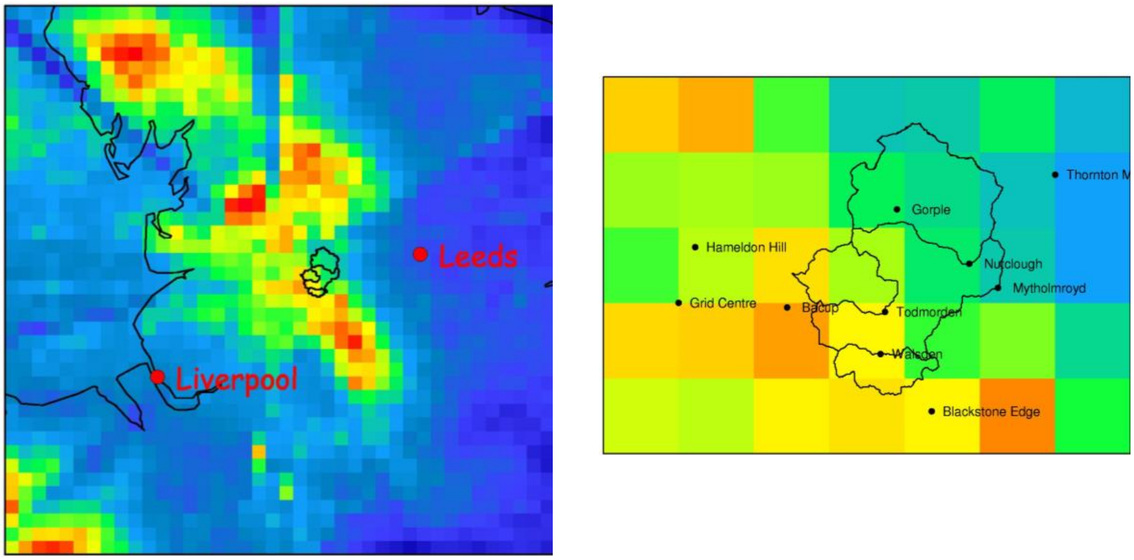

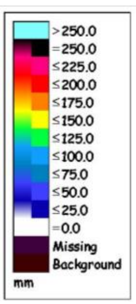

(b) Nimrod 2km analysis

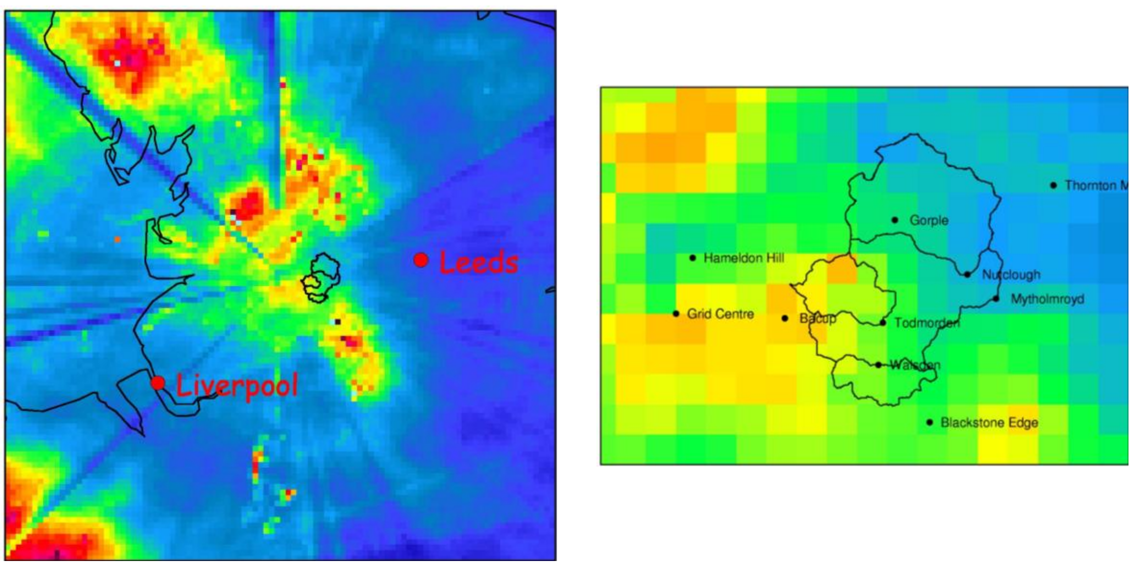

Figure B.9 Rainfall accumulation, using Nimrod 5km and 2km analysis, for Event 10; 9 days to 29 October 2002.

(a) Nimrod 5km analysis

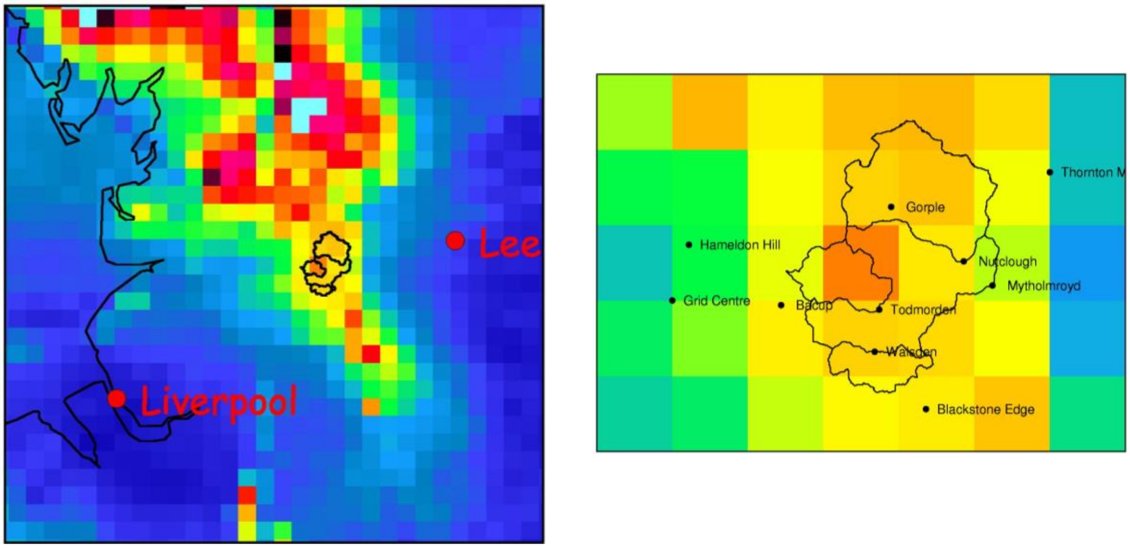

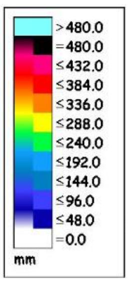

(b) Nimrod 2km analysis

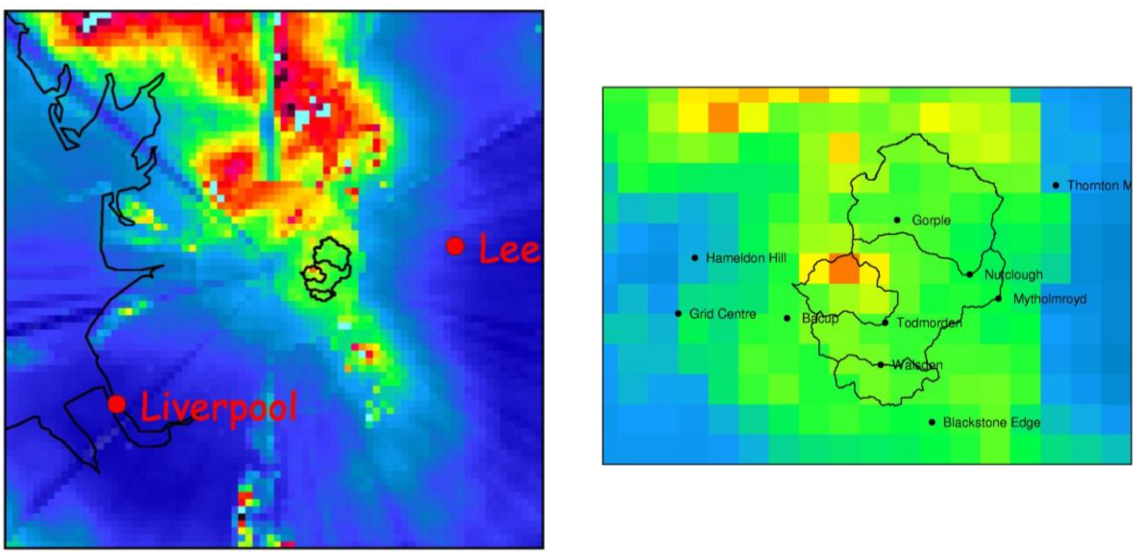

Figure B.10 Rainfall accumulation, using Nimrod 5km and 2km analysis, for Event 11; 33 days to 17 February 2002.

APPENDIX C CUMULATIVE RAINFALL TIME-SERIES

Appendix C compares time-series of cumulative rainfall from radar and raingauges. For each event the cumulative rainfall for each available raingauge is shown along with the four catchment average rainfalls derived from the infilled Nimrod 5km analysis. The Bacup and Gorple raingauges are compared to the radar grid-square which contains them; the Nimrod 5km analysis is used for all events whilst the 2km analysis is used for the 2002 events as well. For the comparison with the two raingauges, the infilled radar data are used in the pre-2001 Met Office data and the *unfilled* radar data are used for the post-2001 CEH data. Missing periods are signified by gaps. For the post-2001 CEH data, this highlights when infill was necessary (also detailed in Table 3.3) and is most apparent in the shorter evaluation events.

(a) Catchment average rainfalls derived from Nimrod 5km analysis

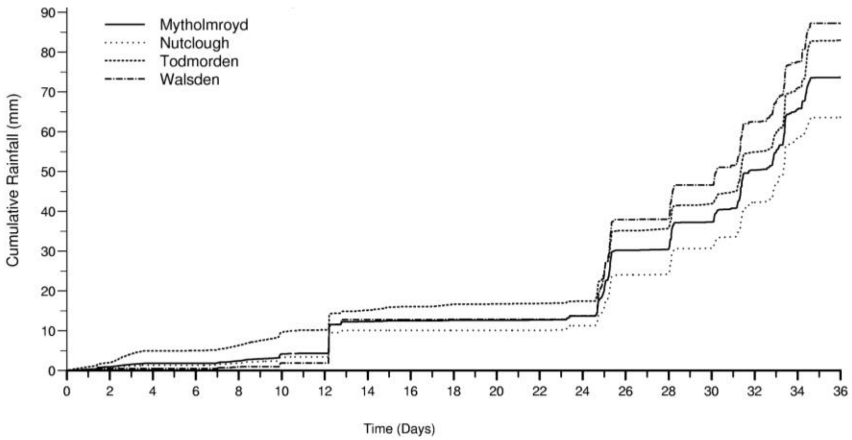

(b) Comparison of the Gorple raingauge (RG) with the 5km radar grid-square containing it (RD)

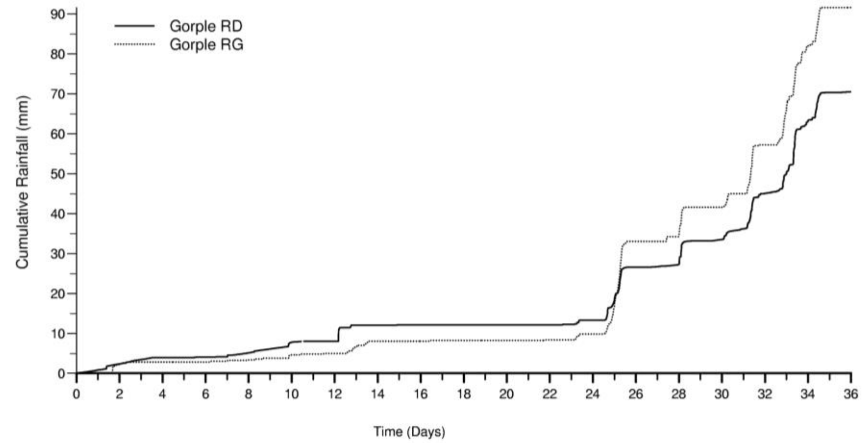

(c) Available raingauges

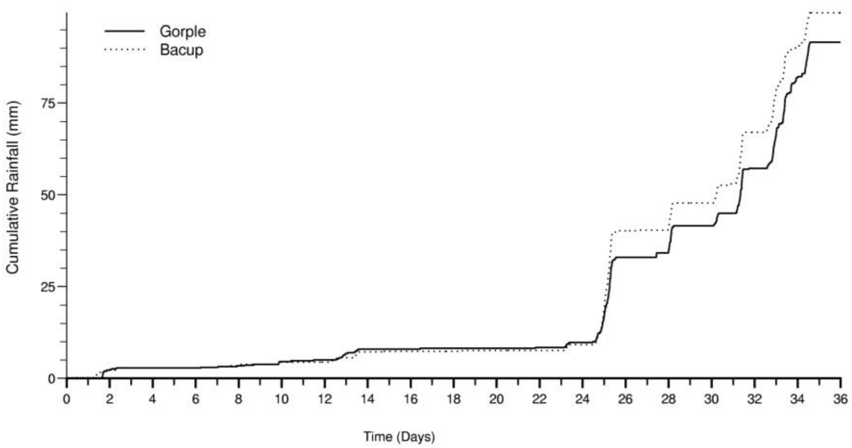

(d) Comparison of the Bacup raingauge (RG) with the 5km radar grid square containing it (RD)

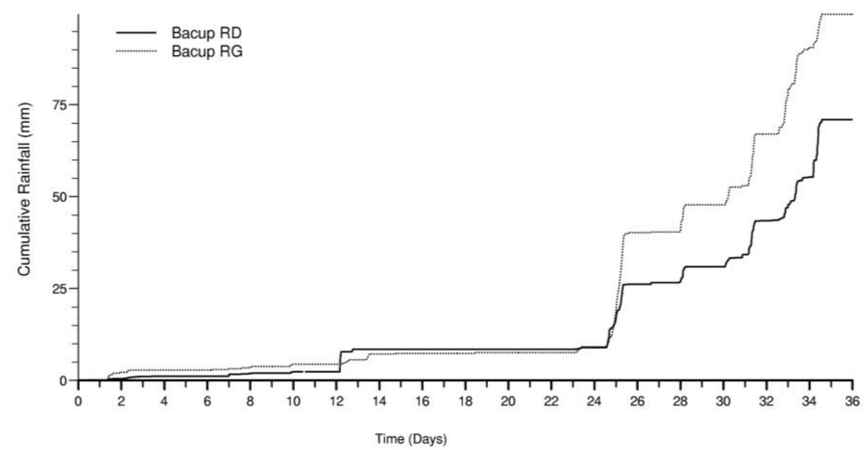

Figure C.1 Cumulative rainfall time-series for Event 1: 10 January to15 February 1997

(a) Catchment average rainfalls derived from Nimrod 5km analysis

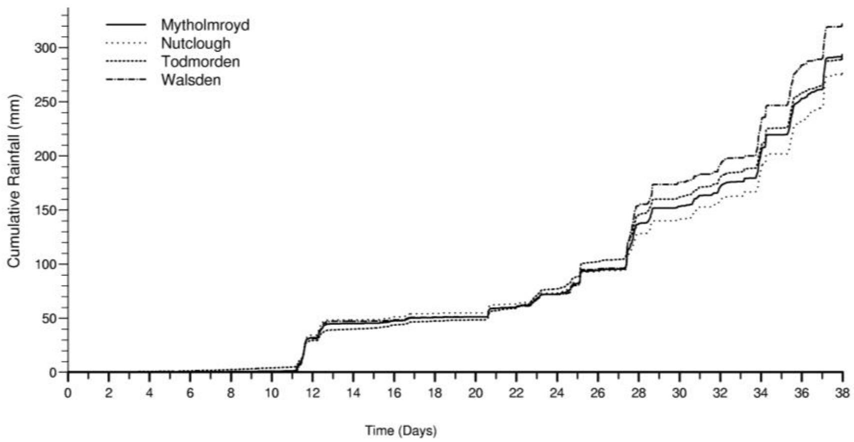

(b) Comparison of the Gorple raingauge (RG) with the 5km radar grid-square containing it (RD)

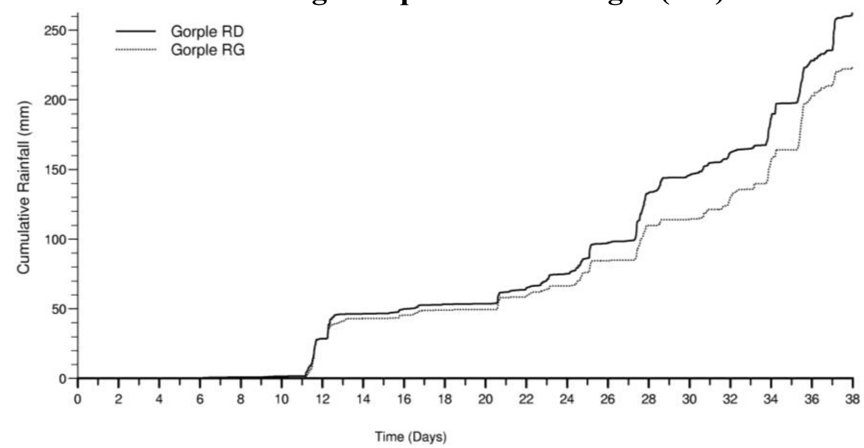

(c) Available raingauges

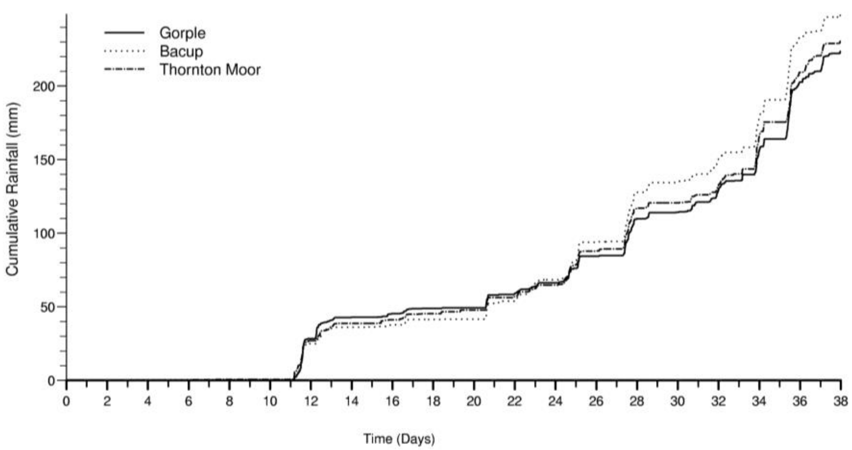

(d) Comparison of the Bacup raingauge (RG) with the 5km radar grid-square containing it (RD)

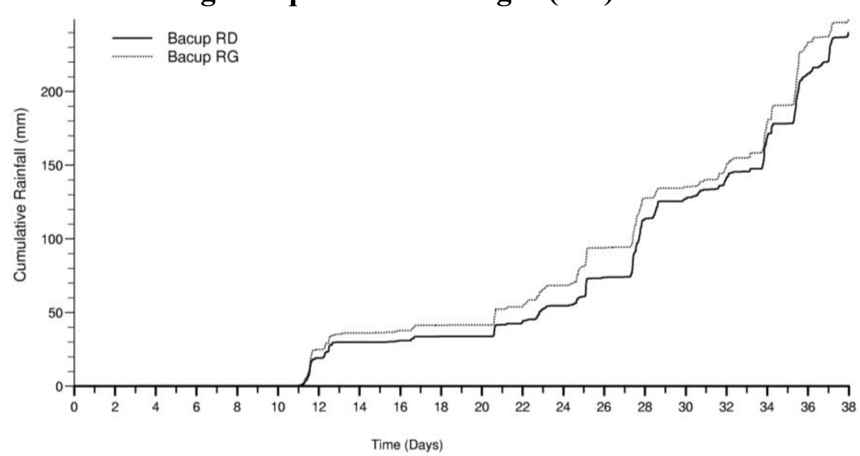

Figure C.2 Cumulative rainfall time-series for Event 2: 19 September to 27 October 1998

(a) Catchment average rainfalls derived from Nimrod 5km analysis

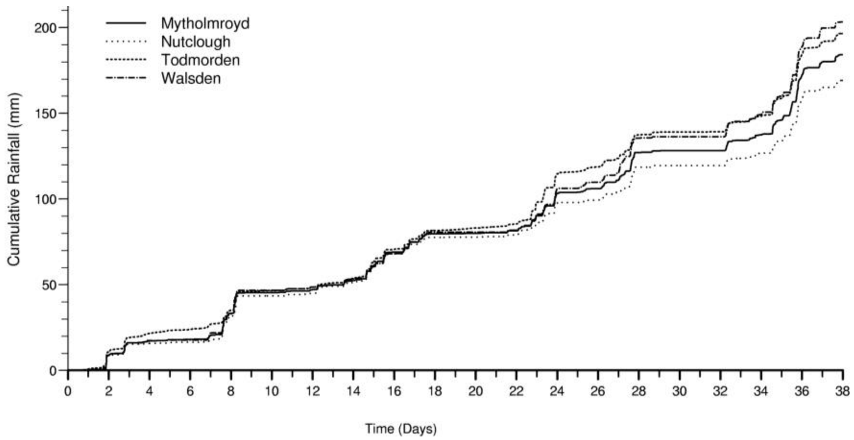

(b) Comparison of the Gorple raingauge (RG) with the 5km radar grid-square containing it (RD)

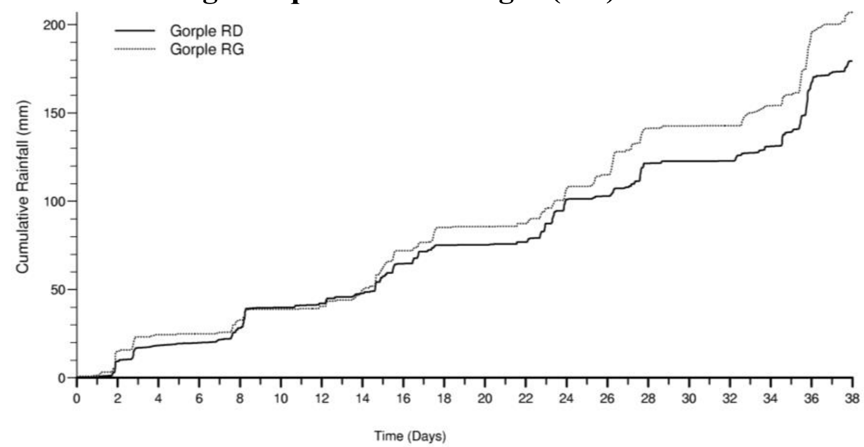

(c) Available raingauges

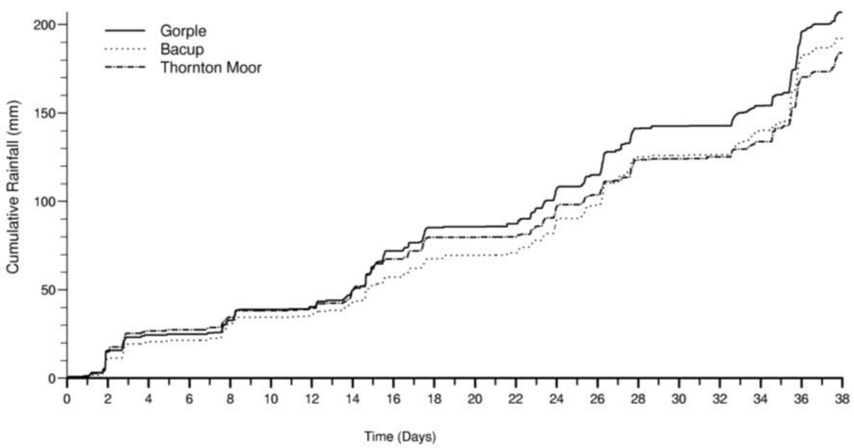

(d) Comparison of the Bacup raingauge (RG) with the 5km radar grid-square containing it (RD)

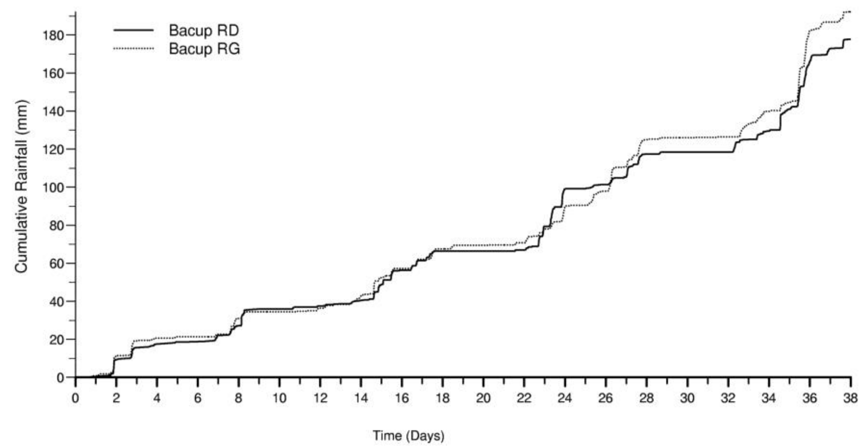

Figure C.3 Cumulative rainfall time-series for Event 3: 11 December 1998 to 18 January 1999

(a) Catchment average rainfalls derived from Nimrod 5km analysis

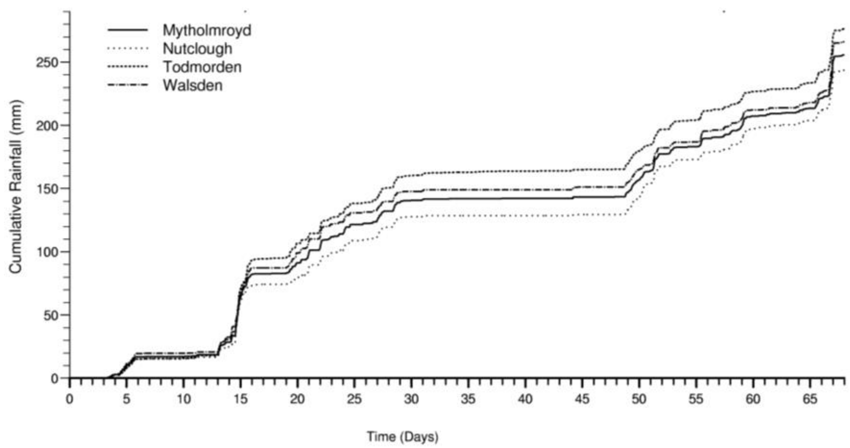

(b) Comparison of the Gorple raingauge (RG) with the 5km radar grid square containing it (RD)

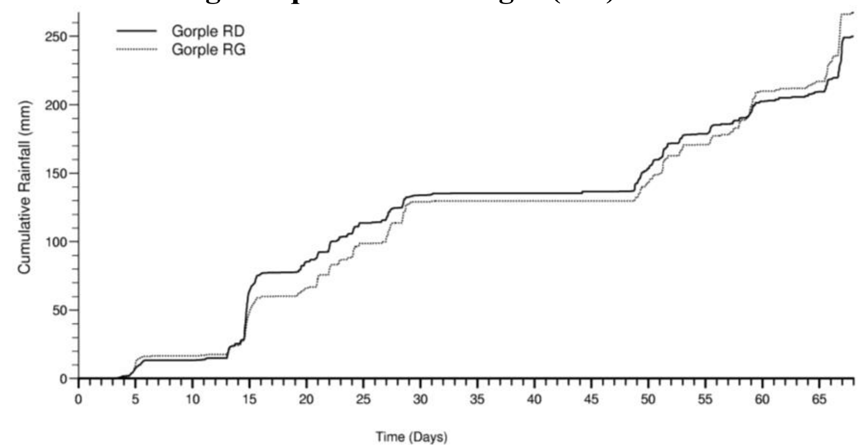

(c) Available raingauges

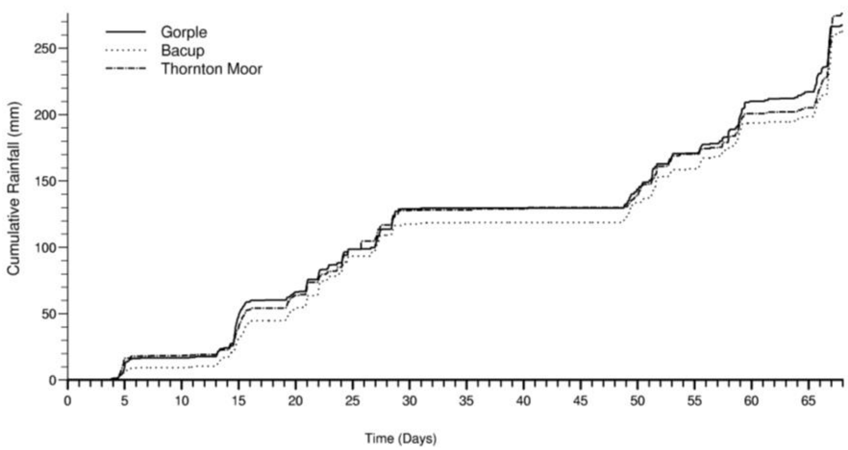

(d) Comparison of the Bacup raingauge (RG) with the 5km radar grid-square containing it (RD)

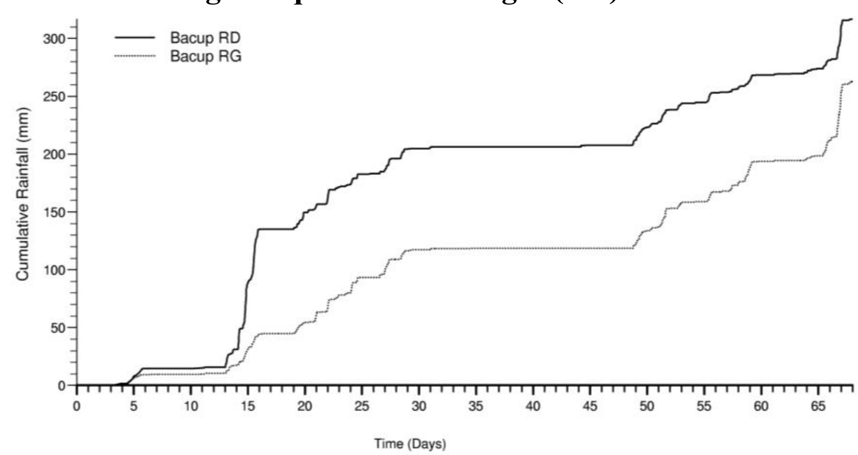

Figure C.4 Cumulative rainfall time-series for Event 4: 29 March to 5 June 2000

(a) Catchment average rainfalls derived from Nimrod 5km analysis

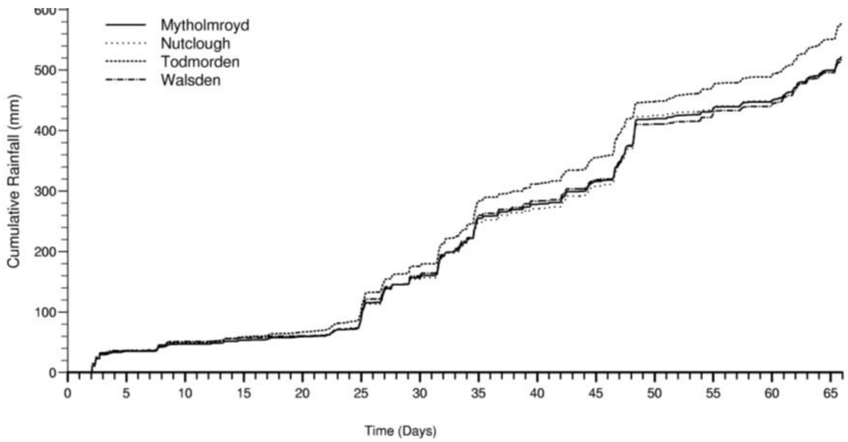

(b) Comparison of the Gorple raingauge (RG) with the 5km radar grid-square containing it (RD)

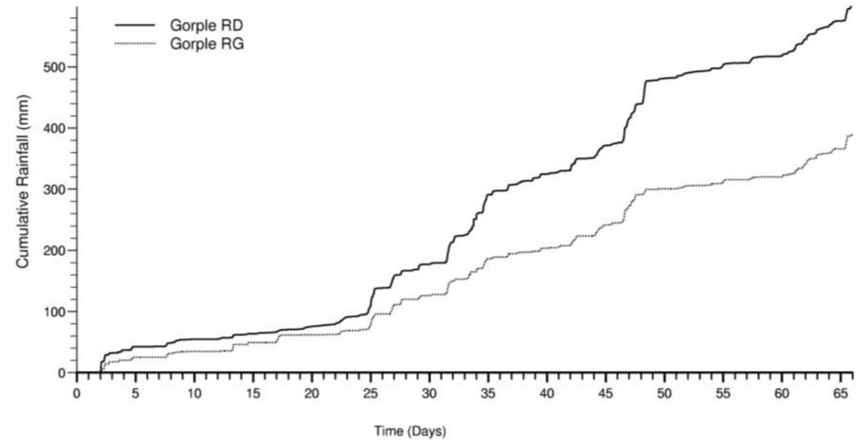

(c) Available raingauges

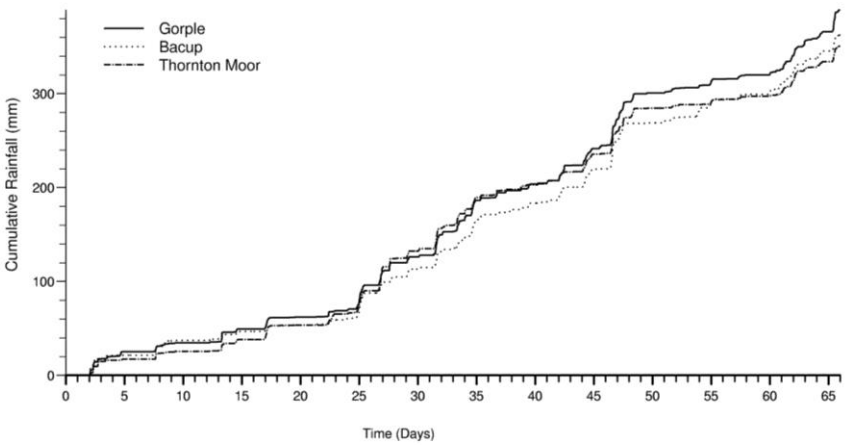

(d) Comparison of the Bacup raingauge (RG) with the 5km radar grid-square containing it (RD)

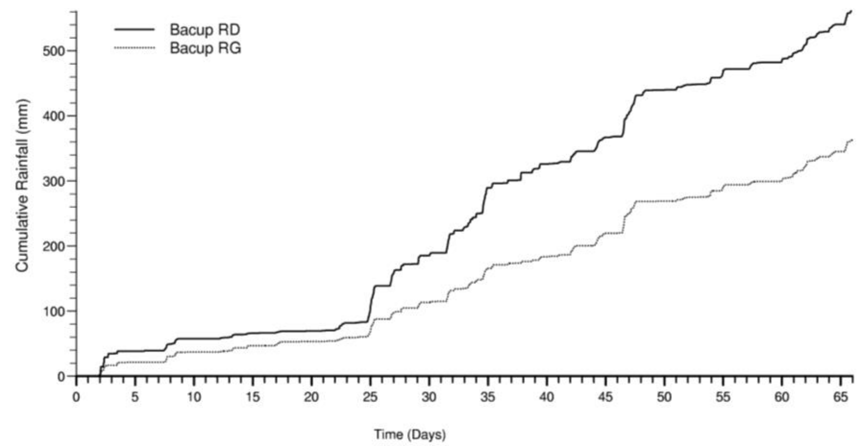

Figure C.5 Cumulative rainfall time-series for Event 5: 24 August to 29 October 2000

(a) Catchment average rainfalls derived from Nimrod 5km analysis

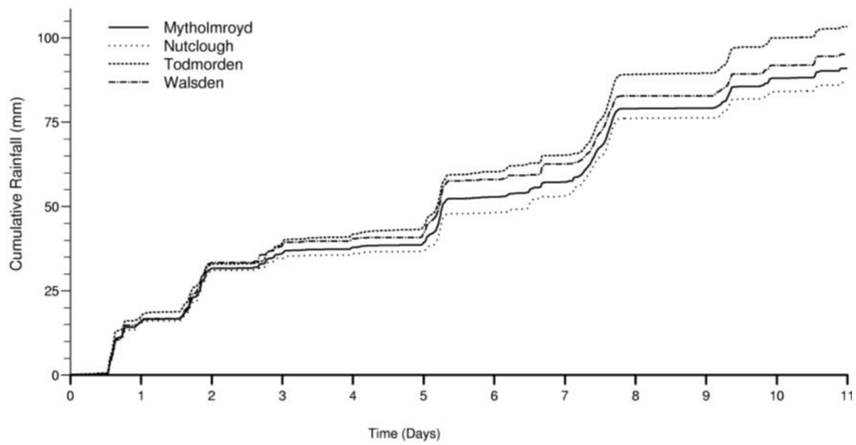

(b) Comparison of the Gorple raingauge (RG) with the 5km and 2km radar grid-squares containing it (RD)

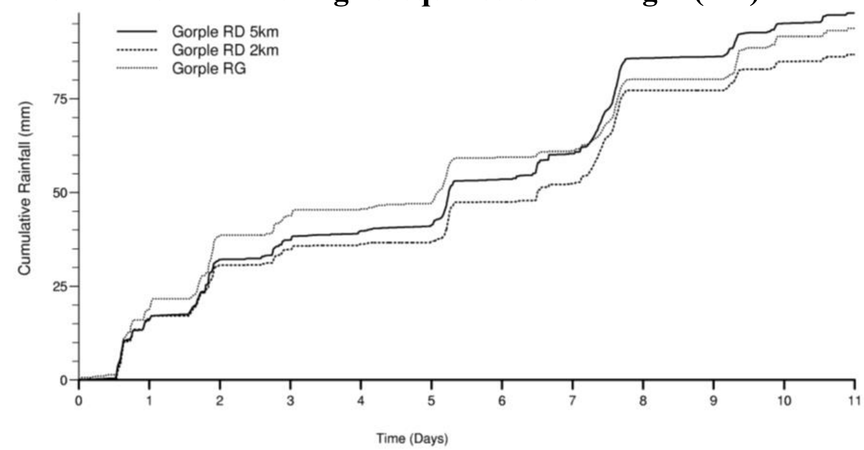

(c) Available raingauges

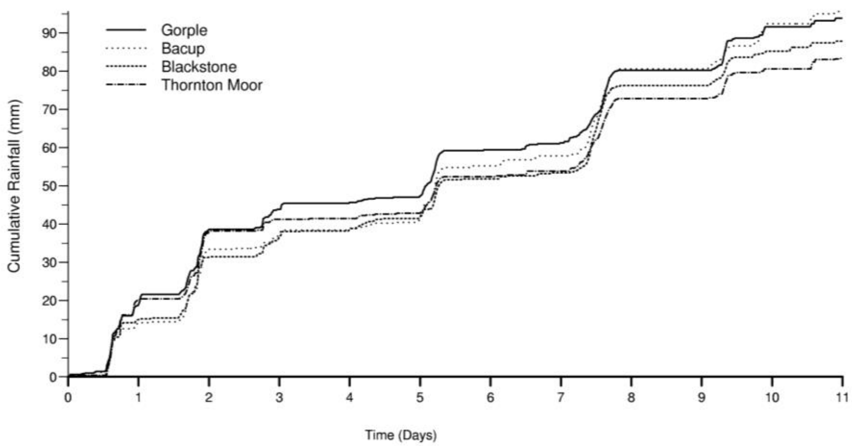

(d) Comparison of the Bacup raingauge (RG) with the 5km and 2km radar grid-squares containing it (RD)

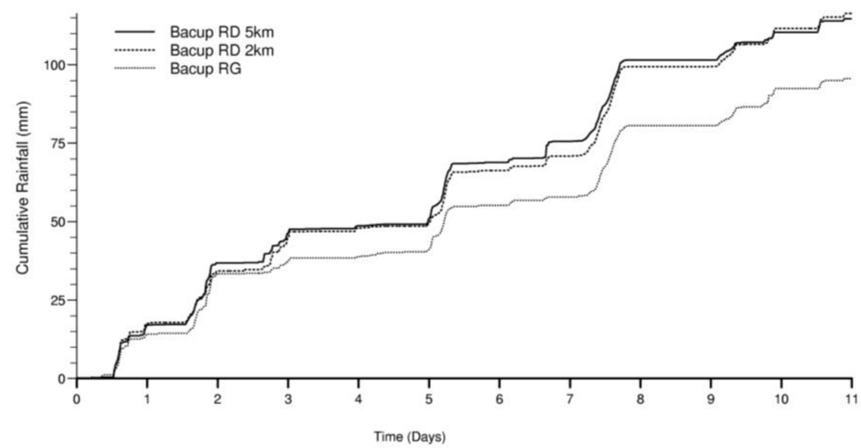

Figure C.6 Cumulative rainfall time-series for Event 6: 1 to 12 November 2002

(a) Catchment average rainfalls derived from Nimrod 5km analysis

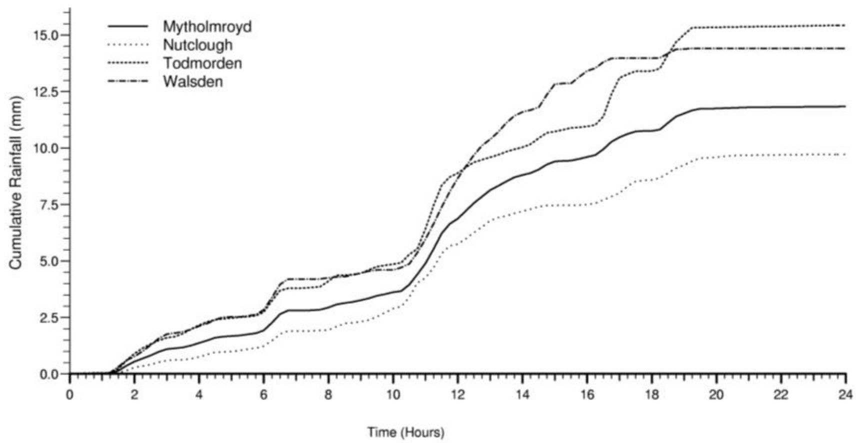

(b) Comparison of the Gorple raingauge (RG) with the 5km and 2km radar grid-squares containing it (RD)

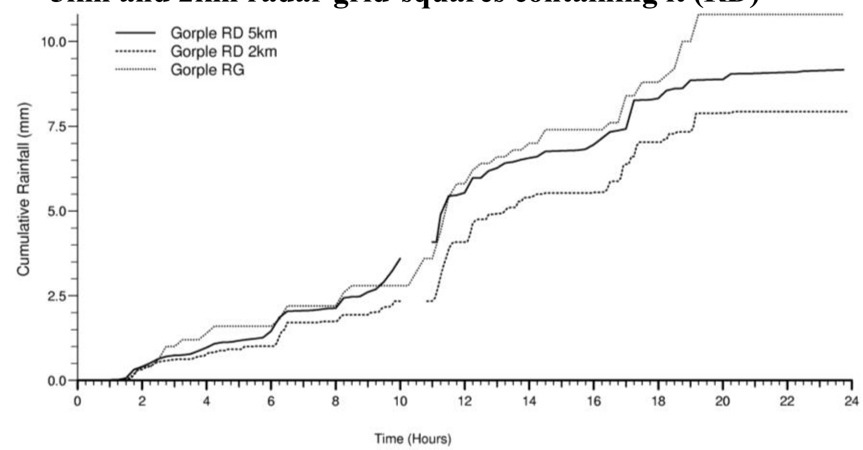

(c) Available raingauges

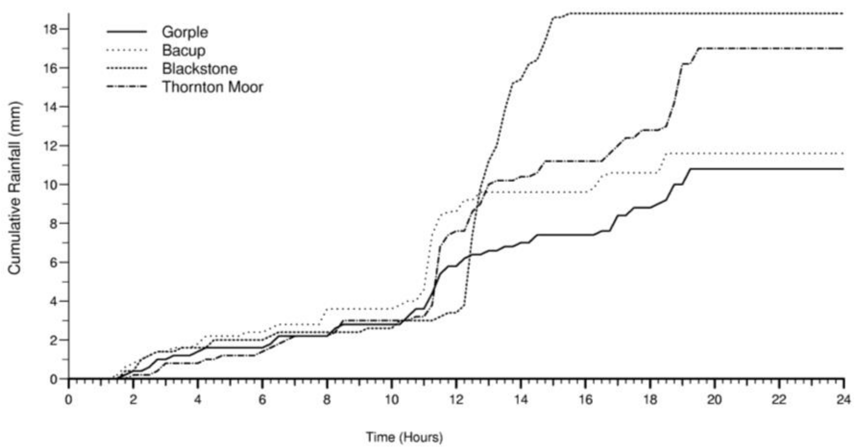

(d) Comparison of the Bacup raingauge (RG) with the 5km and 2km radar grid-squares containing it (RD)

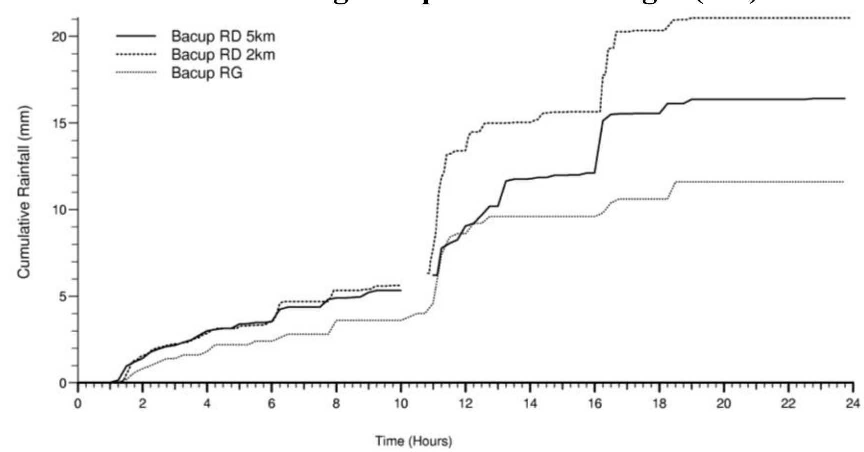

Figure C.7 Cumulative rainfall time-series for Event 7: 10 to 11 June 2002

(a) Catchment average rainfalls derived from Nimrod 5km analysis

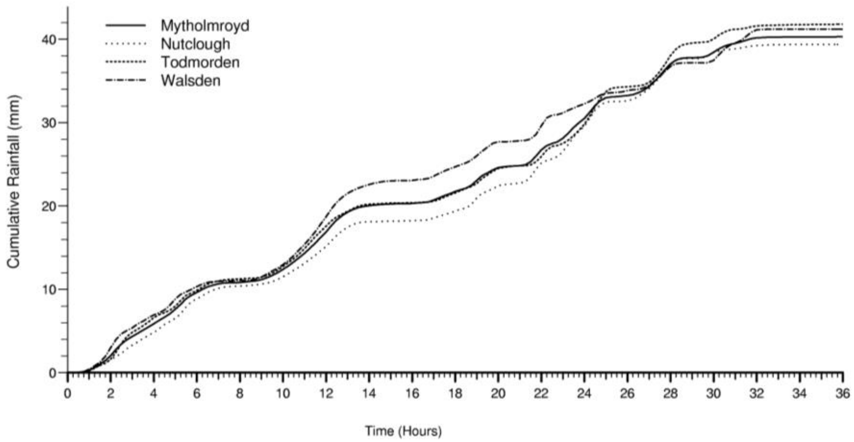

(b) Comparison of the Gorple raingauge (RG) with the 5km and 2km radar grid-squares containing it (RD)

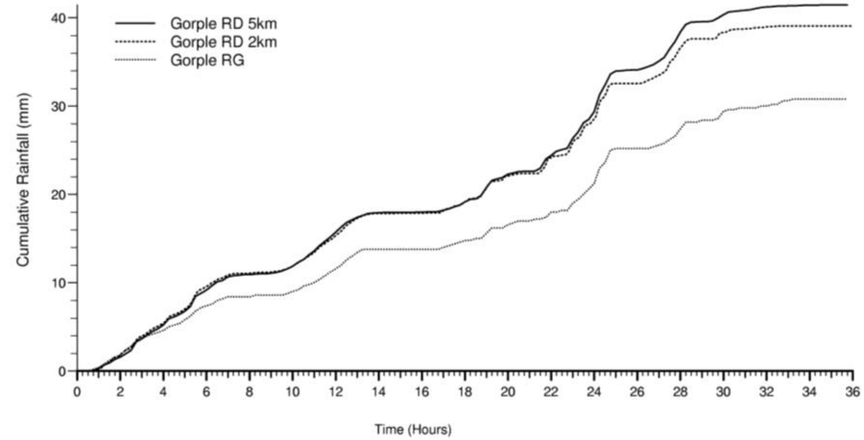

(c) Available raingauges

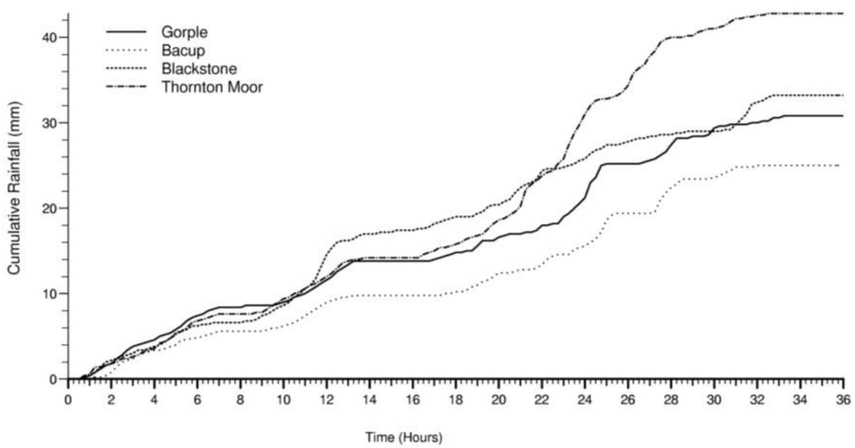

(d) Comparison of the Bacup raingauge (RG) with the 5km and 2km radar grid-squares containing it (RD)

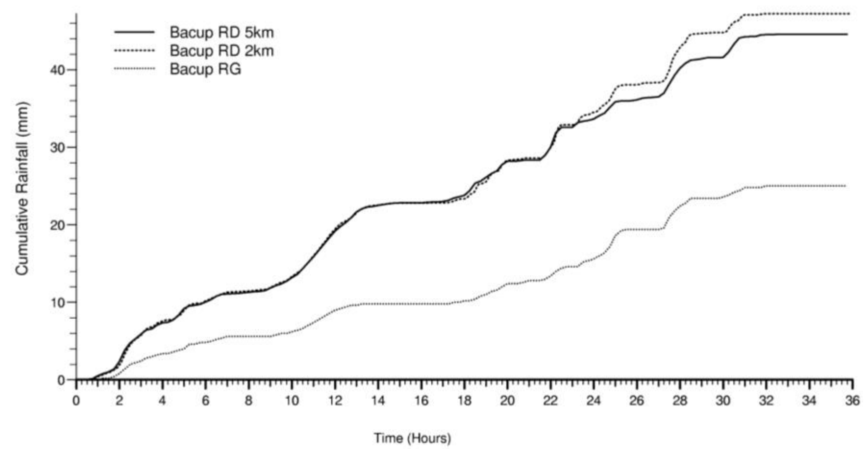

Figure C.8 Cumulative rainfall time-series for Event 8: 00:00 9 August to 12:00 10 August 2002

(a) Catchment average rainfalls derived from Nimrod 5km analysis

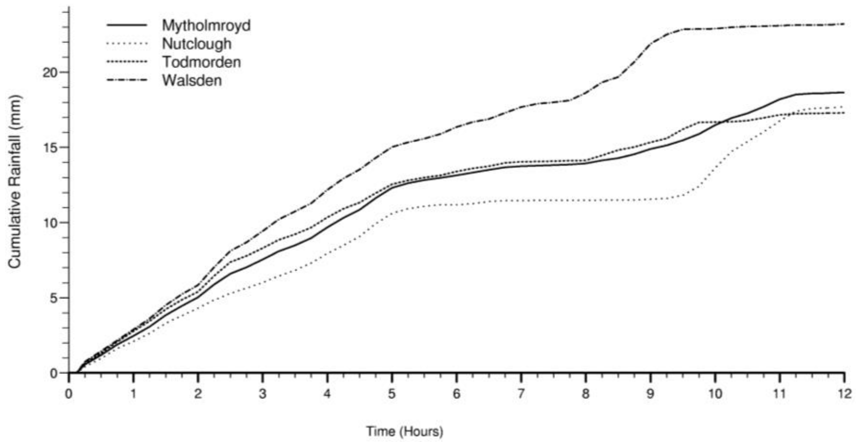

(b) Comparison of the Gorple raingauge (RG) with the 5km and 2km radar grid-squares containing it (RD)

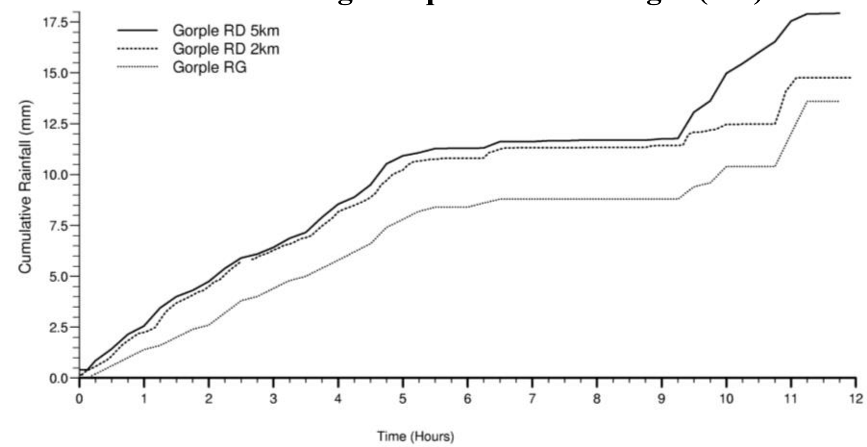

(c) Available raingauges

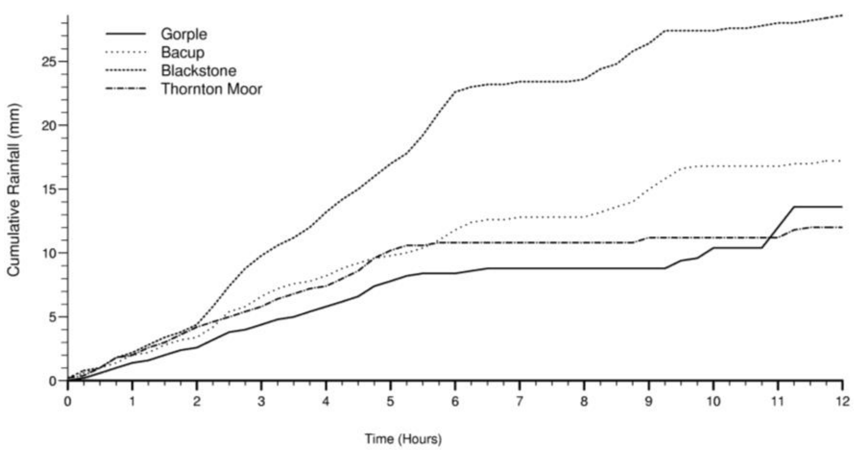

(d) Comparison of the Bacup raingauge (RG) with the 5km and 2km radar grid-squares containing it (RD)

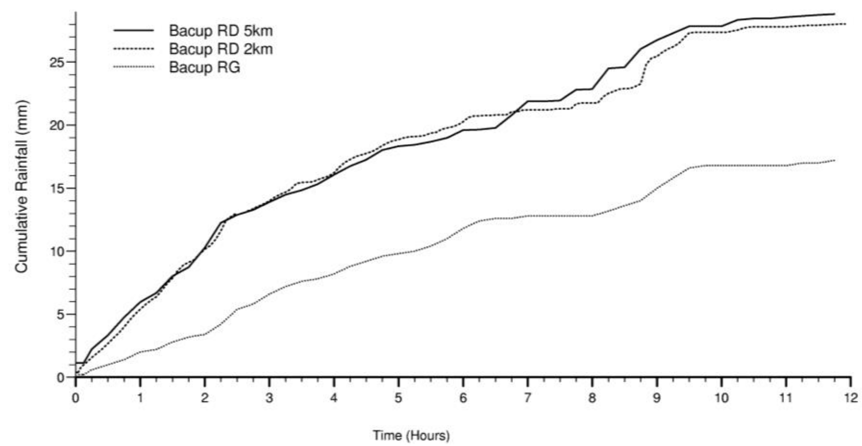

Figure C.9 Cumulative rainfall time-series for Event 9: 12:00 9 September to 00:00 10 September 2002

(a) Catchment average rainfalls derived from Nimrod 5km analysis

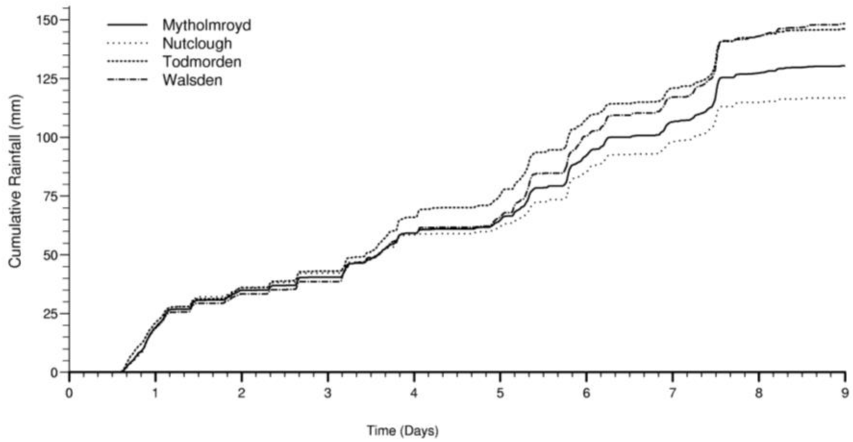

(b) Comparison of the Gorple raingauge (RG) with the 5km and 2km radar grid-squares containing it (RD)

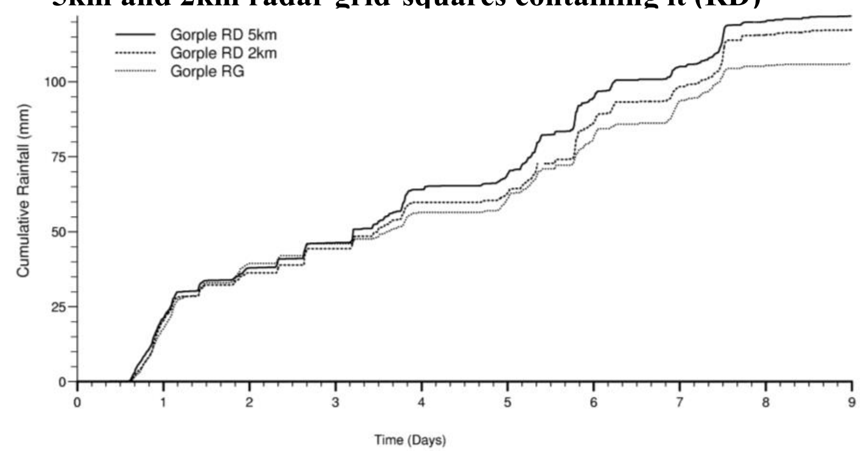

(c) Available raingauges

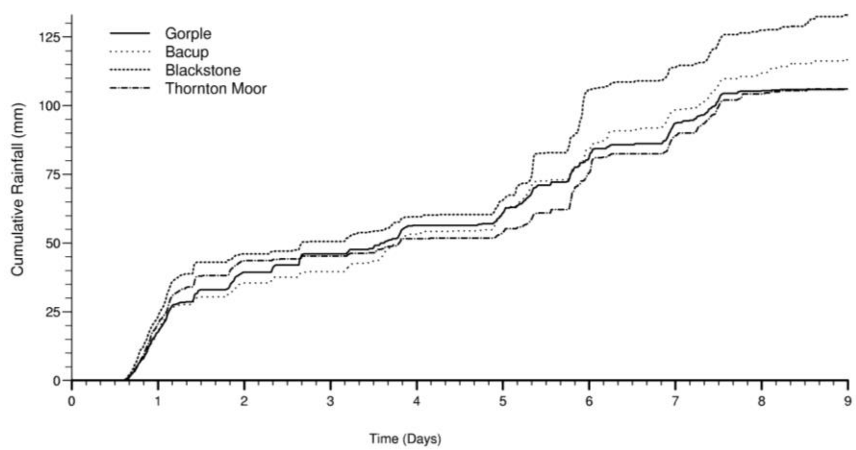

(d) Comparison of the Bacup raingauge (RG) with the 5km and 2km radar grid-squares containing it (RD)

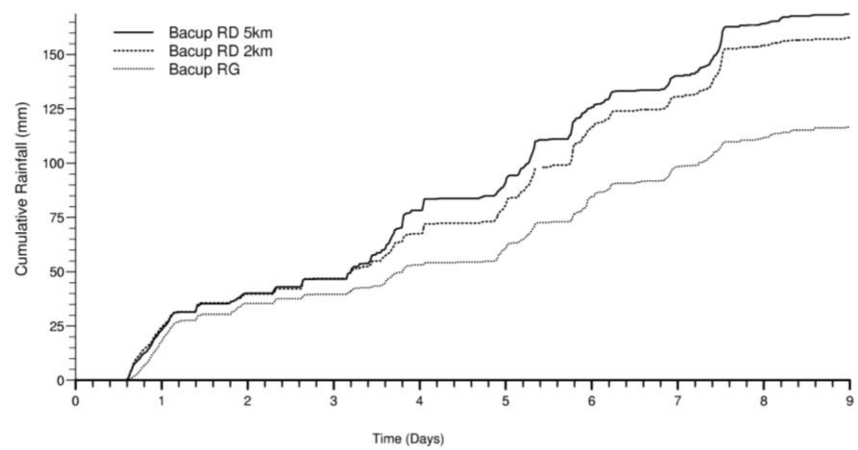

Figure C.10 Cumulative rainfall time-series for Event 10: 20 to 29 October 2002

(a) Catchment average rainfalls derived from Nimrod 5km analysis

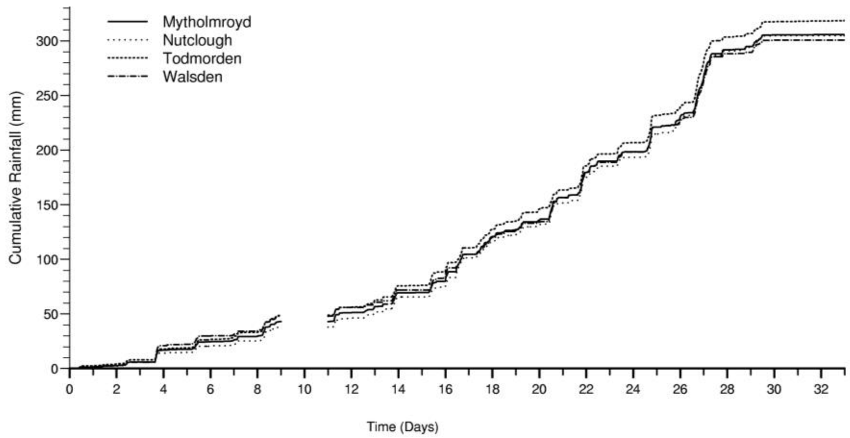

(b) Comparison of the Gorple raingauge (RG) with the 5km and 2km radar grid-squares containing it (RD)

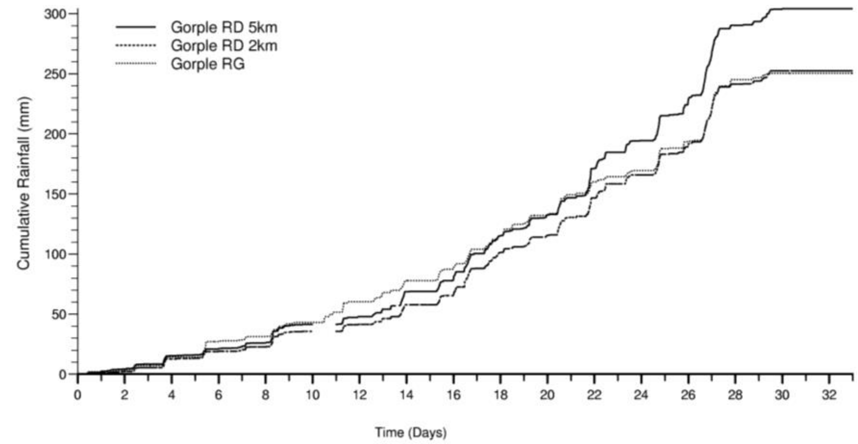

(c) Available raingauges

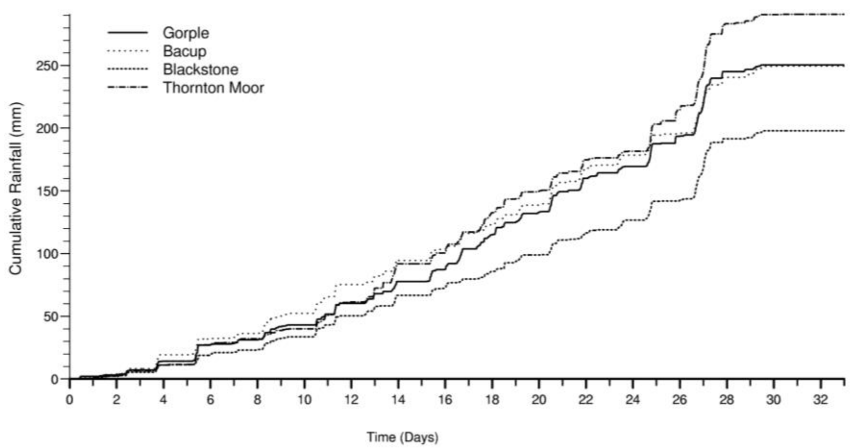

(d) Comparison of the Bacup raingauge (RG) with the 5km and 2km radar grid-squares containing it (RD)

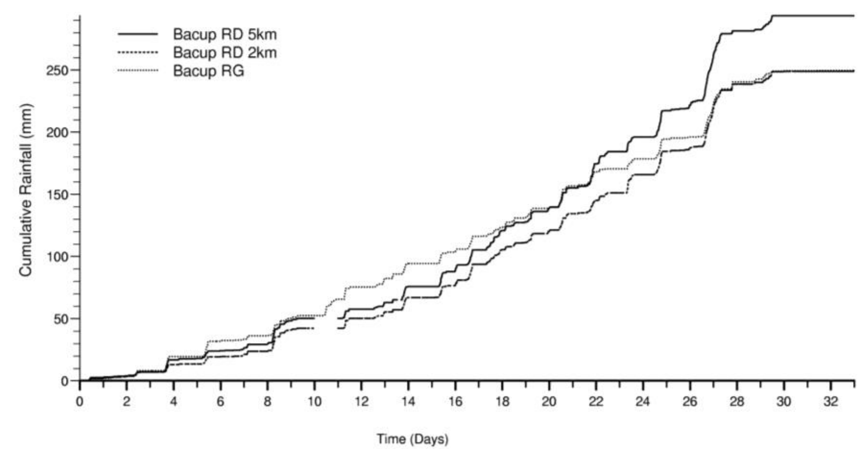

Figure C.11 Cumulative rainfall time-series for Event 11: 15 January to 17 February 2002